Mechanistic Studies of Nickel-Catalyzed Chain-Growth Polymerizations: Additive and Ligand Effects

by

Erica Lynne Lanni

**A dissertation submitted in partial fulfillment
of the requirements for the degree of
Doctor of Philosophy
(Chemistry)
in the University of Michigan
2011**

Doctoral Committee:

**Assistant Professor Anne J. McNeil, Chair
Professor Melanie S. Sanford
Associate Professor John P. Wolfe
Assistant Professor Kenichi Kuroda**

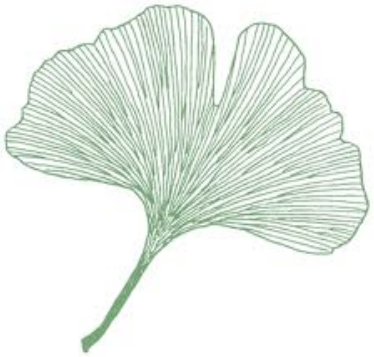

“When we have found all the meanings and lost all the mysteries, we will be alone, on an empty shore.”
- Tom Stoppard, Arcadia

"She would give them order. She would create constellations."
- Thomas Pynchon

“And the roads are covered with a million little molecules...”
- Jack White

2011

Dedication

To my mother, Andrea, for *always* being there to listen.

Acknowledgements

This work would not have been possible without the help, guidance and support of Carolyn and Chris Anderson, Jing Chen, Andrew Higgs, Amanda Hickman, Kelsey King, Beverly Lange, Laura Labut, Se Ryeon Lee, Jonas Locke, John Montgomery, Cheryl Moy, Kathleen Nolta and Tracy Schloemer.

Table of Contents

List of Figures

List of Tables

List of Schemes

List of Appendices

Chapter 1[1]

Introduction: New Conjugated Polymers and Synthetic Methods

Introduction

Organic π-conjugated polymers have unique optical, electrical and redox properties that result from π-electron delocalization along the polymer chain. Consequently, they are being explored for diverse applications, including light-emitting diodes,[1] solar cells,[2] and transistors.[3] Though promising, limitations of the current materials have prevented their widespread application. For example, homopolymers are the most synthetically accessible, however, they often lack one or more of the properties necessary for a functional device (e.g., efficient absorption, exciton dissociation, and charge conduction for solar cells). Accessing more complex polymer architectures has been difficult due to the limitations of current synthetic methods. Typical syntheses of π-conjugated polymers include electrochemical, oxidative, cross-coupling, and metathesis routes. The predominant cross-coupling-based polymerization methods (e.g., Sonogashira,[4] Kumada,[5] Stille,[6] and Suzuki[7]) usually proceed through step-growth mechanisms, where the monomers couple in a random fashion to form oligomers. High molecular weight polymers can only be obtained at high conversions, which are difficult to achieve with these methods. As a result, the polymers typically have low molecular weights with broad molecular weight distributions, and there is limited control over copolymer structure. To advance this field, synthetic methods for accessing a larger variety of well-defined materials are needed.

A major breakthrough occurred in 2004 when Yokozawa[8,9]and McCullough[10,11] simultaneously reported chain-growth syntheses of poly(3-hexylthiophene) utilizing nickel-catalyzed Kumada and Negishi cross-couplings (eq 1)[12]. In chain-growth polymerizations, an initiator reacts with a monomer to start polymerization and subsequent monomer additions occur at the chain end.

---

[1]Excerpted from the manuscript version of McNeil, A. J.; Lanni, E. L. "New Conjugated Polymers and Synthetic Methods." In *Synthesis of Polymers*; Hawker, C.; Junji, S.; Schlüter, D., Eds. Wiley-VCH: Weinheim Germany. *In press.*

If termination pathways are minimal or absent, this method produces polymers with precise molecular weights and narrow molecular weight distributions. Moreover, copolymer microstructure can be controlled by the relative reactivity of the monomers and their order of addition. This chain-growth method has since been modified to polymerize a limited set of monomers, including thiophene derivatives,[13] (2,5-bishexyloxy)phenylene,[14] 9,9-dioctylfluorene,[15] *N*-octylcarbazole,[15b] (2,3-dihexyl)thienopyrazine,[16] and *N*-hexylpyrrole.[17] Although each monomer has required empirical development of chain-growth conditions, this method has provided access to π-conjugated polymers which were previously unobtainable.

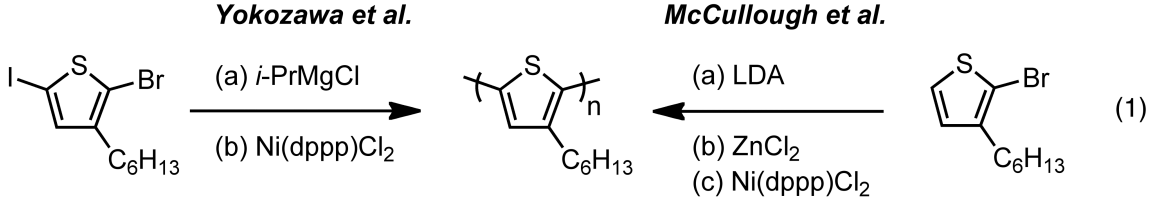

(1)

New Polymers Prepared via Chain-Growth Method

End-Functionalized Polymers. End-functionalized polymers are now accessible with the Ni-catalyzed chain-growth method. These polymers are used as linkers for grafting polymers onto surfaces[18] and as directing groups for self-assembly.[19] In addition, end-functionalized polymers are used as macroinitiators for synthesizing block copolymers. McCullough was the first to demonstrate that poly(3-hexylthiophene) can be selectively functionalized at one chain end by adding a vinyl Grignard reagent post-polymerization (eq 2).[20] Since then, a number of researchers have utilized this method to prepare block copolymers of conjugated polymers with poly(acrylates),[21] polystyrene,[22] polyisoprene,[23] polylactide,[24] and others.[25] These block copolymers formed nanostructured thin-films, and exhibited improved solubilities and film-forming properties compared to their homopolymers. Alternatively, functionalized Ni(II) initiators[26] can be used to graft polymers from surfaces[27] and synthesize block copolymers (eq 3).[28] Although both methods provide access to new materials, competing termination and re-initiation pathways currently result in variable quantities of

unfunctionalized polymers. Consequently, more work is needed to identify robust chain-growth conditions.

End-Functionalization Route to a Block Copolymer

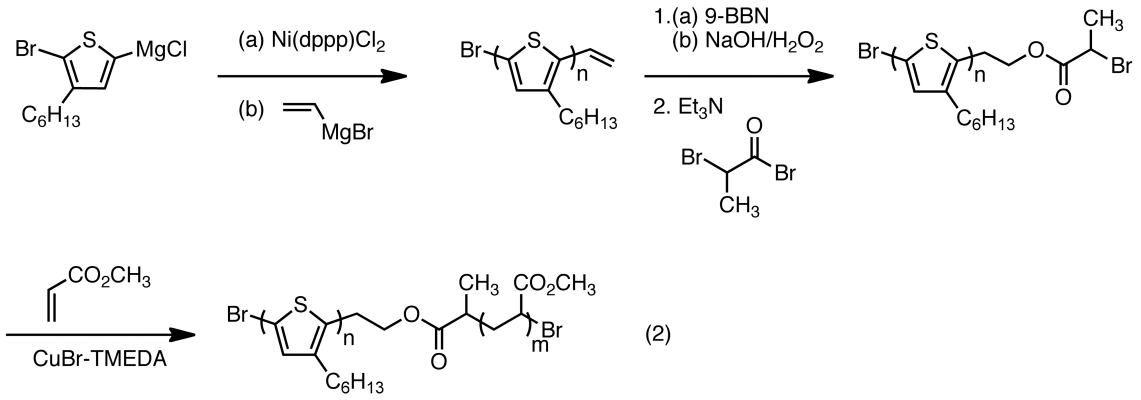

Functionalized Initiator Route to a Block Copolymer

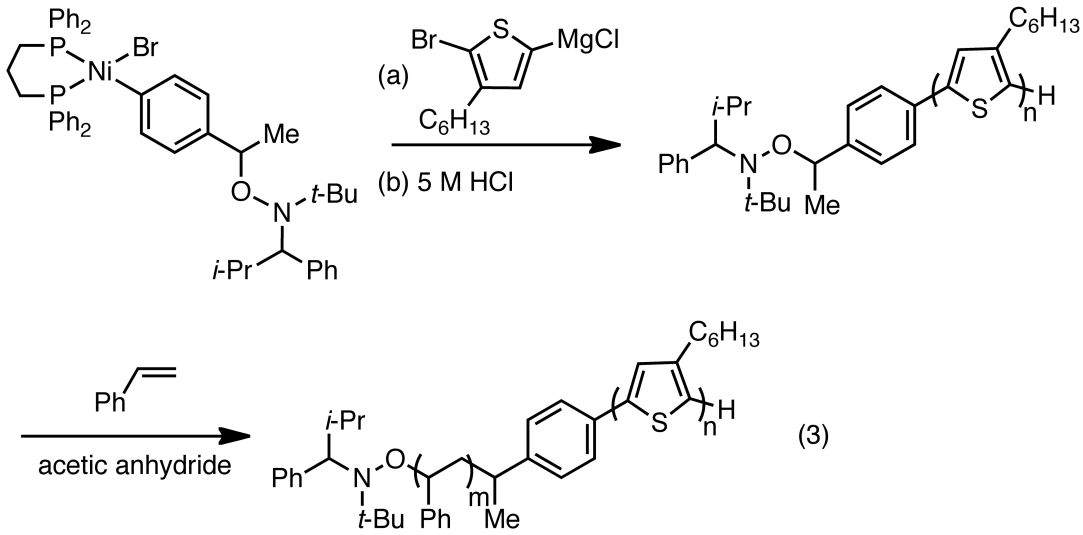

All-Conjugated Block Copolymers. All-conjugated block copolymers can provide access to self-organized, three-dimensional structures in the solid-state (e.g., lamellar), which could lead to improved exciton migration and electron/hole conduction. Most successful copolymerizations employing this chain-growth method have utilized thiophene-based monomers in both blocks.[29] Copolymerizations using structurally different monomers have been demonstrated, but successful formation of block copolymers depended on the order of monomer addition. For example, Yokozawa found that polymerization of 2,5-(bishexyloxy)phenylene must precede the *N*-hexylpyrrole (eq 4); he hypothesized that the extra equiv of dppe necessary for chain-growth

polymerization of pyrrole interferred in the phenylene polymerization.[17] Even when optimized conditions were similar, the order of monomer addition was found to influence copolymer polydispersity; for example, during the polymerization of 3-hexylthiophene with 9,9-dioctylfluorene[30] and 2,5-(bishexyloxy)phenylene.[31] Overall these results suggest inefficient cross-propagation between the two monomers. To rationally expand this methodology to other block copolymers and alternative microstructures, the influence of ligand, monomer, and additive on the reaction mechanism must be understood.

In Situ Synthesis of a Block Copolymer

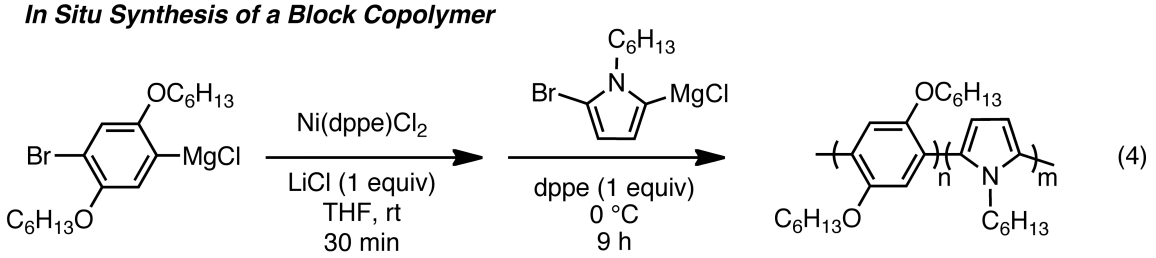

(4)

Mechanism

Initial Observations and Mechanistic Proposal. For over two decades the Kumada polymerization of thiophene[32] was assumed to be step-growth based on conventional cross-coupling mechanisms. In 2004, both Yokozawa[8] and McCullough[10] unexpectedly observed hallmarks of a living, chain-growth mechanism. Most significantly, they observed early formation of high molecular weight polymers, controlled molecular weights based on the ratio of monomer to nickel, and linear increases in molecular weight with conversion. Yokozawa confirmed that the polymerization was living by adding a second batch of monomer to the polymerization and observing that the molecular weight increased while the PDI remained constant. Based on these preliminary results, both McCullough and Yokozawa proposed a new mechanistic pathway for the polymerization where the key difference from conventional cross-coupling mechanisms is formation of an associated Ni(0)-polymer π-complex (**I**, Scheme 1). Subsequent intracomplex oxidative addition is suggested to occur faster than dissociation, leading to successive monomer additions at the chain end. Although Ni(0)-arene π-complexes have precedent, their role in the polymerization mechanism remains uncertain.

Scheme 1.1 Proposed Chain-Growth Mechanism.

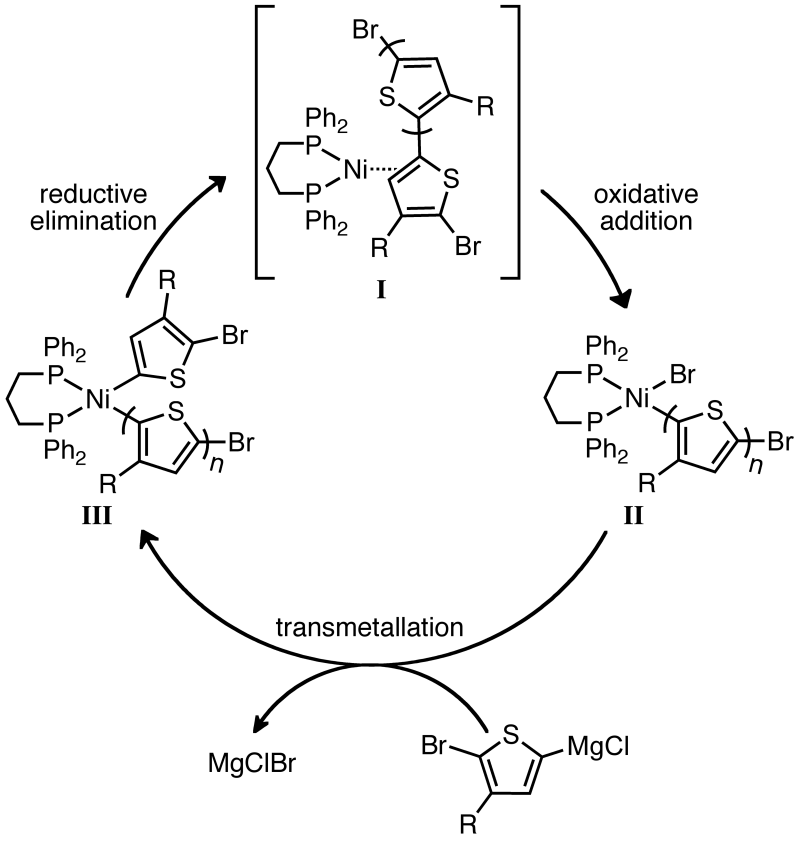

Subsequent Mechanistic Studies

End-Group Analysis. End-group analysis via MALDI-TOF mass spectrometry can provide compelling evidence for a proposed polymerization mechanism. Polymers that result from a living, chain-growth mechanism should exhibit end-groups reflecting the initiating and propagating species. Yokozawa first demonstrated that polymers with a single set of end-groups (H/Br) are obtained in the Ni(dppp)Cl_2-catalyzed polymerization of 3-hexylthiophene (eq 5).[33a] These end-groups are consistent with the proposed catalytic cycle since the reaction should stall at complex **II** once monomer is completely consumed. Subsequent hydrolysis protonates the nickel chain end. Following these early studies, many researchers have employed end-group analysis to determine chain-growth conditions for each polymerization.

End-Group Analysis

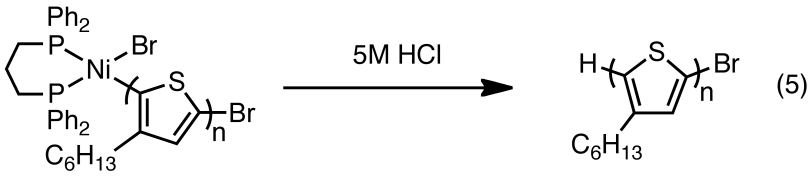

(5)

II

Rate and Spectroscopic Studies. A combination of rate and spectroscopic studies can be used to identify the resting state and rate-determining step of a catalytic cycle. In 2005, McCullough reported limited rate studies which supported a rate-determining transmetallation for Ni(dppp)Cl_2-catalyzed polymerization of 3-hexylthiophene.[Error! Bookmark not defined.i] More recently, he reported similar rate profiles for Ni(dppp)Cl_2-catalyzed polymerization of 9,9-dioctylfluorene.[30] In 2009, we demonstrated that reductive elimination is the rate-determining step for the synthesis of both poly(3-hexylthiophene) and poly(*p*-(2,5-bishexyloxy)phenylene) when using Ni(dppe)Cl_2 – a frequent alternative to Ni(dppp)Cl_2[34]. ^{31}P NMR spectroscopic studies confirmed that the resting state during polymerization was a Ni(II)-bithiophene (**IV**), and after polymerization, the catalytic cycle stalled at a Ni(II) thienyl halide (**V**). We also investigated Ni(dppp)Cl_2-catalyzed polymerization of 3-hexylthiophene and 2,5-(bishexyloxy)phenylene using rate and spectroscopic studies.[35] We observed rate-limiting transmetallation in both cases, consistent with McCullough's preliminary observations. In addition, we characterized the catalyst resting state as the Ni(II) thienyl halide (**II**), consistent with Yokozawa's observation of H/Br end-groups.[33a] Overall, this concomitant change in rate-determining step with catalyst structure indicated that the ligand (dppp versus dppe) has a strong influence over the mechanism. Additionally, the observation of a rate-determining reductive elimination with Ni(dppe)Cl_2 and rate-determining transmetallation with Ni(dppp)Cl_2 suggests that the Ni(0)-polymer π-complex, if formed, is only a fleeting intermediate. As a result, further studies are necessary to probe both the existence and catalytic relevance of Ni(0)-polymer π-complexes in the polymerization. Moreover, additional studies are needed to understand the influence of the ligand on this proposed intermediate.

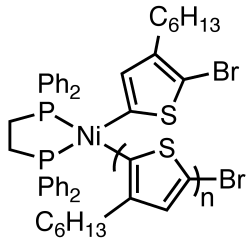

IV

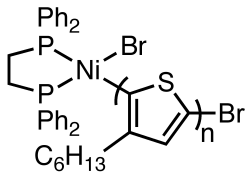

V

Indirect Support for an Intermediate Ni(0)-polymer π-Complex. Although Ni(0)-arene π-complexes have been characterized[36] and implicated as intermediates in oxidative addition[37] and cross-coupling,[38] currently, there is no direct evidence of its intermediacy in the Ni-catalyzed chain-growth polymerization. Kiriy indirectly probed the existence of a π-complex by examining whether the chain-growth mechanism is affected by monomer length.[26e] He observed a decrease in chain-growth behavior for terthiophene compared to bithiophene and thiophene, suggesting that detrimental chain-transfer and termination processes become more prevalent with larger distances between the C-C bond forming site and reactive end-group. In 2010, Kiriy provided evidence that Ni(0) does not stay associated with the chain end but instead performs a near random walk along the polymer backbone via π-bound intermediates (eq 6).[39] This data is consistent with McCullough's observation of end-functionalization at both chain ends when non-vinyl or -alkenyl Grignard reagents were added post-polymerization.[20b] Overall, these results suggest that propagation can occur by oxidative addition into either chain end during the conventional Ni(dppp)Cl_2-catalyzed conditions (c.f., complex **I**, Scheme 1).

Evidence for Random Ni(0) Walking

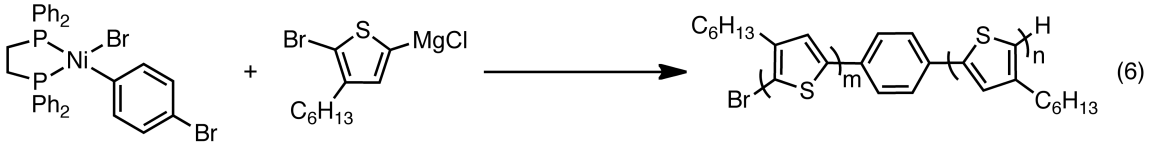

(6)

Competition experiments have also provided indirect support for Ni(0) association with a single polymer chain throughout the polymerization. For example, Yokozawa added 18 mol% of an aryl halide to a thiophene polymerization and observed that most of the aryl halide remained unreacted.[9c] This result suggests that reactive, unassociated Ni(0) was not generated.

Recognizing that aryl halides are less reactive than thiophenes, Kiriy performed a competition experiment where an end-labeled oligothiophene was added to the polymerization.[26e] He saw no evidence of high molecular weight polythiophenes with those end-groups, consistent with Ni(0) remaining associated with a single polymer chain (eq 7).[40]

Competition Experiment

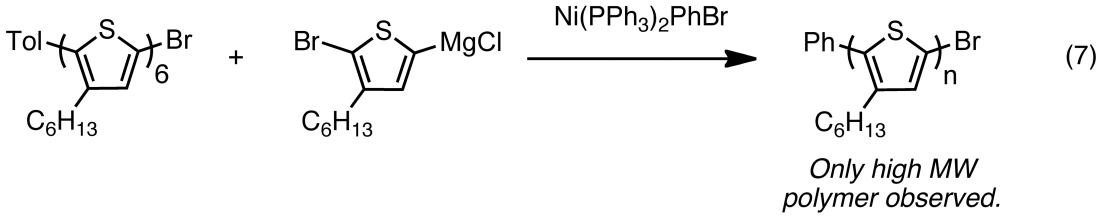

(7)

Conclusion

This dissertation details my work in the McNeil group towards elucidation of the polymerization mechanism. In particular, it describes our group's efforts to improve the method through mechanistic studies and rational ligand design. While we have found that the rate-determining step of the polymerization is strongly influenced by the phosphine bite-angle, alternative structural modifications of the ligand have been shown to enhance or disrupt chain-growth polymerization. The work presented provides a foundation for future investigations into the mechanistic influence of monomers, catalysts, and additives in copolymerizations.

References Cited

(1) Grimsdale, A. C.; Chan K. L.; Martin, R. E.; Jokisz, P. G.; Holmes, A. B. *Chem. Rev.* **2009**, *109*, 897.

(2) (a) Dennler, G.; Scharber, M. C.; Brabec, C. J. *Adv. Mater.* **2009**, *21*, 1323. (b) Hoppe, H.; Sariciftci, N. S. In *Photoresponsive Polymers II,* (eds S. R. Marder and K.-S. Lee), Advances in Polymer Science, Springer Berlin, Heidelberg **214**, pp. 1-86 (2008).

(3) Arias, A. C.; MacKenzie, J. D.; McCulloch, I.; Rivnay, J.; Salleo, A. *Chem. Rev.* **2010**, *110*, 3.

(4) Sanechika, K.; Yamamoto, T.; Yamamoto, A. *Bull. Chem. Soc. Jpn*. **1984**, *57*, 752. For a recent review, see: Bunz, U. H. F.; *Macromol. Rapid Commun*. **2009**, *30*, 772.

(5) Yamamoto, T.; Hayashi, Y.; Yamamoto, A. *Bull. Chem. Soc. Jpn*. **1978**, *51*, 2091.

(6) Bao, Z.; Chan, W.; Yu, L. *Chem. Mater.* **1993**, *5*, 2. See also: Bao, Z.; Chan, W. K.; Yu, L. *J. Am. Chem. Soc.* **1995**, *117*, 12426.

(7) Rehahn, M.; Schlüter, A.-D.; Wegner, G.; Feast, W. J.*Polymer* **1989**, *30*, 1060. For a recent review, see: Sakamoto, J.; Rehahn, M.; Wegner, G.; Schlüter, A. D. *Macromol. Rapid Commun.* **2009**, *30*, 653.

(8) (a) Yokoyama, A.; Miyakoshi, R.; Yokozawa, T. *Macromolecules* **2004**, *37*, 1169. (b) Miyakoshi, R.; Yokoyama, A.; Yokozawa, T. *Macromol. Rapid Commun*. **2004**, *25*, 1663.

(9) For reviews, see: (a) Yokozawa T.; Yokoyama, A. *Chem. Rev.* **2009**, *109*, 5595. (b) Yokozawa, T.; Ajioka, N.; Yokoyama, A. In *New Frontiers in Polymer Synthesis,* (ed S. Kobayashi), Advances in Polymer Science, Springer Berlin, Heidelberg, **2008**, *217*, pp. 1-77. (c) Miyakoshi, R.; Yokoyama, A.; Yokozawa, T. *J. Poly. Sci., Part A: Polym. Chem*. **2008**, *46*, 753.

(10) Sheina, E. E.; Liu, J.; Iovu, M. C.; Laird, D. W.; McCullough, R. D. *Macromolecules* **2004**, *37*, 3526.

(11) For a review, see: Osaka, I.; McCullough, R. D. *Acc. Chem. Res*. **2008**, *41*, 1202.

(12) Note that an apparent chain-growth polymerization method was reported using Pd-catalysts and boronic acids, see: Yokoyama, A.; Suzuki, H.; Kubota, Y.; Ohuchi, K.; Higashimura, H.; Yokozawa, T.; *J. Am. Chem. Soc.* **2007**, *129*, 7236. It has been significnatly less utilized, see: (a) Beryozkina, T.; Boyko, K.; Khanduyeva, N.; Senkovskyy, V.; Horecha, M.; Oertel, U.; Simon, F.; Stamm, M.; Kiriy, A. *Angew. Chem. Int. Ed.* **2009**, *48*, 2695. (b) Huang, W.; Su, L.; Bo, Z.; *J. Am. Chem. Soc.* **2009**, *131*, 10348.

(13) (a) Benanti, T. L.; Kalaydjian, A.; Venkataraman, D. *Macromolecules* **2008**, *41*, 8312. (b) Ouhib, F.; Dkhissi, A.; Iratçabal, P.; Hiorns, R. C.; Khoukh, A.; Desbrières, J.; Pouchan, C.; Dagron-Lartigau, C. *J. Polym. Sci., Part A: Polym. Chem*. **2008**, *46*, 7505. (c) Li, Y.; Xue, Y.; Xia, H.; Xu, B.; Wen, S.; Tian, W. *J. Polym. Sci., Part A: Polym. Chem*. **2008**, *46*, 3970. (d) Vallat, P.; Lamps, J.-P.; Schosseler, F.; Rawiso, M.; Catala, J.-M. *Macromolecules* **2007**, *40*, 2600. (e) Adachi, I.; Miyakoshi, R.; Yokoyama, A.; Yokozawa, T. *Macromolecules* **2006**, *39*, 7793. (f) Koeckelberghs, G.; Vangheluwe, M.; Van Doorsselaere, K.; Robijns, E.; Persoons, A.; Verbiest, T. *Macromol. Rapid Commun*. **2006**, *27*, 1920. (g) Sheina, E. E.; Khersonsky, S. M.; Jones, E. G.; McCullough, R. D. *Chem. Mater.* **2005**, *17*, 3317.

(14) Miyakoshi, R.; Shimono, K.; Yokoyama, A.; Yokozawa, T. *J. Am. Chem. Soc*. **2006**, *128*, 16012.

(15) (a) Huang, L.; Wu, S.; Qu, Y.; Geng, Y.; Wang, F. *Macromolecules* **2008**, *41*, 8944. (b) Stefan, M. C.; Javier, A. E.; Osaka, I.; McCullough, R. D. *Macromolecules* **2009**, *42*, 30.

(16) Wen, L.; Duck, B. C.; Dastoor, P. C.; Rasmussen, S. C. *Macromolecules* **2008**, *41*, 4576.

(17) Yokoyama, A.; Kato, A.; Miyakoshi, R.; Yokozawa, T. *Macromolecules* **2008,** *41*, 7271.

(18) (a) Palaniappan, K.; Murphy, J. W.; Khanam, N.; Horvath, J.; Alshareef, H.; Quevedo-Lopez, M.; Biewer, M. C.; Park, S. Y.; Kim, M. J.; Gnade, B. E.; Stefan, M. C.; *Macromolecules* **2009**, *42*, 3845. (b) Xu, J.; Wang, J.; Mitchell, M.; Mukherjee, P.; Jeffries-EL, M.; Petrich, J. W.; Lin, Z. *J. Am. Chem. Soc.* **2007**, *129*, 12828.

(19) (a) Higashihara, T.; Takahashi, A.; Tajima, S.; Jin, S.; Rho, Y.; Ree, M.; Ueda, M. *Polym. J.* **2010**, *42*, 43. (b) Takahashi, A.; Rho, Y.; Higashihara, T.; Ahn, B.; Ree, M.; Ueda, M. *Macromolecules* **2010**, *43*, 4843.

(20) (a) Jeffries-El, M.; Sauvé, G.; McCullough, R. D. *Macromolecules* **2005**, *38*, 10346. (b) Jeffries-EL, M.; Sauvé, G.; McCullough, R. D. *Adv. Mater.* **2004**, *16*, 1017.

(21) (a) Higashihara, T.; Ueda, M. *React. Funct. Polym*. **2009**, *69*, 457. (b) Lee, J. U.; Cirpan, A.; Emrick, T.; Russell, T. P.; Jo, W. H. *J. Mater. Chem.* **2009**, *19*, 1483. (c) Sommer, M.; Lang, A. S.; Thelakkat, M. *Angew. Chem. Int. Ed.* **2008**, *47*, 7901. (d) Iovu, M. C.; Zhang, R.; Cooper, J. R.; Smilgies, D. M.; Javier, A. E.; Sheina, E. E.; Kowalewski, T.; McCullough, R. D. *Macromol. Rapid Commun*. **2007**, *28*, 1816. (e) Sauvé, G.; McCullough, R. D. *Adv. Mater.* **2007**, *19*, 1822. (f) Iovu, M. C.; Jeffries-EL, M.; Sheina, E. E.; Cooper, J. R.; McCullough, R. D. *Polymer* **2005**, *46*, 8582.

(22) (a) Higashihara, T.; Ohshimizu, K.; Hirao, A.; Ueda, M. *Macromolecules* **2008**, *41*, 9505. (b) Urien, M.; Erothu, H.; Cloutet, E.; Hiorns, R. C.; Vignau, L.; Cramail, H. *Macromolecules* **2008**, *41*, 7033.

(23) Iovu, M. C.; Craley, C. R.; Jeffries-EL, M.; Krankowski, A. B.; Zhang, R.; Kowalewski, T.; McCullough, R. D. *Macromolecules* **2007**, *40*, 4733.

(24) Boudouris, B. W.; Frisbie, C. D.; Hillmyer, M. A. *Macromolecules*, **2008**, *41*, 67.

(25) (a) Craley, C. R.; Zhang, R.; Kowalewski, T.; McCullough, R. D.; Stefan, M. C. *Macromol. Rapid Commun.* **2009**, *30*, 11. (b) Alemseghed, M. G.; Gowrisanker, S.; Servello, J.; Stefan, M. C. *Macromol. Chem. Phys.* **2009**, *210*, 2007. (c) Richard, F.; Brochon, C.; Leclerc, N.; Eckhardt, D.; Heiser, T.; Hadziioannou, G. *Macromol. Rapid Commun.* **2008**, *29*, 885. (d) Dai, C.-A.; Yen, W.-C.; Lee, Y.-H.; Ho, C.-C.; Su, W.-F. *J. Am. Chem. Soc.* **2007**, *129*, 11036. (e) Radano, C. P.; Scherman, O. A.; Stingelin-Stutzmann, N.; Müller, C.; Breiby, D. W.; Smith, P.; Janssen, R. A. J.; Meijer, E. W. *J. Am. Chem. Soc.* **2005**, *127*, 12502.

(26) (a) Doubina, N.; Ho, A.; Jen, K.-Y. A.; Luscombe, C. K. *Macromolecules* **2009**, *42*, 7670. (b) Doubina, N.; Stoddard, M.; Bronstein, H. A.; Jen, A. K.-Y.; Luscombe, C. K.; *Macromol. Chem. Phys.* **2009**, *210*, 1966. (c) Bronstein, H. A.; Luscombe, C. K. *J. Am. Chem. Soc*. **2009**, *131*, 12894. (d) Smeets, A.; Van den Bergh, K.; De Winter, J.; Gerbaux, P.; Verbiest, T.; Koeckelberghs, G.; *Macromolecules* **2009**, *42*, 7638. (e) Beryozkina, T.; Senkovskyy, V.; Kaul, E.; Kiriy, A.; *Macromolecules* **2008**, *41*, 7817.

(27) (a) Tkachov, R.; Senkovskyy, V.; Horecha, M.; Oertel, U.; Stamm, M.; Kiriy, A. *Chem. Commun*. **2010**, *46*, 1425. (b) Marshall, N.; Sontag, S. K.; Locklin, J. *Macromolecules* **2010**, *43*, 2137. (c) Senkovskyy, V.; Tkachov, R.; Beryozkina, T.; Komber, H.; Oertel, U.; Horecha, M.; Bocharova, V.; Stamm, M.; Gevorgyan, S. A.; Krebs, F. C.; Kiriy, A. *J. Am. Chem. Soc.* **2009**, *131*, 16445. (d) Khanduyeva, N.; Senkovskyy, V.; Beryozkina, T.; Horecha, M.; Stamm, M.; Uhrich, C.; Riede, M.; Leo, K.; Kiriy, A. *J. Am. Chem. Soc.* **2009**, *131*, 153. (e) Sontag, S. K.; Marshall, N.; Locklin, J. *Chem. Commun*. **2009**, 3354. (f) Khanduyeva, N.; Senkovskyy, V.; Beryozkina, T.; Bocharova, V.; Simon, F.; Nitschke, M.; Stamm, M.; Grötzschel, R.; Kiriy, A. *Macromolecules* **2008**, *41*, 7383. (g) Senkovskyy, V.; Khanduyeva, N.; Komber, H.; Oertel, U.; Stamm, M.; Kuckling, D.; Kiriy, A. *J. Am. Chem. Soc.* **2007**, *129*, 6626.

(28) Kaul, E.; Senkovskyy, V.; Tkachov, R.; Bocharova, V.; Komber, H.; Stamm, M.; Kiriy, A. *Macromolecules* **2010**, *43*, 77.

(29) (a) Van den Bergh, K.; Cosemans, I.; Verbiest, T.; Koeckelberghs, G.; *Macromolecules* **2010**, *43*, 3794. (b) Clément, S.; Meyer, F.; De Winter, J.; Coulembier, O.; Vande Velde, C. M. L.; Zeller, M.; Gerbaux, P.; Balandier, J.-Y.; Sergeyev, S.; Lazzaroni, R.; Geerts, Y.; Dubois, P. *J. Org. Chem*. **2010**, *75*, 1561. (c) Zhang, Y.; Tajima, K.; Hashimoto, K.; *Macromolecules* **2009**, *42*, 7008. (d) Wu, P.-T.; Ren, G.; Li, C.; Mezzenga, R.; Jenekhe, S. A. *Macromolecules* **2009**, *42*, 2317. (e) Ouhib, F.; Khoukh, A.; Ledeuil, J.-B.; Martinez, H.; Desbrières, J.; Dagron-Lartigau, C.

Macromolecules **2008**, *41*, 9736. (f) Ohshimizu, K.; Ueda, M. *Macromolecules* **2008**, *41*, 5289. (g) Ouhib, F.; Hiorns, R. C.; de Bettignies, R.; Bailly, S.; Desbrières, J.; Dagron-Lartigau, C.; *Thin Solid Films* **2008**, *516*, 7199. (h) Zhang, Y.; Tajima, K.; Hirota, K.; Hashimoto, K. *J. Am. Chem. Soc*. **2008**, *130*, 7812. (i) Van den Bergh, K.; Huybrechts, J.; Verbiest, T.; Koeckelberghs, G.*Chem. Eur. J.* **2008**, *14*, 9122. (j) Yokozawa, T.; Adachi, I.; Miyakoshi, R.; Yokoyama, A. *High Perform. Polym*. **2007**, *19*, 684. (k) Iovu, M. C.; Sheina, E. E.; Gil, R. R.; McCullough, R. D. *Macromolecules* **2005**, *38*, 8649.

(30) Javier, A. E.; Varshney, S. R.; McCullough, R. D. *Macromolecules* **2010**, *43*, 3233.

(31)Miyakoshi, R.; Yokoyama, A.; Yokozawa, T. *Chem. Lett*. **2008**, *37*, 1022. See also: Wu, S.; Bu, L.; Huang, L.; Yu, X.; Han, Y.; Geng, Y.; Wang, F. *Polymer* **2009**, *50*, 6245.

(32) (a) Lin, J. W.-P.; Dudek, L. P. *J. Polym. Sci.: Polym. Chem. Ed.* **1980**, *18*, 2869. (b) Yamamoto, T.; Sanechika, K.; Yamamoto, A. *J. Polym. Sci.: Polym. Lett. Ed*. **1980**, *18*, 9.

(33) (a) R. Miyakoshi, A. Yokoyama, and T. Yokozawa, *J. Am. Chem. Soc*., **127**, 17542 (2005). (b) See also: A. Yokoyama and T. Yokozawa, *Macromolecules* **2007**, *40*, 4093.

(34) Lanni, E. L.; McNeil, A. J. *J. Am. Chem. Soc.* **2009**, *131*, 16573.

(35) Lanni, E. L.; McNeil, A. J. *Macromolecules* **2010**, *43*, 8039.

(36) (a) Johnson, S. A.; Huff, C. W.; Mustafa, F.; Saliba, M. *J. Am. Chem. Soc.*, **2008**, *130*, 17278. (b) Stanger, A.; Shazar, A. *J. Organomet. Chem.* **1993**, *458*, 233. (c) Boese, R.; Stanger, A.; Stellberg, P.; Shazar, A. *Angew. Chem., Int. Ed.* **1993**, *32*, 1475. (d) Stanger, A.; Vollhardt, K. P. C.; *Organometallics* **1992**, *11*, 317. (e) Stanger, A.; Boese, R. *J. Organomet. Chem*. **1992**, *430*, 235. (f) Scott, F.; Krüger, C.; Betz, P. *J. Organomet. Chem*. **1990**, *387*, 113. (g) Choe, S.-B.; Klabunde, K. J.; *J. Organomet. Chem.* **1989**, *359*, 409. (h) Benn, R.; Mynott, R.; Topalović, I.; Scott, F. *Organometallics* **1989**, *8*, 2299. (i) Brauer, D. J.; Krüger, C. *Inorg. Chem.* **1977**, *16*, 884.

(37) (a) Zenkina, O. V.; Karton, A.; Freeman, D.; Shimon, L. J. W.; Martin, J. M. L.; van der Boom, M. E. *Inorg. Chem*. **2008**, *47*, 5114. (b) Ateşin, T. A.; Li, T.; Lachaize, S.; García, J. J.; Jones, W. D. *Organometallics* **2008**, *27*, 3811. (c) Reinhold, M.; McGrady, J. E.; Perutz, R. N. *J. Am. Chem. Soc.* **2004**, *126*, 5268. (d) García, J. J.; Brunkan, N. M.; Jones, W. D. *J. Am. Chem. Soc.* **2002**, *124*, 9547. (e) Braun, T.; Cronin, L.; Higgitt, C. L.; McGrady, J. E.; Perutz, R. N.; Reinhold, M. *New J. Chem*. **2001**, *25*, 19. (f) Bach, I.; Pörschke, K.-R.; Goddard, R.; Kopiske, C.; Krüger, C.; Rufińska, A.; Seevogel, K. *Organometallics* **1996**, *15*, 4959.

(38) Yoshikai, N.; Matsuda, H.; Nakamura, E. *J. Am. Chem. Soc.* **2008**, *130*, 15258.

(39) Tkachov, R.; Senkovskyy, V.; Komber, H.; Sommer, J.-U.; Kiriy, A. *J. Am. Chem. Soc*. **2010**, *132*, 7803.

(40) For an alternative mechanism, see:. Achord, B. C.; Rawlins, J. W. *Macromolecules* **2009**, *42*, 8634.

Chapter 2[1]

Evidence for Rate-Determining Reductive Elimination in Ni(dppe)Cl_2-catalyzed Chain-Growth Polymerizations.

Introduction

Organic π-conjugated polymers are the active components of numerous emerging technologies, including thin-film solar cells[1] and light-emitting diodes.[2] The predominant cross-coupling-based polymerization methods[3] used to synthesize these materials (e.g., Sonogashira,[4] Kumada,[5] Stille,[6] Suzuki,[7] Heck,[8] and Negishi[9] couplings) typically proceed through *step-growth* mechanisms, leading to broad molecular weight distributions and limited control over copolymer microstructure. In 2004, Yokozawa[10] and McCullough[11] simultaneously reported *chain-growth* syntheses of poly(3-hexylthiophene) utilizing Ni-catalyzed cross-coupling reactions. Yokozawa[12] and McCullough[13] independently proposed a novel mechanistic pathway for this polymerization, where the key step is formation of an associated Ni^0-arene π-complex after reductive elimination. Subsequent intra-complex oxidative addition is suggested to occur faster than dissociation, leading to successive monomer additions at the chain end. Although Ni^0-arene π-complexes are known,[14] this mechanistic hypothesis remains speculative.

If broadly applicable, this chain growth method has the potential to provide access to polymers with controlled molecular weights,[15] narrow molecular weight distributions, and well-defined microstructures.[16] This method has since been modified to polymerize a small set of other monomers in solution[17] and on surfaces,[18] including (2,5-bishexyloxy)phenylene,[19] 9,9-dioctylfluorene,[20] (2,3-dihexyl)thienopyrazine,[21] *N*-octylcarbazole,[20b] 3-alkoxythiophene,[22] and *N*-hexylpyrrole.[23] However, without mechanistic data, each monomer has required empirical development of unique reaction conditions to achieve chain growth. Preliminary attempts at preparing simple block copolymers have highlighted the

---

[1]Reproduced with permission from Lanni, E. L.; McNeil, A. J. "Mechanistic Studies on Ni(dppe)Cl_2-catalyzed Polymerizations: Evidence for Rate-Determining Reductive Elimination." *J. Am. Chem. Soc.* **2009**, *131*, 16573-16579. Copyright 2009 American Chemical Society.

challenges involved when each monomer requires highly specific conditions.[23,24] For example, Yokozawa reported that the order of polymerization had a significant effect on the molecular weight distribution in the synthesis of poly(2,5-bishexyloxybenzene-*b*-*N*-hexylpyrrole).[23] He suggested that the excess dppe ligand, which is required for chain-growth polymerization of the pyrrole, interfered with the phenylene polymerization. However, the mechanistic influences of the ligand and other additives that are reported to promote chain-growth have not been explored. In order to rationally expand this methodology to other monomers and copolymerizations, and to develop improved catalysts with a broader substrate scope, a detailed understanding of the reaction mechanism - particularly the role of ligand, monomer and additives - is essential.

To date, the few mechanistic studies that have been performed on these Ni-catalyzed chain growth polymerizations have focused solely on thiophenes.[12,13,25,26] Most notably, rate studies by McCullough on the Ni(dppp)Cl_2-catalyzed polymerization of thiophene found the reaction was first-order in monomer, suggesting rate-determining transmetallation.[13a] Given the narrow substrate scope, we sought to elucidate the mechanistic influences of both monomer and ligand structure. Herein we report the results of rate and spectroscopic studies for polymerization (2,5-bishexyloxy)phenylene and 3-hexylthiophene, using Ni(dppe)Cl_2 – a frequent alternative to Ni(dppp)Cl_2.[12b,19,23] We provide strong evidence for rate-determining reductive elimination and identify Ni^{II}-biaryl and Ni^{II}-bithiophene complexes as the catalyst resting states. Further, we show that an additive (LiCl) reported to be beneficial in controlled polymerizations of (2,5-bishexyloxy)phenylene[19] has no effect on the rate-determining step or on the molecular weight distribution under our reaction conditions. These results, combined with the rate data previously reported by McCullough for Ni(dppp)Cl_2-catalyzed polymerization,[13a] suggest that the ligand structure has a strong influence on the polymerization mechanism.

Results

Grignard Metathesis. Monomer **2a** was generated in situ from **1** via Grignard metathesis (GRIM) with *i*-PrMgCl (eq 1).[27] In the presence of 1 equiv LiCl, rate

studies demonstrated that the reaction is four times faster than in the absence of salt (Appendix 1). Furthermore, a peak shift is observed in the aromatic region of the product's no-D NMR spectrum depending on the presence and absence of LiCl (Figure 2.1A). These results suggest that a mixed aggregate (**2b**) is formed between LiCl and the ArMgCl.[28] The aggregation state (e.g., 1:1 mixed dimer versus 2:2 mixed tetramer) for this species was not determined, however Knochel has suggested that related aryl Grignards form 1:1 mixed dimers with LiCl in THF.[27f] Though **2a** or **2b** are the major products, several minor products (< 5%) were frequently observed in the aromatic region of the no-D ^{1}H NMR spectrum (Figure 2.1B). These products were identified by independent synthesis and co-injection into the NMR sample (Appendix 1). THF-adducts **3** and **4** were unexpected; however, a related coupling reaction between electron-rich aryl Grignards and THF has previously been reported and was suggested to proceed through a radical pathway.[29] Importantly, these by-products are not consumed during the polymerization; however, monomers **2a** and **2b** were titrated immediately prior to each kinetic run to account for their formation (Appendix 1).

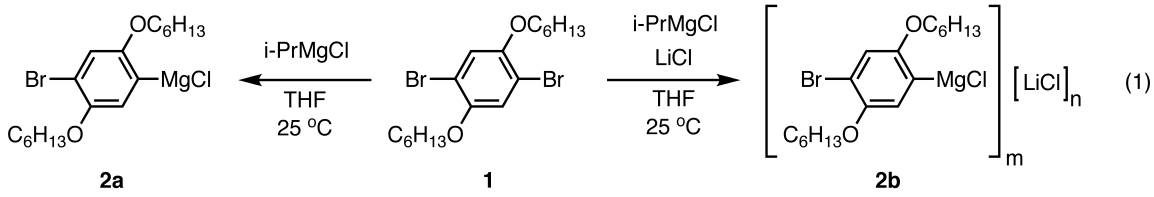

(1)

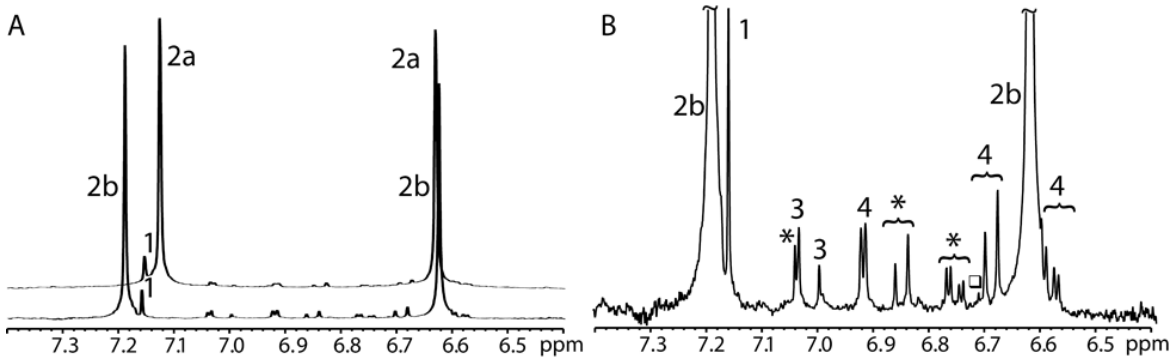

Figure 2.1 ^{1}H NMR Spectra of (A) **2a** and **2b** and (B) **2b** with by-products (*quenched monomer, ▫ 1,4-bishexyloxybenzene).

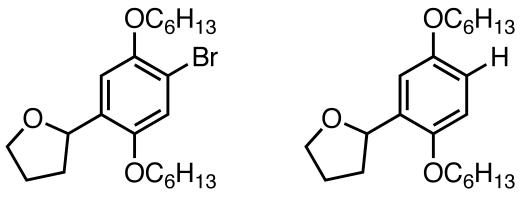

3 **4**

Monomer **6** was generated in situ from **5** via GRIM with *i*-PrMgCl (eq 2). ^{1}H NMR spectroscopic analysis revealed an 80:20 ratio of regioisomers. Unlike monomers **2a** or **2b**, no by-products were observed after the GRIM reaction.

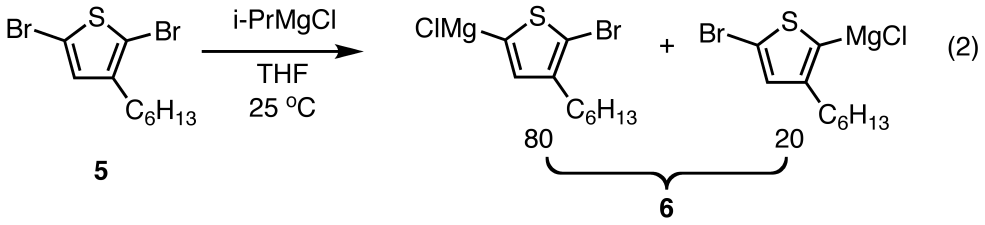

5 **6** (2)

Rate Studies. Rate studies were carried out to ascertain the rate-determining step (RDS) in the Ni(dppe)Cl_2-catalyzed chain-growth polymerization of **2a** and **6** (eqs 3-4). Polymerization of **2a** was monitored by in situ IR spectroscopy, while GC analysis of aliquots was used to monitor the polymerization of **6** relative to an internal standard. Due to the insolubility of Ni(dppe)Cl_2 we found it convenient to initiate this pre-catalyst with 5-7 equiv of monomer before starting the rate studies (see Appendix 1 for details);[30] pre-initiation also avoided any potential complications resulting from sluggish Ni(dppe)Cl_2 reduction.

For polymerization of monomer **2a** with Ni(dppe)Cl_2, a plot of the initial rate versus [monomer] showed a zero-order dependence while a plot of initial rate versus [catalyst] displayed a first-order dependence (Figure 2.2A-B). Similarly, for the polymerization of **6** by Ni(dppe)Cl_2, the reaction was zero-order in monomer and first-order in catalyst (Figure 2.3A-B). These data eliminate transmetallation as a plausible RDS because it would exhibit a first-order dependence on [monomer]. However, these rate studies are not able to distinguish between rate-limiting reductive elimination and intra-complex oxidative addition because both cases would exhibit zero- and first-order dependencies on [monomer] and [catalyst], respectively. We used NMR

spectroscopic studies to characterize the catalyst structure at the resting state to differentiate between these two steps.

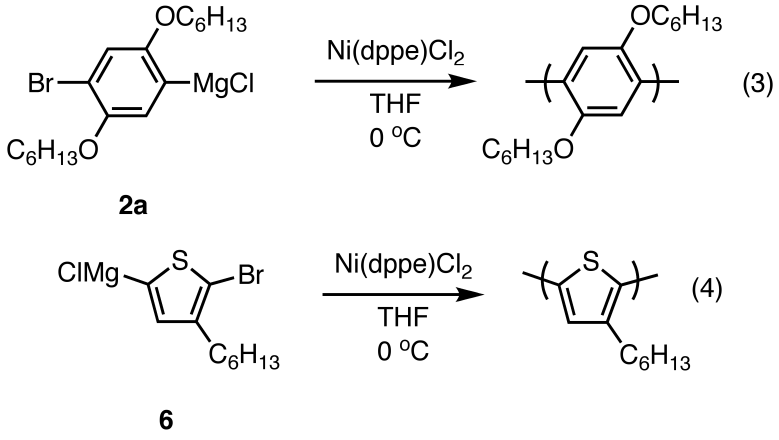

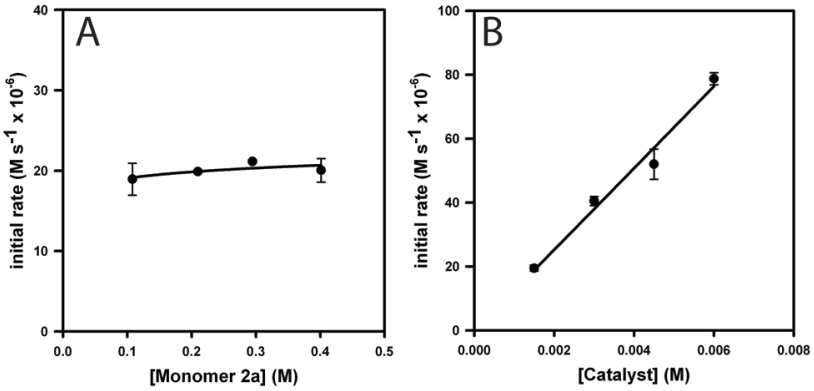

Figure 2.2 (A) Plot of initial rate versus [monomer] for the polymerization of **2a** in THF at 0 °C ([Ni(dppe)Cl_2] = 0.0015 M). The curve depicts an unweighted least-squares fit to initial rate = *a*[monomer]^n, where *a* = 22 ± 1 and *n* = 0.06 ± 0.04. (B) Plot of initial rate versus [catalyst] for the polymerization of **2a** in THF at 0 °C ([**2a**] = 0.20 M). The curve depicts an unweighted least-squares fit to initial rate = *a*[catalyst]^n, where *a* = 1.3 ± 0.1 x 10^4 and *n* = 1.01 ± 0.01.

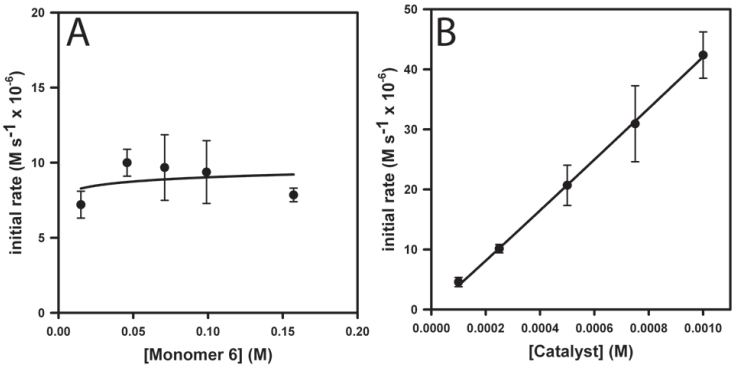

Figure 2.3 (A) Plot of initial rate versus [monomer] for the polymerization of **6** in THF at 0 ^{o}C ([Ni(dppe)Cl$_2$] = 0.00025 M). The curve depicts an unweighted least-squares fit to initial rate = a[monomer]^{n}, where a = 10 ± 3 and n = 0.05 ± 0.09. (B) Plot of initial rate versus [catalyst] for the polymerization of **6** in THF at 0 ^{o}C ([**6**] = 0.10 M). The curve depicts an unweighted least-squares fit to initial rate = a[catalyst]^{n}, where a = 4.9 ± 0.8 x 10^4 and n = 1.02 ± 0.02.

Spectroscopic Studies. ^{31}P NMR spectroscopic studies were used to identify the catalyst resting state in the chain-growth polymerization of **2a** and **6**. These studies were performed on samples with higher [catalyst] than in the polymerization to obtain sufficient signal. According to the proposed catalytic cycles, the resting states would be complexes **I** and **IV** if oxidative addition were rate-limiting, and complexes **III** and **VI** if reductive elimination were rate-limiting (Scheme 2.1).

During the polymerization of **2a**, the ^{31}P NMR spectrum revealed two proximate, broad doublets (J_{PP} = 11 Hz, Figure 2.4A). The coupling constant is consistent with a Ni^{II} species[14d] and the small Δδ is suggestive of complex **III** (with two similar phosphorus nuclei). We synthesized a model Ni^0-anthracene π-complex (**7**) for comparison (Figure 2.4B). This π-complex exhibited a relatively large coupling constant (J_{PP} = 68 Hz) when compared to the observed resting state. Based on this data we assigned the catalyst resting state as complex **III**.

During the polymerization of **6**, the ^{31}P NMR spectrum also revealed two proximate signals (J_{PP} = 24 Hz, Figure 2.4C), which we assigned as complex **VI** based on analogy to **2a**. However, the spectrum clearly shows additional, related species. Since both regioisomers of **6** are consumed under these low

[monomer]/[catalyst] ratios (see Appendix I), we tentatively attribute these peaks as resulting from regioisomeric Ni^0-bithiophene complexes. These results, combined with the first-order rate dependence on [catalyst] and zero-order rate dependence on [monomer], support reductive elimination as the rate-determining step for the chain-growth polymerization of both **2a** and **6**.

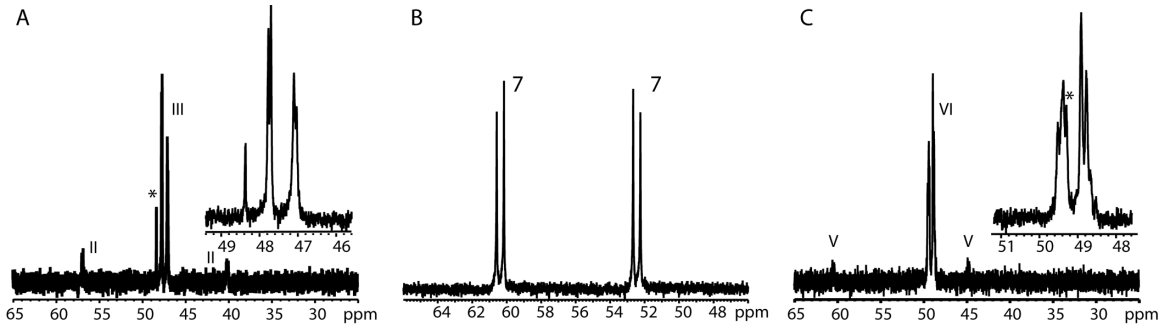

Figure 2.4 ^{31}P NMR Spectra for (A) the resting state during polymerization of **2a**, (B) Ni^0-anthracene complex **7**, and (C) the resting state during polymerization of **6**. *We tentatively assign this species as $Ni(dppe)_2X_2$.[31]

Interestingly, different Ni complexes are observed in the ^{31}P NMR spectra when polymerization of **2a** and **6** are complete. After **2a** is consumed, two doublets appear, which we hypothesized was complex **II** (J_{PP} = 25 Hz, Figure 2.5A). We synthesized a related Ni^{II} model complex (**8**), which showed a similar spectrum (J_{PP} = 15 Hz, Figure 2.5B), supporting this assignment. After **6** was consumed, the ^{31}P NMR spectrum also showed two new doublets (J_{PP} = 36 Hz, Figure 2.5C), which we hypothesized was complex **V**. The proximate, lower intensity doublets were again attributed to regioisomeric Ni^{II}-complexes since both regioisomers of **6** were consumed under these conditions. These results are consistent with the proposed catalytic cycle since the reaction should stall at complexes **II** and **V** when the monomers are consumed. Note that complexes **III** and **VI** cannot be isolated because of this facile conversion to **II** and **V** once polymerization is complete.[32]

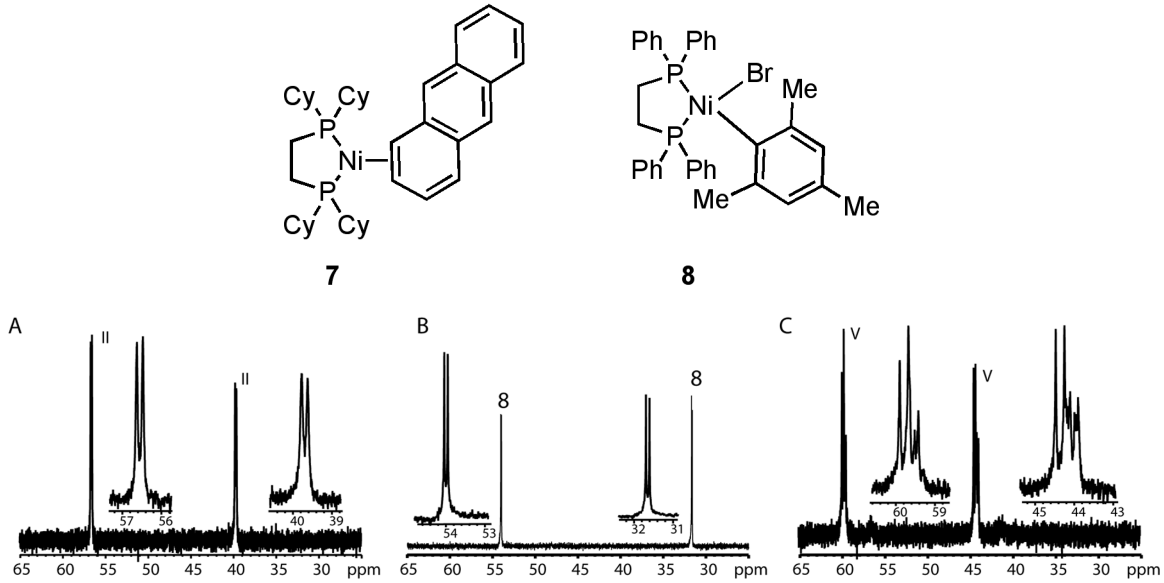

Figure 2.5 ^{31}P NMR Spectra for (A) after consumption of **2a**, (B) complex **8**, and (C) after consumption of **6**.

Scheme 2.1 Proposed Mechanism for Chain-Growth Polymerization of **2** and **6**.

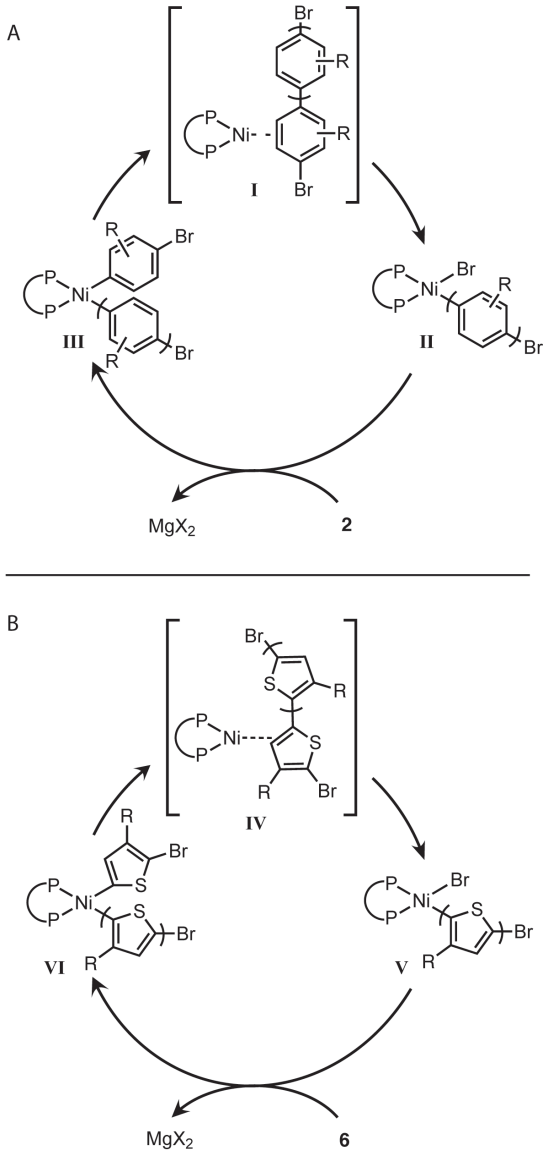

Role of LiCl. Yokozawa reported that LiCl accelerated the Ni(dppe)Cl_2-catalyzed polymerization of **2b** (eq 5) and led to a narrower molecular weight distribution (PDI).[19] We anticipated that to produce such a rate acceleration, the LiCl must not only aggregate with the monomer but also change the rate-determining step since (1) the polymerization rate was shown to be independent of [monomer] for **2a**, and (2) transmetallation with either **2a** or aggregate **2b** should result in the same Ni^{II}-biaryl complex. Instead, initial rate measurements on the polymerization of **2b** gave zero- and first-order dependencies in

[monomer] and [catalyst], respectively (Figure 2.6A-B). Moreover, the absolute initial rates were nearly identical to the rates without LiCl (c.f., Figure 2.2A-B), indicating that LiCl has no effect on the rate. Initial rates were also measured for polymerizations with *excess* LiCl to determine if a rate acceleration could be caused by non-aggregated salt. As evident in Figure 2.7A, the rate remains unchanged with greater than 1 equiv LiCl. Further evidence came from temperature-dependent rate data, which provided nearly identical activation parameters (Figure 2.7B). In the presence of LiCl the activation enthalpy and entropy were 18.4 ± 0.7 kcal/mol and 0 ± 3 cal/mol·K, respectively, while in the absence of LiCl the activation enthalpy and entropy were 18 ± 1 kcal/mol and -3 ± 5 cal/mol·K. Last, the ^{31}P NMR spectroscopic studies on the catalyst resting state showed two proximate doublets (J_{PP} = 9 Hz, Figure 2.8A), consistent with complex **III** and rate-limiting reductive elimination. Complex **II** is observed once conversion of monomer (**2b**) is complete (Figure 2.8B). Altogether these data imply that there is no substantive effect of LiCl on the absolute rate and the rate-determining step.

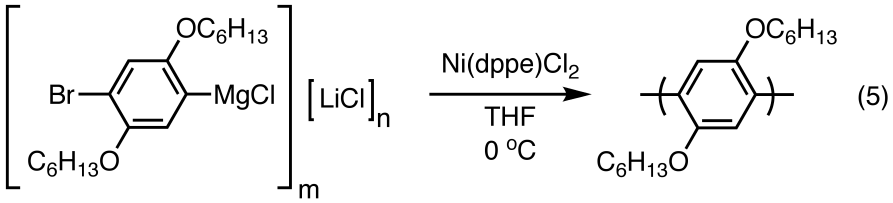

2b (5)

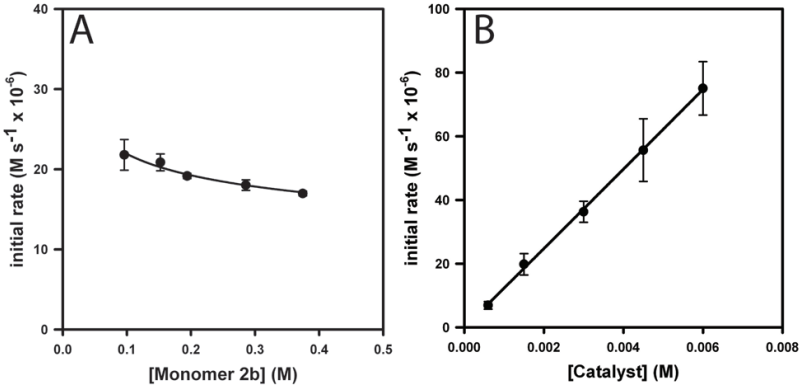

Figure 2.6 (A) Plot of initial rate versus [monomer] for the polymerization of **2b** in THF at 0 °C ([Ni(dppe)Cl_2] = 0.0015 M). The curve depicts an unweighted least-squares fit to initial rate = *a*[monomer]^n, where *a* = 14.2 ± 0.5 and *n* = -0.19 ± 0.02. (B) Plot of initial rate versus [catalyst] for the polymerization of **2b** in THF at 0 °C ([**2b**] = 0.20 M). The curve depicts an unweighted least-squares fit to initial rate = *a*[catalyst]^n, where *a* = 1.3 ± 0.2 x 10^4 and *n* = 1.01 ± 0.03.

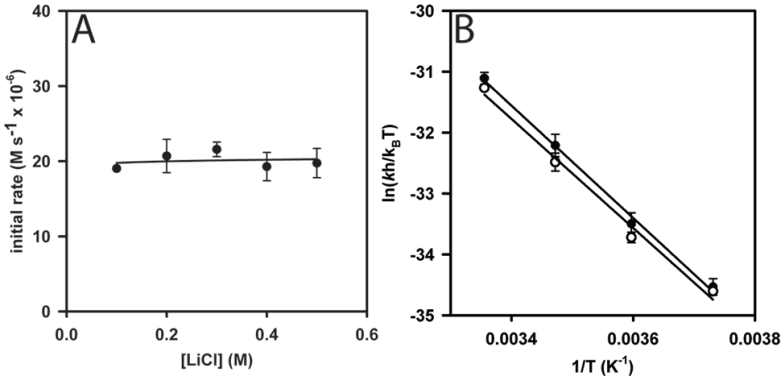

Figure 2.7 (A) Plot of initial rates versus [LiCl] for the Ni(dppe)Cl_2-catalyzed polymerization of **2b** in THF at 0 °C ([**2b**] = 0.20 M, [Ni(dppe)Cl_2] = 0.0015 M). The curve depicts an unweighted least-squares fit to initial rate = *a*[LiCl]^n, where *a* = 20 ± 1 and *n* = 0.02 ± 0.05. (B) Plot of ln(*k*h/k_bT) versus 1/T for the polymerization of **2a** and **2b** in THF ([**2a**] = [**2b**] = 0.20 M, [Ni(dppe)Cl_2] = 0.001 M). The curves depict unweighted least squares fits to ln(*k*h/k_bT) = -($\Delta H^{‡}$/RT) + $\Delta S^{‡}$/R, providing a $\Delta H^{‡}$ of 18 ± 1 kcal/mol and a $\Delta S^{‡}$ of -3 ± 5 cal·mol^{-1}·K^{-1} for **2a** and a $\Delta H^{‡}$ of 18.4 ± 0.7 kcal/mol and a $\Delta S^{‡}$ of 0 ± 3 cal·mol^{-1}·K^{-1} for **2b**.

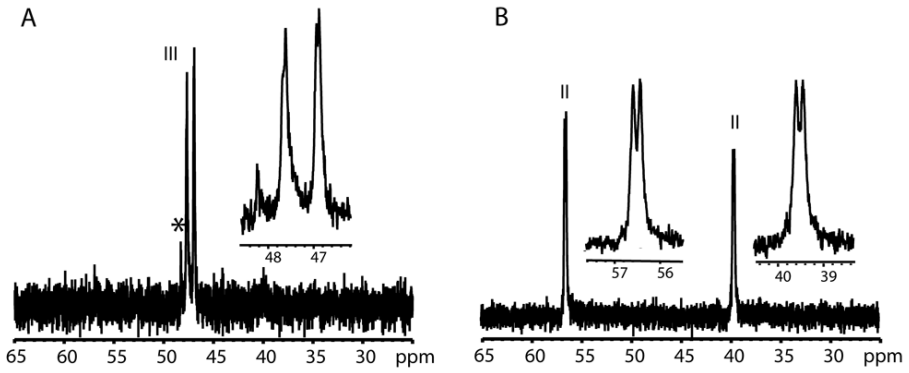

Figure 2.8 ^{31}P NMR Spectra for (A) the resting state during polymerization of **2b**, (B) after consumption of **2b**. *We tentatively assign this species as $Ni(dppe)_2X_2$.[31]

Comparing plots of the number average molecular weight and PDI versus conversion for the polymerization of **2a** and **2b** revealed that, in contrast to the report by Yokozawa,[19] LiCl also had no effect on the PDI (Figure 2.9A-B). In this case, however, a subtle difference between the two reports may be playing an important role. In chain-growth polymerizations, the relative rate of initiation versus propagation will influence the molecular weight distribution.[33] We avoided this relative rate issue by pre-initiating the $Ni(dppe)Cl_2$ with 5-7 equiv of monomer before beginning the rate studies. In contrast, Yokozawa initiated his catalyst in situ, where the influence of LiCl on the initiation rate may be significant. This hypothesis is supported by the identification of a monomer-LiCl mixed aggregate (**2b**) which would be involved in initiation.

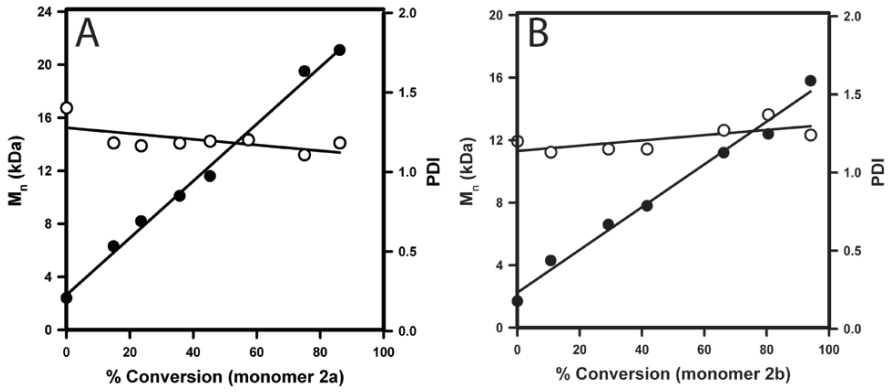

Figure 2.9 M_n and PDI versus conversion for the Ni(dppe)Cl_2-catalyzed polymerization of (A) **2a** and (B) **2b** in THF at 0 ^oC ([**2a**] = 0.10 M; [**2b**] = 0.20 M; [Ni(dppe)Cl_2] = 0.0015 M).

Discussion

Despite the general utility of Ni-catalyzed cross-coupling reactions[34] in both small molecule[35] and polymer syntheses,[3,5,9,36] the operative mechanisms are still highly debated.[37] Moreover, the extrapolation of small molecule-based mechanistic studies to the polymerization is not straightforward. Yokozawa[12] and McCullough[13] independently proposed a new mechanistic pathway for this polymerization where the key step is formation of an associated Ni^0-thiophene π-complex (e.g., complexes **I** and **IV**). Subsequent intra-complex oxidative addition leads to chain growth. Although Ni^0-arene π-complexes have precedent,[14] their role in the polymerization mechanism remains uncertain. Both the potential of this method to provide access to novel well-defined polymers as well as its current limitations motivated us to explore the mechanism in more detail, particularly the influence of the ligand, monomer and additives, with the aim of generating improved catalysts.

Mechanism. Through a combination of rate and spectroscopic studies, we found evidence supporting a rate-determining *reductive elimination* for the polymerization of monomers **2a**, **2b** and **6** using Ni(dppe)Cl_2. Interestingly, the monomer structure (arene versus thiophene) had no influence on the rate-determining step of the catalytic cycle. Notably, McCullough found evidence for a rate-determining *transmetallation* for polymerization of **6** using a different catalyst

– Ni(dppp)Cl_2.[13a] Combined, these results point to a significant mechanistic influence of the ligand on the polymerization, and suggest that alternative ligand structures may lead to catalysts with improved reactivities.[38,39] Finally, though LiCl formed a mixed aggregate with the arene monomer, our rate and spectroscopic studies showed that this additive has no effect on either the polymerization rate or mechanism. Nevertheless, the role of LiCl on the initiation step may be significant and future studies are needed to address this issue.

Chain-Growth via Ni^0 π-complexes? The structure[40] and reactivity[41] of Ni^0-*olefin* π-complexes has been widely documented. For example, van der Boom recently demonstrated that alkene coordination to Ni^0 is kinetically preferred over the oxidative addition of an aryl-I and aryl-Br bond.[42] In addition, they only observed products resulting from intra-complex oxidation addition after alkene coordination. Far fewer studies have been reported for Ni^0-arene π-complexes. Moreover, evidence of an intermediate Ni^0 π-complex in the chain-growth polymerization has only been circumstantial: (1) Kiriy indirectly probed the existence of a π-complex by examining whether the chain-growth mechanism depends on monomer size.[25] They observed a decrease in chain-growth behavior for terthiophene compared to thiophene, suggesting that detrimental chain-transfer and termination processes become more prevalent with larger distances between the C-C bond forming site and the reactive end-group. (2) McCullough observed an unexpected double substitution reaction to generate thiophene trimers when using a 2:1 ratio of monomer to catalyst.[11] Such preferential double substitutions have also been observed in Pd-catalyzed cross-coupling reactions of small molecules[43] and polymers.[44] Interestingly, Kumada observed a similar preferential Ni-catalyzed double alkylation in 1976 when using bifunctional arenes (e.g., 1,4-dichlorobenzene) despite having a 2-fold excess of the arene reagent compared to the alkyl Grignard.[34c] He suggested that such substrates undergo a "mechanistically different" reaction but provided no further explanation.

Our observation of a rate-determining reductive elimination and McCullough's observation of a rate-determining transmetallation indicate that the Ni^0 π-

complex, if formed, is only a fleeting, post-rate-limiting intermediate. Moreover, our extensive spectroscopic studies identified the catalyst species both during and after polymerization and neither was consistent with a Ni^0 π-complex. This result was further supported by our synthesis and characterization of a model Ni^0 π-complex with anthracene. As a result, further studies are necessary to probe both the existence and catalytic relevance of Ni^0 π-complexes in the polymerization.

Conclusion

Rate and spectroscopic studies support a rate-limiting reductive elimination for the Ni(dppe)Cl_2-catalyzed syntheses of poly(*p*-(2,5-bishexyloxy)phenylene) and poly(3-hexylthiophene). These results, combined with the data from McCullough[13a] using Ni(dppp)Cl_2, suggest that the ligand has a strong influence over the rate-determining step. Ni^{II}-biaryl and Ni^{II}-bithiophene complexes, though unstable to isolation, were identified as the active catalyst resting states. These studies also revealed that the role of LiCl is complex and may be unnecessary under certain reaction conditions. By addressing the mechanistic influences of monomer and catalyst structure as well as the role of additives, these results provide a strong foundation for future studies aimed at preparing novel polymers and developing improved catalysts. In addition, we are now in a position to explore the more complex, yet intriguing copolymerization mechanisms.

References Cited

(1) Dennler, G.; Scharber, M. C.; Brabec, C. J. *Adv. Mater.* **2009**, *21*, 1323-1338. Hoppe, H.; Sariciftci, N. S. In *Photoresponsive Polymers II*; Marder, S. R., Lee, K.-S., Eds.; Advances in Polymer Science; Springer-Verlag: Berlin, 2008; Vol. 214, pp 1-86. Thompson, B. C.; Fréchet, J. M. J. *Angew. Chem. Int. Ed.* **2008**, *47*, 58-77. Coakley, K. M.; McGehee, M. D. *Chem. Mater.* **2004**, *16*, 4533-4542.

(2) Grimsdale, A. C.; Chan, K. L.; Martin, R. E.; Jokisz, P. G.; Holmes, A. B. *Chem. Rev.* **2009**, *109*, 897-1091. Perepichka, I. F.; Perepichka, D. F.; Meng, H.; Wudl, F. *Adv. Mater.* **2005**, *17*, 2281-2305. Kulkarni, A. P.; Tonzola, C. J.; Babel, A.; Jenekhe, S. A. *Chem. Mater.* **2004**, *16*, 4556-4573.

(3) Cheng, Y.-J.; Luh, T.-Y. *J. Organomet. Chem.* **2004**, *689*, 4137-4148. Babudri, F.; Farinola, G. M.; Naso, F. *J. Mater. Chem.* **2004**, *14*, 11-34. Yamamoto, T. *J. Organomet. Chem.* **2002**, *653*, 195-199.

(4) Sanechika, K.; Yamamoto, T.; Yamamoto, A. *Bull. Chem. Soc. Jpn.* **1984**, *57*, 752-755. For a recent review, see: Bunz, U. H. F. *Macromol. Rapid Commun.* **2009**, *30*, 772-805.

(5) (a) Yamamoto, T.; Hayashi, Y.; Yamamoto, A. *Bull. Chem. Soc. Jpn.* **1978**, *51*, 2091-2097. (b) For a recent review, see: Miyakoshi, R.; Yokoyama, A.; Yokozawa, T. *J. Poly. Sci., Part A: Polym. Chem.* **2008**, 46, 753-765.

(6) Bao, Z.; Chan, W.; Yu, L. *Chem. Mater.* **1993**, *5*, 2-3. See also: Bao, Z.; Chan, W. K.; Yu, L. *J. Am. Chem. Soc.* **1995**, *117*, 12426-12435.

(7) Rehahn, M.; Schlüter, A. D.; Wegner, G.; Feast, W. J. *Polymer* **1989**, *30*, 1060-1062. For a recent review, see: Sakamoto, J.; Rehahn, M.; Wegner, G.; Schlüter, A. D. *Macromol. Rapid Commun.* **2009**, *30*, 653-687.

(8) Heitz, W.; Brügging, W.; Freund, L.; Gailberger, M.; Greiner, A.; Jung, H.; Kampschulte, U.; Nießner, N.; Osan, F.; Schmidt, H.-W.; Wicker, M. *Makromol. Chem.* **1988**, *189*, 119-127. For a recent review, see: Lee, Y.; Liang, Y.; Yu, L. *Synlett* **2006**, *18*, 2879-2893.

(9) Yamamoto, T.; Osakada, K.; Wakabayashi, T.; Yamamoto, A. *Makromol. Chem., Rapid Commun.* **1985**, *6*, 671-674. See also: Chen, T.-A.; Wu, X.; Rieke, R. D. *J. Am. Chem. Soc.* **1995**, *117*, 233-244.

(10) Yokoyama, A.; Miyakoshi, R.; Yokozawa, T. *Macromolecules* **2004**, 37, 1169-1171. Miyakoshi, R.; Yokoyama, A.; Yokozawa, T. *Macromol. Rapid Commun.* **2004**, *25*, 1663-1666.

(11) Sheina, E. E.; Liu, J.; Iovu, M. C.; Laird, D. W.; McCullough, R. D. *Macromolecules* **2004**, *37*, 3526-3528.

(12) (a) Miyakoshi, R.; Yokoyama, A.; Yokozawa, T. *J. Am. Chem. Soc.* **2005**, *127*, 17542-17547. (b) Adachi, I.; Miyakoshi, R.; Yokoyama, A.; Yokozawa, T. *Macromolecules* **2006**, *39*, 7793-7795. (c) Yokoyama, A.; Yokozawa, T. *Macromolecules* **2007**, *40*, 4093-4101. (d) See also: ref 5b.

(13) (a) Iovu, M. C.; Sheina, E. E.; Gil, R. R.; McCullough, R. D. *Macromolecules* **2005**, *38*, 8649-8656. (b) Osaka, I.; McCullough, R. D. *Acc. Chem. Res.* **2008**, *41*, 1202-1214.

(14) (a) Yoshikai, N.; Matsuda, H.; Nakamura, E. *J. Am. Chem. Soc.* **2008**, *130*, 15258-15259. (b) Johnson, S. A.; Huff, C. W.; Mustafa, F.; Saliba, M. *J. Am. Chem. Soc.* **2008**, *130*, 17278-17280. (c) Ateşin, T. A.; Li, T.; Lachaize, S.; García, J. J.; Jones, W. D. *Organometallics* **2008**, *27*, 3811-3817. (d) García, J. J.; Brunkan, N. M.; Jones, W. D. *J. Am. Chem. Soc.* **2002**, *124*, 9547-9555. (e) Braun, T.; Cronin, L.; Higgitt, C. L. McGrady, J. E.; Perutz, R. N.; Reinhold, M. *New J. Chem.* **2001**, *25*, 19-21. (f) Bach, I.; Pörschke, K.-R.; Goddard, R.; Kopiske, C.; Krüger, C.; Rufińska, A.; Seevogel, K. *Organometallics* **1996**, *15*, 4959-4966. (g) Stanger, A.; Shazar, A. *J. Organomet. Chem.* **1993**, *458*, 233-236. (h) Boese, R.; Stanger, A.; Stellberg, P.; Shazar, A. *Angew. Chem., Int. Ed.* **1993**, *32*, 1475-1477. (i) Stanger, A.; Vollhardt, K. P. C. *Organometallics* **1992**, *11*, 317-320. (j) Stanger, A.; Boese, R. *J. Organomet. Chem.* **1992**, *430*, 235-243. (k) Scott, F.; Krüger, C.; Betz, P. *J. Organomet. Chem.* **1990**, *387*, 113-121. (l) Choe, S.-B.; Klabunde, K. J. *J. Organomet. Chem.* **1989**, *359*, 409-418. (m) Benn, R.; Mynott, R.; Topalović, I.; Scott, F. *Organometallics* **1989**, *8*, 2299-2305. (n) Brezinski, M. M.; Klabunde, K. J. *Organometallics* **1983**, *2*, 1116-1123. (o) Brauer, D. J.; Krüger, C. *Inorg. Chem.* **1977**, *16*, 884-891. (p) Jonas, K. *J. Organomet. Chem.* **1974**, *78*, 273-279.

(15) Hiorns, R. C.; Bettignies, R.; Leroy, J.; Bailly, S.; Firon, M.; Sentein, C.; Khoukh, A.; Preud'homme, H.; Dagron-Lartigau, C. *Adv. Funct. Mater.* **2006**, *16*, 2263-2273.

(16) For syntheses of end-functionalized polymers via this method, see: (a) Urien, M.; Erothu, H.; Cloutet, E.; Hiorns, R. C.; Vignau, L.; Cramail, H. *Macromolecules* **2008**, *41*, 7033-7040. (b) Hiorns, R. C.; Khoukh, A.; Gourdet, B.; Dagron-Lartigau, C. *Polym. Int.* **2006**, *55*, 608-620. (c) Jeffries-EL, M.; Sauvé, G.; McCullough, R. D. *Macromolecules* **2005**, *38*, 10346-10352. (d) Iovu, M. C.; Jeffries-EL, M.; Sheina, E. E.; Cooper, J. R.; McCullough, R. D. *Polymer* **2005**, *46*, 8582-8586. (e) Jeffries-EL, M.; Sauvé, G.; McCullough, R. D. *Adv. Mater.* **2004**, *16*, 1017-1019. For examples of controlled microstructure polymers via this method, see: (a) Wu, P.-T.; Ren, G.; Li, C.; Mezzenga, R.; Jenekhe, S. A. *Macromolecules* **2009**, *42*, 2317-2320. (b) Ouhib, F; Khoukh, A.; Ledeuil, J.-B.; Martinez, H.; Desbrières, J.; Dagron-Lartigau, C. *Macromolecules* **2008**, *41*, 9736-9743. (c) Ohshimizu, K.; Ueda, M. *Macromolecules* **2008**, *41*, 5289–5294. (d) Zhang, Y.; Tajima, K.; Hirota, K.; Hashimoto, K. *J. Am. Chem. Soc.* **2008**, *130*, 7812-7813.

(17) For polymerization of thiophene derivatives via this method, see: (a) Benanti, T. L.; Kalaydjian, A. Venkataraman, D. *Macromolecules* **2008**, *41*, 8312–8315. (b) Li, Y.; Xue, L.; Xia, H.; Xu, B.; Wen S.; Tian W. *J. Poly. Sci., Part A: Polym. Chem.* **2008**, 46, 3970-3984. (c) Ouhib, F.; Dkhissi, A.; Iratcabal, P.; Hiorns R. C.; Khoukh, A .; Desbrières, J.; Pouchan, C.; Dagron-Lartigau, C. *J. Poly. Sci., Part A: Polym. Chem.* **2008**, 46, 7505-7516. (d) Vallat, P.; Lamps, J.-P.; Schosseler, F.; Rawiso, M.; Catala, J.-M. *Macromolecules* **2007**, *40*, 2600–2602.

(18) (a) Sontag, S. K.; Marshall, N.; Locklin, J. *Chem. Commun.* **2009**, 3354-3356. (b) Khanduyeva, N.; Senkovskyy, V.; Beryozkina, T.; Horecha, M.; Stamm, M.; Uhrich, C.; Riede, M.; Leo, K.; Kiriy, A. *J. Am. Chem. Soc.* **2009**, *131*, 153-161. (c) Beryozkina, T.; Boyko, K.; Khanduyeva, N.; Senkovskyy, V.; Horecha, M.; Oertel, U.; Simon, F.; Stamm, M.; Kiriy, A. *Angew. Chem. Int. Ed.* **2009**, *48*, 2695-2698. (d) Khanduyeva, N.; Senkovskyy, V.; Beryozkina, T.; Bocharova, V.; Simon, F.; Nitschke, M.; Stamm, M.; Grötzschel, R.; Kiriy, A. *Macromolecules* **2008**, *41*, 7383-7389. (e) Senkovskyy, V.; Khanduyeva, N.; Komber, H.; Oertel, U.; Stamm, M.; Kuckling, D.; Kiriy, A. *J. Am. Chem. Soc.* **2007**, *129*, 6626-6632.

(19) Miyakoshi, R.; Shimono, K.; Yokoyama, A.; Yokozawa, T. *J. Am. Chem. Soc.* **2006**, *128*, 16012-16013.

(20) (a) Huang, L.; Wu, S.; Qu, Y.; Geng, Y.; Wang, F. *Macromolecules* **2008**, *41*, 8944-8947. (b) Stefan, M. C.; Javier, A. E.; Osaka, I.; McCullough, R. D. *Macromolecules* **2009**, *42*, 30-32.

(21) Wen, L.; Duck, B. C.; Dastoor, P. C.; Rasmussen, S. C. *Macromolecules* **2008**, *41*, 4576-4578.

(22) (a) Sheina, E. E.; Khersonsky, S. M.; Jones, E. G.; McCullough, R. D. *Chem. Mater.* **2005**, *17*, 3317-3319. (b) See also: ref 12b.

(23) Yokoyama, A.; Kato, A.; Miyakoshi, R.; Yokozawa, T. *Macromolecules* **2008**, *41*, 7271-7273.

(24) Miyakoshi, R.; Yokoyama, A.; Yokozawa, T. *Chem. Lett.* **2008**, *37*, 1022-1023.

(25) Beryozkina, T.; Senkovskyy, V.; Kaul, E.; Kiriy, A. *Macromolecules* **2008**, *41*, 7817-7823.

(26) Mao, Y.; Wang, Y.; Lucht, B. L. *J. Poly. Sci., Part A: Polym. Chem.* **2004**, 42, 5538-5547.

(27) (a) Shi, L.; Chu, Y.; Knochel, P.; Mayr, H. *Org. Lett.* **2009**, *11*, 3502-3505. (b) Shi, L.; Chu, Y.; Knochel, P.; Mayr, H. *J. Org. Chem.* **2009**, *74*, 2760-2764. (c) Shi, L.; Chu, Y.; Knochel, P.; Mayr, H. *Angew. Chem. Int. Ed.* **2008**, *47*, 202-204. (d) Krasovskiy, A.; Straub, B. F.; Knochel, P. *Angew. Chem. Int. Ed.* **2006**, *45*, 159-162. (e) Hauk, D.; Lang, S.; Murso, A. *Org. Process Res. Dev.* **2006**, *10*, 733-738. (f) Krasovskiy, A.; Knochel, P. *Angew. Chem. Int. Ed.* **2004**, *43*, 3333-3336. (g) Knochel, P.; Dohle, W.; Gommermann, N.; Kneisel, F. F.; Kopp, F.; Korn, T.;

Sapountzis, I.; Vu, V. A. *Angew. Chem. Int. Ed*. **2003**, *42*, 4302-4320. (h) Boymond, L.; Rottländer, M.; Cahiez, G.; Knochel, P. *Angew. Chem. Int. Ed.* **1998**, *37*, 1701-1703.

(28) For an X-ray crystal structure of a related mixed aggregate, see: Buttrus, N. H.; Eaborn, C.; El-Kheli, M. N. A.; Hitchcock, P. B.; Smith, J. D.; Sullivan, A. C.; Tavakkoli, K. *Dalton Trans.* **1988**, 381-391.

(29) Inoue, A.; Shinokubo, H.; Oshima, K. *Synlett* **1999**, 1582-1584.

(30) Note that we obtained slower polymerization rates when using commercial batches of Ni(dppe)Cl_2 that contained impurities observable by ^{31}P NMR spectroscopy.

(31) Jarrett, P. S.; Sadler, P. J. *Inorg. Chem.* **1991**, *30*, 2098-2104.

(32) Ni^{II} biaryl complexes with chelating ligands have previously been reported to be unstable to isolation due to facile reductive elimination. For example, see: Coronas, J. M.; Muller, G.; Rocamora, M.; Miravitlles, C.; Solans, X. *Dalton Trans.* **1985**, 2333-2341.

(33) Odian, G. Ionic Chain Polymerization. *Principles of Polymerization*, 4th ed.; Wiley: Hoboken, NJ, 2004; pp 422-436.

(34) (a) Tamao, K.; Sumitani, K.; Kumada, M. *J. Am. Chem. Soc.* **1972**, *94*, 4374-4376. (b) Corriu, R. J. P.; Masse, J. P. *Chem. Commun*. **1972**, 144. (c) Tamao, K.; Sumitani, K.; Kiso, Y.; Zembayashi, M.; Fujioka, A.; Kodama, S.; Nakajima, I.; Minato, A.; Kumada, M. *Bull. Chem. Soc. Jpn.* **1976**, *49*, 1958-1969. (d) Tamao, K.; Kodama, S.; Nakajima, I.; Kumada, M.; Minato, A.; Suzuki, K. *Tetrahedron* **1982**, *38*, 3347-3354.

(35) (a) Takahashi, T.; Kanno, K. Nickel-catalyzed Cross-coupling Reactions. In *Modern Organonickel Chemistry*; Tamaur, Y., Ed.; Wiley-VCH: Weinheim, 2005; pp 41-55. (b) Phapale, V. B.; Cárdenas, D. J. *Chem. Soc. Rev.* **2009**, *38*, 1598-1607. (c) Hassan, J.; Sévignon, M.; Gozzi, C.; Schulz, E.; Lemaire, M. *Chem. Rev.* **2002**, *102*, 1359-1469.

(36) (a) Yamamoto, T.; Koizumi, T. *Polymer* **2007**, *48*, 5449-5472. (b) Yamamoto, T. *Synlett* **2003**, 425-450.

(37) (a) Jin, L.; Zhang, H.; Li, P.; Sowa, J. R., Jr.; Lei, A. *J. Am. Chem. Soc.* **2009**, *131*, 9892-9893. (b) Amatore, C.; Jutand, A. *Organometallics* **1988**, *7*, 2203-2214. (c) Colon, I.; Kelsey, D. R. *J. Org. Chem.* **1986**, *51*, 2627-2637. (d) Semmelhack, M. F.; Helquist, P.; Jones, L. D.; Keller, L.; Mendelson, L.; Ryono, L. S.; Smith, J. G.; Stauffer, R. D. *J. Am. Chem. Soc.* **1981**, *103*, 6460-6471. (e) Smith, G.; Kochi, J. K. *J. Organomet. Chem.* **1980**, *198*, 199-214. (f) Tsou, T. T.; Kochi, J. K. *J. Am. Chem. Soc.* **1979**, *101*, 6319-6332. (g) Tsou, T. T.; Kochi, J. K. *J. Am. Chem. Soc.* **1979**, *101*, 7547-7560. (h) Tsou, T. T.; Kochi, J. K. *J. Am. Chem. Soc.* **1978**, *100*, 1634-1635. (i) Morrell, D. G.; Kochi, J. K. *J. Am. Chem. Soc.* **1975**, *97*, 7262-7270.

(38) For an example of the influence of ligand (dppe versus dppp) on reductive elimination in Ni^{II} dimethyl complexes, see: Kohara, T.; Yamamoto, T.; Yamamoto, A. *J. Organomet. Chem.* **1980**, *192*, 265-274.

(39) For examples of alternative initiators, see: (a) Doubina, N.; Ho, A.; Jen, A. K.-Y. Luscombe, C. K. *Macromolecules* **2009**, DOI: 10.1021/ma901410k. (b) Bronstein, H. A.; Luscombe, C. K. *J. Am. Chem. Soc.* **2009**, *131*, 12894-12895. (c) See also: ref 18e.

(40) (a) Massera, C.; Frenking, G. *Organometallics* **2003**, *22*, 2758-2765. (b) Tolman, C. A.; Seidel, W. C.; Gosser, L. W. *Organometallics* **1983**, *2*, 1391-1396. (c) Tolman, C. A. *J. Am. Chem. Soc.* **1974**, *96*, 2780-2789. (d) Tolman, C. A.; Seidel, W. C. *J. Am. Chem. Soc.* **1974**, *96*,

2774-2780. (e) Brauer, D. J.; Krüger, C. *J. Organomet. Chem.* **1974**, *77*, 423-438. (f) Tolman, C. A.; Seidel, W. C.; Gerlach, D. H. *J. Am. Chem. Soc.* **1972**, *94*, 2669-2676. (g) Cheng, P.-T.; Cook, C. D.; Nyburg, S. C.; Wan, K. Y. *Inorg. Chem.* **1971**, *10*, 2210-2213. (h) Ittel, S. D. *Inorg. Chem.* **1977**, *16*, 2589-2597.

(41) For leading references, see: Johnson, J. B.; Rovis, T. *Angew. Chem. Int. Ed.* **2008**, *47*, 840-871.

(42) Zenkina, O. V.; Karton, A.; Freeman, D.; Shimon, L. J. W.; Martin, J. M. L.; van der Boom, M. E. *Inorg. Chem.* **2008**, *47*, 5114-5121.

(43) (a) Weber, S. K.; Galbrecht, F.; Scherf, U. *Org. Lett.* **2006**, *8*, 4039-4041. (b) Sinclair, D. J.; Sherburn, M. S. *J. Org. Chem.* **2005**, *70*, 3730-3733. (c) Dong, C.-G.; Hu, Q.-S. *J. Am. Chem. Soc.* **2005**, *127*, 10006-10007.

(44) Yokoyama, A.; Suzuki, H.; Kubota, Y.; Ohuchi, K.; Higashimura, H.; Yokozawa, T. *J. Am. Chem. Soc.* **2007**, *129*, 7236-7237.

Chapter 3[1]

Evidence for Ligand-Dependent Mechanistic Changes in Nickel-Catalyzed Chain-Growth Polymerizations

Introduction

Organic π-conjugated polymers are promising materials for thin-film solar cells,[1] light-emitting diodes,[2] and transistors[3] because they exhibit tunable optical and electrical properties and can be solution-processed onto large, flexible substrates. However, these materials have several limitations that prevent their widespread application. For example, homopolymers are the most synthetically accessible but often lack one or more properties that are necessary for device operation. To advance the field, synthetic methods that provide access to new polymers are needed. In 2004, Yokozawa[4] and McCullough[5] reported the first chain-growth synthesis of poly(3-hexylthiophene). This initial result garnered much interest[6,7] because living, chain-growth methods can be used to synthesize polymers with sequence-control[8] and end-functionalization.[9] However, efforts toward expanding the scope and utility of this method have been hindered by the highly monomer-specific reaction conditions necessary to achieve chain-growth. As a result, even simple block copolymers have been difficult to synthesize.[10] To develop a general synthetic method, a mechanistic understanding of the role of monomer, ligand, and additives on the chain-growth pathway is needed.

Yokozawa[4,11,12] and McCullough[5,13,14] independently proposed a new mechanism to account for the unexpected chain-growth behavior wherein the key difference from conventional cross-coupling mechanisms is formation of a π-complex[15,16] between the polymer chain and Ni^0 following reductive elimination.[17] Subsequent intramolecular oxidative addition leads to chain-growth. Indirect evidence supporting this mechanism has been provided.[18] Most significantly, MALDI-TOF MS data on polymer samples revealed end-groups consistent with the structure of the initiating and propagating species, which is characteristic of

---

[1]Reproduced with permission from Lanni, E. L.; McNeil, A. J. "Evidence for Ligand-Dependent Mechanistic Changes in Nickel-Catalyzed Chain-Growth Polymerizations." *Macromolecules* **2010**, *43*, 8039-8044. Copyright 2010 American Chemical Society.

chain-growth polymerizations.[11] In addition, aryl and thienyl halides that can undergo competitive oxidative addition with Ni^0 were shown to be unreactive during polymerization, consistent with Ni^0-polymer π-complex formation and intramolecular oxidative addition.[12b,18b] Nevertheless, the sensitivity of this synthetic method to changes in monomer, ligand, and additives suggests that the chain-growth mechanism is competing with other reaction pathways like chain-transfer and termination. As a result, a detailed mechanistic understanding of each reaction pathway will be necessary to guide the rational development of an improved synthetic method.

In 2009, we reported the influence of monomer structure and additives on the mechanism of Ni(dppe)Cl_2-catalyzed syntheses of poly(*p*-(2,5-bishexyloxy)phenylene) and poly(3-hexylthiophene).[19] Rate and spectroscopic studies were consistent with rate-limiting reductive elimination for both monomers. Further studies showed that although LiCl forms a mixed aggregate with the arene monomer, the salt did not affect the propagation rate or mechanism. Because McCullough reported that an alternative catalyst (Ni(dppp)Cl_2) lead to different rate behavior,[10a,13] we anticipated that the ligand might be a key mechanistic determinant. In this report, we provide detailed rate and spectroscopic evidence for a ligand-dependent change in rate-determining step. Specifically, we demonstrate that Ni(dppp)Cl_2-catalyzed syntheses of both poly(*p*-(2,5-bishexyloxy)phenylene) and poly(3-hexylthiophene) proceed through a rate-determining transmetallation. Moreover, we show that LiCl influences the reaction order in monomer and, consequently, the polymerization rate. Given the important mechanistic influence of ligand, these results suggest that modifying the ligand structure may lead to new catalysts that are effective for a broader range of monomers.

Results and Discussion

Rate Studies. Monomers **2a** and **4** were generated in situ from **1** and **3** via Grignard metathesis (GRIM) with *i*-PrMgCl (eqs 1-2).[20] Although **4** is an approximately 80:20 mixture of regioisomers, the minor regioisomer is not significantly consumed during polymerization (see Figure S18 in Appendix 2). To

generate a soluble catalyst species, the Ni(dppp)Cl_2 was pre-initiated with 5-7 equiv of monomer prior to starting the rate studies. Initial rates of polymerization were measured by in situ IR spectroscopy[21] or GC analysis of aliquots at varying concentrations of monomer and catalyst (Appendix 2). For the Ni(dppp)Cl_2-catalyzed polymerization of both **2a** and **4**, an approximate first-order dependence of the initial rate on both [catalyst] and [monomer] was observed (Figures 3.1-2).[22] These monomer reaction orders are different than those obtained with Ni(dppe)Cl_2,[19] suggesting a ligand-dependent change in rate-determining step. Indeed, the rate data obtained with Ni(dppp)Cl_2 are consistent with either rate-determining transmetallation or intermolecular oxidative addition because both steps involve the monomer and catalyst. To distinguish between these two scenarios, in situ NMR spectroscopic studies were used to characterize the catalyst resting state during polymerization.

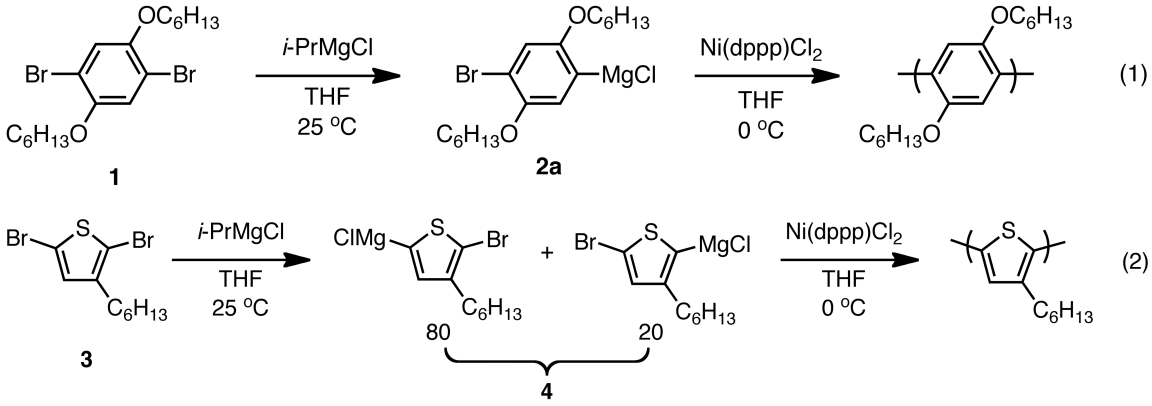

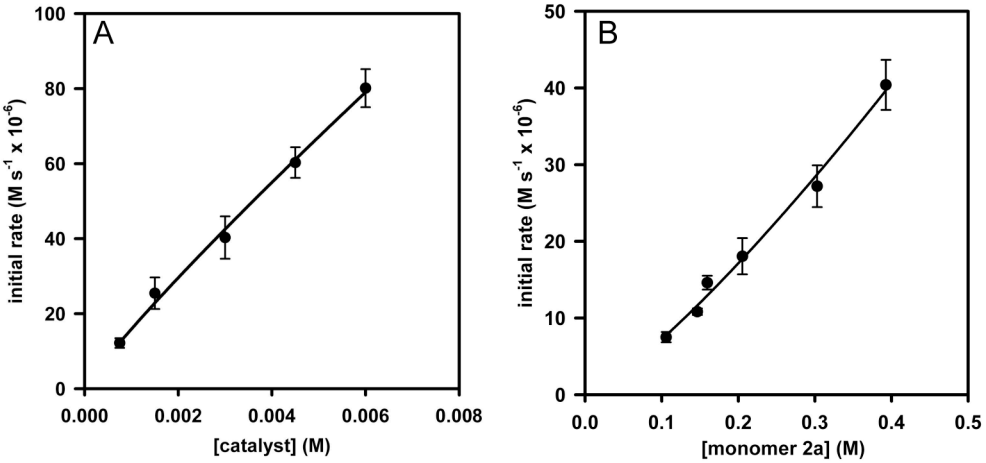

Figure 3.1. (A) Plot of initial rate versus [catalyst] for the polymerization of **2a** in THF at 0 °C ([**2a**] = 0.20 M). The curve depicts an unweighted least-squares fit to the expression initial rate = a[catalyst]^n that gave a = 8 ± 2 x 10^3 and n = 0.89 ± 0.05. (B) Plot of initial rate versus [monomer] for the polymerization of **2a** in THF at 0 °C ([Ni(dppp)Cl_2] = 0.0015 M). The curve depicts an unweighted least-squares fit to the expression initial rate = a[monomer]^n that gave a = 1.3 ± 0.1 x 10^2 and n = 1.24 ± 0.07.

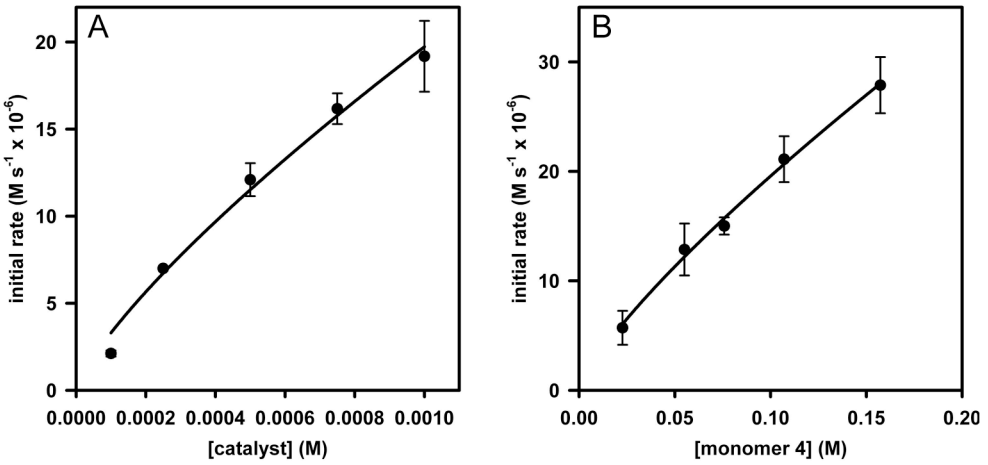

Figure 3.2. (A) Plot of initial rate versus [catalyst] for the polymerization of **4** in THF at 0 °C ([**4**] = 0.05 M). The curve depicts an unweighted least-squares fit to the expression initial rate = a[catalyst]^n that gave a = 4 ± 2 x 10^3 and n = 0.78 ± 0.07. (B) Plot of initial rate versus [monomer] for the polymerization of **4** in THF at 0 °C ([Ni(dppp)Cl_2] = 0.00025 M). The curve depicts an unweighted least-squares fit to the expression initial rate = a[monomer]^n that gave a = 12 ± 1 x 10^1 and n = 0.79 ± 0.04.

NMR Spectroscopic Studies. The polymerizations were followed by ^{1}H and ^{31}P NMR spectroscopy to identify the catalyst resting states. During the polymerization of both **2a** and **4**, two doublets with similar intensities were observed in each ^{31}P NMR spectrum (**2a**: J_{PP} = 52 Hz, **4**: J_{PP} = 66 Hz, Figure 3.3A,B). This result, coupled with the relatively large Δδ, is consistent with complexes **II** and **V** as the polymerization resting states (Scheme 3.1). Because the catalytic cycle will stall at complexes **II** and **V** when the monomer is depleted, further support for this assignment was provided by the fact that the spectra remain unchanged even after the monomer was consumed (see Figures S26 and S28 in Appendix 2). However, the coupling constants for these dppp-based Ni^{II} complexes were significantly larger than those observed for the related dppe-based Ni^{II} complexes.[19] Therefore, two model complexes (**5** and **6**) were synthesized and characterized by ^{31}P NMR spectroscopy. Complexes **5** and **6** exhibited similar chemical shifts and coupling constants to the polymerization resting states (**5**: J_{PP} = 59 Hz, **6**: J_{PP} = 64 Hz, see Figures S6 and S7 in Appendix 2), supporting these assignments. These resting-states are different than those observed with Ni(dppe)Cl_2,[19] consistent with a ligand-dependent change in rate-determining step. Overall, the observed first-order rate dependence on both [catalyst] and [monomer], and the identification of complexes **II** and **V** as the catalyst resting states, support transmetallation as the rate-determining step in the Ni(dppp)Cl_2-catalyzed polymerization of **2a** and **4**.

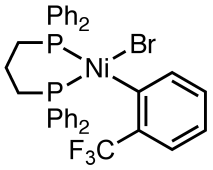

5

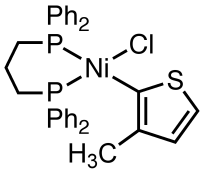

6

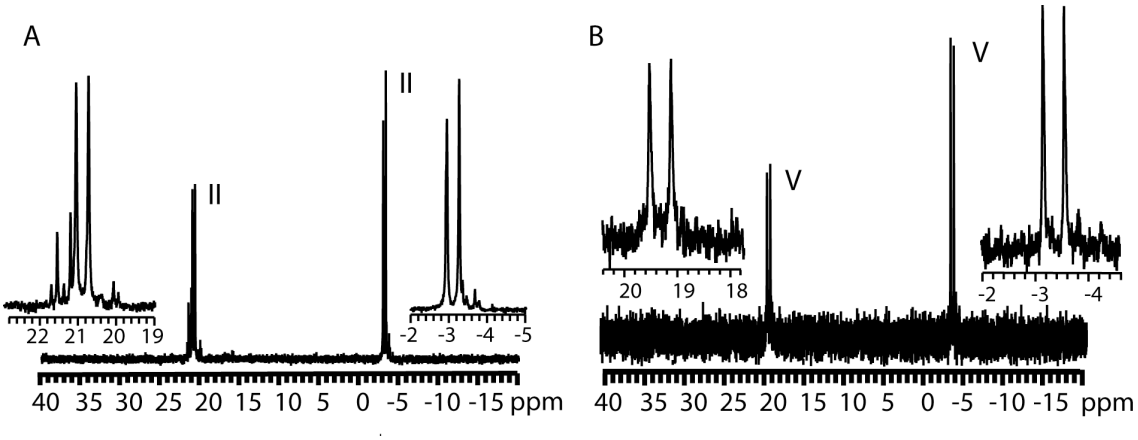

Figure 3.3. ^{31}P NMR spectra for the resting state during polymerization of (A) **2a** and (B) **4**.

Role of Ligand. The change in rate-determining step from reductive elimination (dppe) to transmetallation (dppp) points to a significant mechanistic role of the ligand in the polymerization. The principle differences between the two ligands are the bite angle, with dppp (91°) exhibiting a larger bite angle than dppe (85°), and the conformation of the chelate rings. As a result, differences in reactivity may be observed due to changes in the sterics, electronics and geometry of the nickel complex. These ligand effects are well documented in the small-molecule cross-coupling literature.[23] For example, Yamamoto observed faster rates for reductive elimination from (P-P)$NiMe_2$ when using dppp versus dppe.[24] Similarly, the chain-growth polymerizations are known to be highly sensitive to ligand structure.[25] However, the interpretation of these effects is often ambiguous because the elementary steps in the catalytic cycle can be affected differently by changes in the ligand. For example, in the Ni-catalyzed polymerizations reported herein, it is difficult to pinpoint the affect of ligand on either the rate of transmetallation or reductive elimination because the rate-determining step changes with the different ligands. Therefore, future studies are needed to elucidate the affect of ligand structure on the elementary steps of both the chain-growth and competing reaction pathways.

Scheme 3.1. Proposed Mechanism for the Chain-Growth Polymerizations of (A) **2** and (B) **4**.

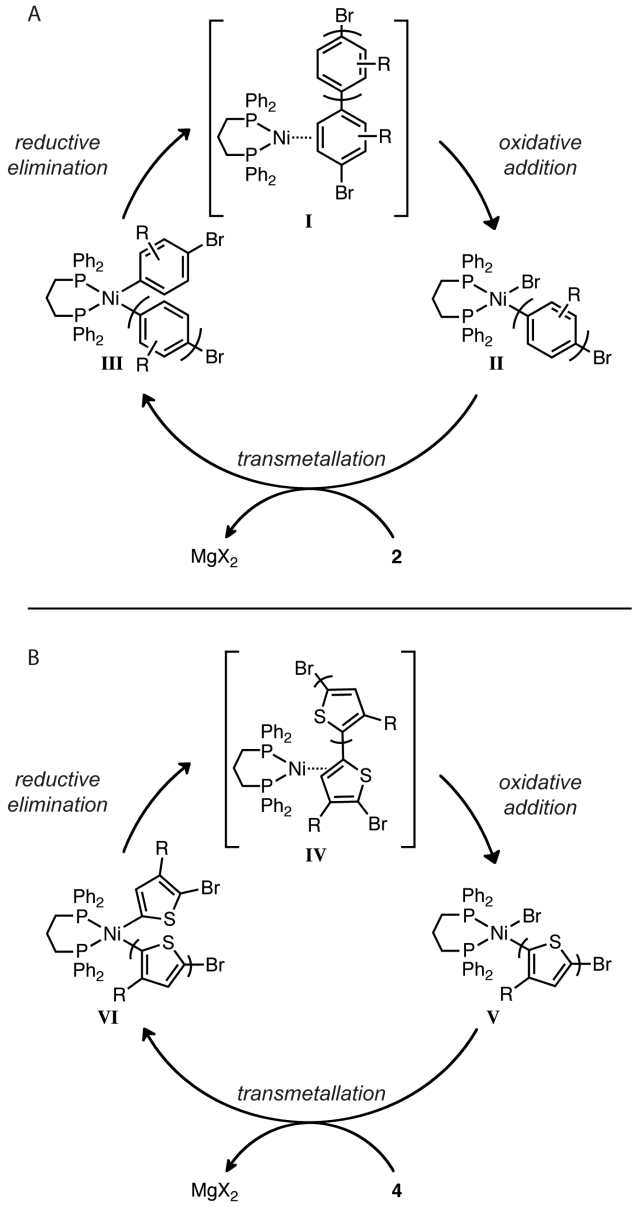

Role of LiCl. In our previous studies with Ni(dppe)Cl_2, LiCl had no effect on the polymerization rate of **2** even though ^{1}H NMR spectroscopic studies revealed that LiCl aggregates with the monomer.[19] These results are consistent with the observed rate-determining reductive elimination since the monomer is not involved in this step. In contrast, because transmetallation involves the monomer, a rate-dependence on LiCl was anticipated in the Ni(dppp)Cl_2-

catalyzed polymerization of **2b**. Indeed, rate studies in the presence of one equiv LiCl revealed an approximate first-order dependence on [catalyst] and half-order dependence on [monomer] (eq 3 and Figure 3.4). Non-integer reaction orders are common for aggregated species and a half-order dependence suggests a higher order aggregate (e.g., a mixed tetramer, $(ArMgCl)_2(LiCl)_2$). However, ^1H NMR spectroscopic studies provided evidence that multiple aggregates may be equilibrating in solution; the aromatic protons of monomer **2** shifted downfield with increasing either [LiCl] or [**2b**] (see Figures S31 and S32 in Appendix 2). Polymerization rate studies performed with excess LiCl revealed slower rates with higher [LiCl], consistent with [LiCl]-dependent changes in aggregate structure (see Figure S23 in Appendix 3). Because solution-based characterization techniques for Grignard reagents remain limited,[26,27] no further insight into the structure of **2b** was obtained. One interesting consequence of the change in monomer reaction order is that the rate effect of LiCl will depend on [monomer] (Figure 3.5). For example, the polymerization of **2b** will be faster than **2a** at low monomer concentrations (< 0.4 M), and slower at high monomer concentrations (> 0.4 M).

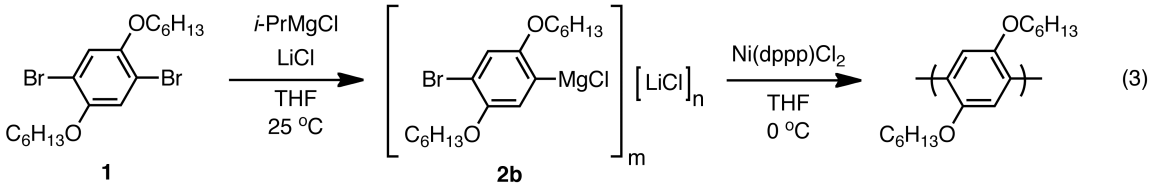

(3)

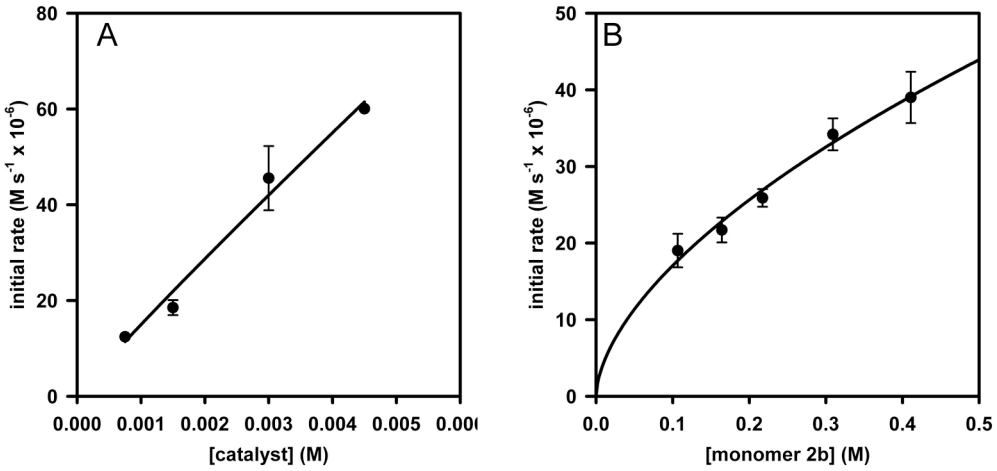

Figure 3.4. (A) Plot of initial rate versus [catalyst] for the polymerization of **2b** in THF at 0 °C ([**2b**] = 0.20 M). The curve depicts an unweighted least-squares fit to the expression initial rate = a[catalyst]^n that gave a = 1.0 ± 0.7 x 10^4 and n = 0.9 ± 0.1. (B) Plot of initial rate versus [monomer] for the polymerization of **2b** in THF at 0 °C ([Ni(dppp)Cl_2] = 0.0015 M). The curve depicts an unweighted least-squares fit to the expression initial rate = a[monomer]^n that gave a = 66 ± 4 and n = 0.59 ± 0.05.

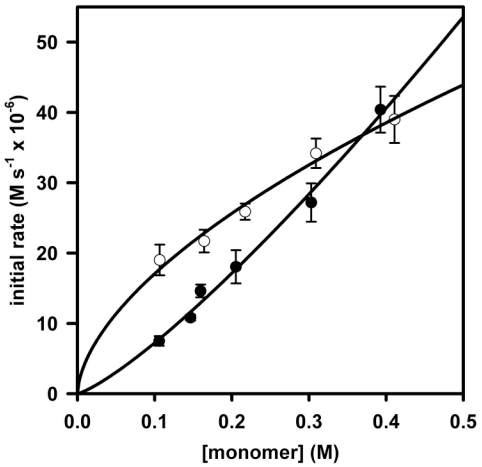

Figure 3.5. Plot of initial rate versus [monomer] for the polymerization of **2a** (●) and **2b** (○) in THF at 0 °C ([Ni(dppp)Cl_2] = 0.0015 M).

In contrast to data reported by Yokozawa,[7e] plots of the M_n and PDI versus conversion revealed that adding one equiv of LiCl resulted in small changes to the M_n and PDI (see Table S1 in Appendix 2). We previously reported a similar result with Ni(dppe)Cl_2,[19] and ascribed this discrepancy to differences in catalyst preparation: Yokozawa used Ni(dppp)Cl_2 and Ni(dppe)Cl_2 as initiators, which are

both insoluble in THF and must react with the monomer to enter the catalytic cycle. The relative rates of these heterogeneous initiation reactions[28] to propagation may depend on LiCl since it is aggregated with the monomer. We avoided this relative rate issue by pre-initiating these insoluble complexes with 5-7 equiv of monomer before beginning the polymerizations.

Conclusion

Our finding that the rate-determining step changes from reductive elimination to transmetallation when the ligand is varied from dppe to dppp points to a strong mechanistic influence of the ligand on the polymerization. As a result, substantial improvements in the synthetic method may be possible through advances in ligand design. However, to rationally select new ligands, it will be necessary to understand the influence of ligand structure on the rate-determining steps, the stability and reactivity of key intermediates – including the hypothesized Ni^0-polymer π-complexes[29] – and the competing reaction pathways. Future studies are aimed at addressing these issues.

References Cited

(1) Cai, W.; Gong, X.; Cao, Y. *Sol. Energy Mater. Sol. Cells* **2010**, *94*, 114-127. Po, R.; Maggini, M.; Camaioni, N. *J. Phys. Chem. C* **2010**, *114*, 695-706. Li, C.; Liu, M.; Pschirer, N. G.; Baumgarten, M.; Müllen, K. *Chem. Rev.* **2010**, *110*, 6817–6855.

(2) Grimsdale, A. C.; Chan, K. L.; Martin, R. E.; Jokisz, P. G.; Holmes, A. B. *Chem. Rev.* **2009**, *109*, 897-1091.

(3) Arias, A. C.; MacKenzie, J. D.; McCulloch, I.; Rivnay, J.; Salleo, A. *Chem. Rev.* **2010**, *110*, 3-24.

(4) Yokoyama, A.; Miyakoshi, R.; Yokozawa, T. *Macromolecules* **2004**, 37, 1169-1171. Miyakoshi, R.; Yokoyama, A.; Yokozawa, T. *Macromol. Rapid Commun.* **2004**, *25*, 1663-1666.

(5) Sheina, E. E.; Liu, J.; Iovu, M. C.; Laird, D. W.; McCullough, R. D. *Macromolecules* **2004**, *37*, 3526-3528.

(6) For chain-growth polymerization of thiophene derivatives, see: (a) Wu, S.; Sun, Y.; Huang, L.; Wang, J.; Zhou, Y.; Geng, Y.; Wang, F. *Macromolecules* **2010**, *43*, 4438-4440. (b) Benanti, T. L.; Kalaydjian, A. Venkataraman, D. *Macromolecules* **2008**, *41*, 8312–8315. (c) Li, Y.; Xue, L.; Xia, H.; Xu, B.; Wen, S.; Tian W. *J. Poly. Sci., Part A: Polym. Chem.* **2008**, *46*, 3970-3984. (d) Ouhib, F.; Dkhissi, A.; Iratçabal, P.; Hiorns, R. C.; Khoukh, A.; Desbrières, J.; Pouchan, C.; Dagron-Lartigau, C. *J. Poly. Sci., Part A: Polym. Chem.* **2008**, *46*, 7505-7516. (e) Vallat, P.; Lamps, J.-P.; Schosseler, F.; Rawiso, M.; Catala, J.-M. *Macromolecules* **2007**, *40*, 2600–2602. (f) Adachi, I.; Miyakoshi, R.; Yokoyama, A.; Yokozawa, T. *Macromolecules* **2006**, *39*, 7793-7795. (g) Koeckelberghs, G.; Vangheluwe, M.; Van Doorsselaere, K.; Robijns, E.; Persoons, A.; Verbiest,

T. *Macromol. Rapid Commun*. **2006**, *27*, 1920-1925. (h) Sheina, E. E.; Khersonsky, S. M.; Jones, E. G.; McCullough, R. D. *Chem. Mater.* **2005**, *17*, 3317-3319.

(7) For chain-growth polymerization of other monomers, see: (a) Stefan, M. C.; Javier, A. E.; Osaka, I.; McCullough, R. D. *Macromolecules* **2009**, *42*, 30-32. (b) Yokoyama, A.; Kato, A.; Miyakoshi, R.; Yokozawa, T. *Macromolecules* **2008**, *41*, 7271-7273. (c) Huang, L.; Wu, S.; Qu, Y.; Geng, Y.; Wang, F. *Macromolecules* **2008**, *41*, 8944-8947. (d) Wen, L.; Duck, B. C.; Dastoor, P. C.; Rasmussen, S. C. *Macromolecules* **2008**, *41*, 4576-4578. (e) Miyakoshi, R.; Shimono, K.; Yokoyama, A.; Yokozawa, T. *J. Am. Chem. Soc.* **2006**, *128*, 16012-16013.

(8) Block copolymers with thiophene-based monomers in both blocks have been successfully synthesized. For recent examples, see: (a) Van den Bergh, K.; Cosemans, I.; Verbiest, T.; Koeckelberghs, G. *Macromolecules* **2010**, *43*, 3794-3800. (b) Clément, S.; Meyer, F.; De Winter, J.; Coulembier, O.; Vande Velde, C. M. L.; Zeller, M.; Gerbaux, P.; Balandier, J.-Y.; Sergeyev, S.; Lazzaroni, R.; Geerts, Y.; Dubois, P. *J. Org. Chem.* **2010**, *75*, 1561-1568. (c) Zhang, Y.; Tajima, K.; Hashimoto, K. *Macromolecules* **2009**, *42*, 7008-7015. (d) Wu, P.-T.; Ren, G.; Li, C.; Mezzenga, R.; Jenekhe, S. A. *Macromolecules* **2009**, *42*, 2317-2320.

(9) For recent examples of syntheses of end-functionalized polymers via this method, see: (a) Kaul, E.; Senkovskyy, V.; Tkachov, R.; Bocharova, V.; Komber, H.; Stamm, M.; Kiriy, A. *Macromolecules* **2010**, *43*, 77-87. (b) Higashihara, T.; Takahashi, A.; Tajima, S.; Jin, S. Rho, Y.; Ree, M.; Ueda, M. *Polym. J.* **2010**, *42*, 43-50. (c) Palaniappan, K.; Murphy, J. W.; Khanam, N.; Horvath, J.; Alshareef, H.; Quevedo-Lopez, M.; Biewer, M. C.; Park, S. Y.; Kim, M. J.; Gnade, B. E.; Stefan, M. C. *Macromolecules* **2009**, *42*, 3845-3848. (d) Alemseghed, M. G.; Gowrisanker, S.; Servello, J.; Stefan, M. C. *Macromol. Chem. Phys.* **2009**, *210*, 2007-2014.

(10) (a) Javier, A. E.; Varshney, S. R.; McCullough, R. D. *Macromolecules* **2010**, *43*, 3233-3237. (b) Miyakoshi, R.; Yokoyama, A.; Yokozawa, T. *Chem. Lett.* **2008**, *37*, 1022-1023. (c) Wu, S.; Bu, L.; Huang, L.; Yu, X.; Han, Y.; Geng, Y.; Wang, F. *Polymer* **2009**, *50*, 6245-6251. (d) See also, ref 7b.

(11) Miyakoshi, R.; Yokoyama, A.; Yokozawa, T. *J. Am. Chem. Soc.* **2005**, *127*, 17542-17547.

(12) For recent reviews, see: (a) Yokozawa, T.; Yokoyama, A. *Chem. Rev.* **2009**, *109*, 5595-5619. (b) Miyakoshi, R.; Yokoyama, A.; Yokozawa, T. *J. Poly. Sci., Part A: Polym. Chem*. **2008**, *46*, 753-765. (c) Yokozawa, T.; Ajioka, N.; Yokoyama, A. In *New Frontiers in Polymer Synthesis;* Kobayashi, S., Ed.; Advances in Polymer Science, Vol 217; Springer Berlin: Heidelberg, 2008, pp 1-77. (d) Yokoyama, A.; Yokozawa, T. *Macromolecules* **2007**, *40*, 4093-4101.

(13) Iovu, M. C.; Sheina, E. E.; Gil, R. R.; McCullough, R. D. *Macromolecules* **2005**, *38*, 8649-8656.

(14) For a recent review, see: Osaka, I.; McCullough, R. D. *Acc. Chem. Res.* **2008**, *41*, 1202-1214.

(15) For examples of Ni^0-arene π-complexes, see: (a) Johnson, S. A.; Huff, C. W.; Mustafa, F.; Saliba, M. *J. Am. Chem. Soc.* **2008**, *130*, 17278-17280. (b) Garcia, J. J.; Brunkan, N. M.; Jones, W. D. *J. Am. Chem. Soc.* **2002**, *124*, 9547-9555. (c) Braun, T.; Cronin, L.; Higgitt, C. L.; McGrady, J. E.; Perutz, R. N.; Reinhold, M. *New J. Chem*. **2001**, *25*, 19-21. (d) Bach, I.; Pörschke, K.-R.; Goddard, R.; Kopiske, C.; Krüger, C.; Rufińska, A.; Seevogel, K. *Organometallics* **1996**, *15*, 4959-4966. (e) Stanger, A.; Shazar, A. *J. Organomet. Chem.* **1993**, *458*, 233-236. (f) Boese, R.; Stanger, A.; Stellberg, P.; Shazar, A. *Angew. Chem. Int. Ed.* **1993**, *32*, 1475-1477. (g) Stanger, A.; Vollhardt, K. P. C. *Organometallics* **1992**, *11*, 317-320. (h) Stanger, A.; Boese, R. *J. Organomet. Chem*. **1992**, *430*, 235-243. (i) Scott, F.; Krüger, C.; Betz, P. *J. Organomet. Chem.*

1990, *387*, 113-121. (j) Benn, R.; Mynott, R.; Topalović, I.; Scott, F. *Organometallics* **1989**, *8*, 2299-2305. (k) Brauer, D. J.; Krüger, C. *Inorg. Chem.* **1977**, *16*, 884-891.

(16) Ni^0-arene π-complexes have previously been implicated as intermediates in oxidative addition reactions. For examples, see (a) Yoshikai, N.; Matsuda, H.; Nakamura, E. *J. Am. Chem. Soc.* **2008**, *130*, 15258-15259. (b) Zenkina, O. V.; Karton, A.; Freeman, D.; Shimon, L. J. W.; Martin, J. M. L.; van der Boom, M. E. *Inorg. Chem*. **2008**, *47*, 5114-5121. (c) Ateşin, T. A.; Li, T.; Lachaize, S.; García, J. J.; Jones, W. D. *Organometallics* **2008**, *27*, 3811-3817. (d) Reinhold, M.; McGrady, J. E.; Perutz, R. N. *J. Am. Chem. Soc.* **2004**, *126*, 5268-5276. (e) See also, refs 15b, 15c, and 15d.

(17) An alternative mechanism has been proposed, see: Achord, B. C.; Rawlins, J. W. *Macromolecules* **2009**, *42*, 8634-8639.

(18) (a) Tkachov, R.; Senkovskyy, V.; Komber, H.; Sommer, J.-U.; Kiriy, A. *J. Am. Chem. Soc.* **2010**, *132*, 7803-7810. (b) Beryozkina, T.; Senkovskyy, V.; Kaul, E.; Kiriy, A. *Macromolecules* **2008**, *41*, 7817-7823. (c) Boyd, S. D.; Jen, A.K.-Y.; Luscombe, C. K. *Macromolecules* **2009**, *42*, 9387-9389.

(19) Lanni, E. L.; McNeil, A. J. *J. Am. Chem. Soc.* **2009**, *131*, 16573-16579.

(20) (a) Shi, L.; Chu, Y.; Knochel, P.; Mayr, H. *Org. Lett.* **2009**, *11*, 3502-3505. (b) Shi, L.; Chu, Y.; Knochel, P.; Mayr, H. *J. Org. Chem*. **2009**, *74*, 2760-2764. (c) Shi, L.; Chu, Y.; Knochel, P.; Mayr, H. *Angew. Chem. Int. Ed*. **2008**, *47*, 202-204. (d) Krasovskiy, A.; Straub, B. F.; Knochel, P. *Angew. Chem. Int. Ed.* **2006**, *45*, 159-162. (e) Hauk, D.; Lang, S.; Murso, A. *Org. Process Res. Dev*. **2006**, *10*, 733-738. (f) Krasovskiy, A.; Knochel, P. *Angew. Chem. Int. Ed*. **2004**, *43*, 3333-3336. (g) Knochel, P.; Dohle, W.; Gommermann, N.; Kneisel, F. F.; Kopp, F.; Korn, T.; Sapountzis, I.; Vu, V. A. *Angew. Chem. Int. Ed.* **2003**, *42*, 4302-4320. (h) Boymond, L.; Rottländer, M.; Cahiez, G.; Knochel, P. *Angew. Chem. Int. Ed.* **1998**, *37*, 1701-1703.

(21) In situ UV-vis spectroscopy has also been used to monitor polymerization rates. For reference, see: Lamps, J.-P.; Catala, J.-M. *Macromolecules* **2009**, *42*, 7282-7284.

(22) Many of the first-order rate dependencies are ± 0.2 from the anticipated value of 1.0. For the initial rate versus [monomer] plots, this effect may be due to concentration-dependent changes in the Grignard structure.

(23) For leading references on phosphine ligand effects in transition metal catalysis, see: (a) Gillespie, J. A.; Dodds, D. L.; Kamer, P. C. J. *Dalton Trans.* **2010**, *39*, 2751-2764. (b) Birkholz, M.-N.; Freixa, Z.; van Leeuwen, P. W. N. M. *Chem. Soc. Rev.* **2009**, *38*, 1099-1118. (c) van Leeuwen, P. W. N. M.; Kamer, P. C. J.; Reek, J. N. H.; Dierkes, P. *Chem. Rev.* **2000**, *100*, 2741-2769. (d) Dierkes, P.; van Leeuwen, P. W. N. M. *Dalton Trans.* **1999**, 1519-1529.

(24) Kohara, T.; Yamamoto, T.; Yamamoto, A. *J. Organomet. Chem*. **1980**, *192*, 265-274.

(25) For examples, see: (a) Doubina, N.; Stoddard, M.; Bronstein, H. A.; Jen, A. K.-Y.; Luscombe, C. K. *Macromol. Chem. Phys*. **2009**, *210*, 1966-1972. (b) Mao, Y.; Wang, Y.; Lucht, B. L. *J. Polym. Sci., Part A: Polym. Chem.* **2004**, *42*, 5538-5547. (c) See also, refs 6f, 12b.

(26) X-ray crystallography remains the most popular characterization method even though the solid-state structures do not necessary represent the species present in solution. For reviews, see: (a) Holloway, C. E.; Melnik, M. *Coord. Chem. Rev.* **1994**, *135/136*, 287- 301. (b) Holloway, C. E.; Melnik, M. *J. Organomet. Chem.* **1994**, *465*, 1-63.

(27) Recently, coldspray ionization mass spectrometry and diffusion-ordered NMR spectroscopy have been used to characterize Grignard reagents in solution. For examples, see: (a) Sakamoto, S.; Imamoto, T.; Yamaguchi, K. *Org. Lett.* **2001**, *3*, 1793-1795. (b) Armstrong, D. R.; García-Álvarez, P.; Kennedy, A. R.; Mulvey, R. E.; Parkinson, J. A. *Angew. Chem. Int. Ed.* **2010**, *49*, 3185-3188.

(28) Aryl- and thienyl-functionalized initiators have recently been explored as soluble alternatives to L_2NiCl_2. For recent examples, see: (a) Bronstein, H. A.; Luscombe, C. K. *J. Am. Chem. Soc.* **2009**, *131*, 12894-12895. (b) Doubina, N.; Ho, A.; Jen, A. K.-Y.; Luscombe, C. K. *Macromolecules* **2009**, *42*, 7670-7677. (c) Smeets, A.; Van den Bergh, K.; De Winter, J.; Gerbaux, P.; Verbiest, T.; Koeckelberghs, G. *Macromolecules* **2009**, *42*, 7638-7641. (d) Senkovskyy, V.; Tkachov, R.; Beryozkina, T.; Komber, H.; Oertel, U.; Horecha, M.; Bocharova, V.; Stamm, M.; Gevorgyan, S. A.; Krebs, F. C.; Kiriy, A. *J. Am. Chem. Soc.* **2009**, *131*, 16445-16453. (e) Senkovskyy, V.; Khanduyeva, N.; Komber, H.; Oertel, U.; Stamm, M.; Kuckling, D.; Kiriy, A. *J. Am. Chem. Soc.* **2007**, *129*, 6626-6632. (f) See also, 18c.

(29) Studies on Ni^0-*olefin* π-complexes indicate that chelating, electron-rich phosphine ligands may be optimal in the chain-growth polymerizations because they could stabilize the π-complex and, as a result, limit competitive dissociation pathways. For leading references, see: (a) Massera, C.; Frenking, G. *Organometallics* **2003**, *22*, 2758-2765. (b) Tolman, C. A.; Seidel, W. C.; Gosser, L. W. *Organometallics* **1983**, *2*, 1391-1396.

Chapter 4[1]

Preliminary Results for Ligand-based Steric Effects in Ni-catalyzed Chain-growth Polymerizations using Bis(dialkylphosphino)ethanes

Introduction

In 2004, McCullough[1] and Yokozawa[2] reported a chain-growth method for synthesizing π-conjugated polymers that gained attention because previously inaccessible materials, like all-conjugated block[3] and gradient[4] copolymers, could now be prepared. In the intervening years, however, it has become evident that the original chain-growth method is limited to a relatively narrow scope of monomers.[5,6] Furthermore, the mechanistic underpinnings of this limitation remain unclear today. In addition, only a limited number of copolymers have been prepared because of inefficiencies in the cross-propagation step;[7] these results also lack a clear mechanistic explanation.[8,9] To advance this field, a mechanistic understanding of the key factors controlling the competition between the desired chain-growth pathway[10,11,12] and the detrimental side-reactions is needed. We recently reported that the ligand scaffold had a substantial influence on the chain-growth polymerization mechanism.[11,12] Specifically, we showed that the syntheses of both poly(*p*-(2,5-bishexyloxy)phenylene) and poly(3-hexylthiophene) proceed through different rate-limiting steps when different ligands (diphenylphosphinoethane (dppe)[11] and diphenylphosphinopropane (dppp))[12] were used. Therefore, we hypothesized that alternative ligand scaffolds might provide catalysts with a broader substrate scope and facile cross-propagation abilities.

To account for the unexpected chain-growth nature of the cross-coupling polymerization, a Ni^0-arene π-complex[13] (**III** in Scheme 4.2) has been proposed as a key intermediate.[10,11,12] We further postulated that the detrimental, competing reaction pathways stem from a breakdown of this key intermediate. Therefore, we selected bis(dialkylphosphino)ethane ligands for this study

---

[1] Reproduced in part with permission from Lanni, E. L.; Locke, J. R.; Gleave, C. M.; McNeil, A. J. manuscript in preparation, 2011

because we anticipated that their increased electron-donating ability (relative to dppe and dppp)[14] would increase the polymer-binding affinities to nickel (intermediate **III**)[15] and minimize the competing reaction pathways. To probe the influence of steric effects on the polymerization we selected a series of bis(dialkylphosphino)ethane ligands with different alkyl substituents.[16]

Herein, we report that poly(*p*-(2,5-bishexyloxy)phenylene) can be prepared via chain-growth polymerization using one of these catalysts, $Ni(depe)Cl_2$. Mechanistic studies were consistent with a rate-determining reductive elimination. Steric effects played a significant role in the polymerization, with the most hindered phosphine leading to low molecular weight oligomers. On the other hand, the least hindered phosphine led to significant amounts of decomposition. In addition, we identified previously uncharacterized intermediates in the initiation process. $Ni(depe)Cl_2$ was also an effective chain-growth catalyst for synthesizing poly(3-hexylthiophene). Overall, these results highlight the important mechanistic role of ligands in Ni-catalyzed chain-growth polymerizations[11,12] and indicate that future studies should continue to focus on optimizing the ligand scaffold.

Results and Discussion

Catalyst Design and Synthesis. Nickel complexes **1**-**3** were synthesized from commercially available $NiCl_2•(H_2O)_6$ and the corresponding bis(dialkylphosphino)ethane.[17] With the exception of **1**, the ligand complexation reactions resulted in quantitative conversion in one step. The resulting Ni complexes were precipitated from EtOH to give analytically pure compounds (Appendix 3).

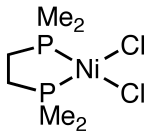

$Ni(dmpe)Cl_2$

1

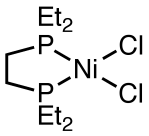

$Ni(depe)Cl_2$

2

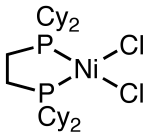

$Ni(dcpe)Cl_2$

3

The steric properties of ligands are generally defined by the Tolman cone angle,[18] which is based on molecular models and describes the opening of a cone that encompasses the metal and the outermost atoms of a ligand. An alternative measure of steric properties is the solid angle,[19] which is based on experimental data and describes the size of a shadow that the ligand creates on a sphere if the metal is a point-source of light. Weigand and co-workers[20] recently reported an extension of this model by performing a comprehensive analysis of 900 crystal structures of Pt complexes with bidendate phosphines. In this work they calculated a "generalized equivalent cone angle" which we will use in this paper. The generalized equivalent cone angles for the ligands used in this study are bis(dimethylphosphino)ethane (dmpe, 155°), bis(diethylphosphino)ethane (depe, 175°), and bis(dicyclohexylphosphino)ethane (dcpe, 191°). For chelating phosphines, the natural bite angle[21] is another parameter that can influence the steric properties.[22] The bite angle refers to the preferred chelation angle (P-M-P) and is determined by the ligand backbone. Because we previously showed that changes in ligand bite angles altered the polymerization mechanism,[11,12] we intentionally selected three phosphine ligands with similar bite angles (~85°) for this study. Overall, these ligands provide large variation in the steric crowding near the metal center and thus the influence of steric properties on the polymerization can be elucidated.

Catalyst Screening: Polymerization of Monomer 4a. Monomer **4a**[23] was selected for catalyst screening because it is known to undergo a robust chain-growth polymerization with both Ni(dppp)Cl_2 and Ni(dppe)Cl_2.[6e,11,12] Thus, polymerization of **4a** using catalysts **1**-**3** was first attempted at room temperature (eq 1). The results were quite surprising; complex **2** was the only catalyst capable of producing polymer at room temperature (Appendix 3). At elevated temperatures (60 °C), all three catalysts were active in the polymerization of **4a** (Table 4.1). Under these reaction conditions, Ni(depe)Cl_2 (**2**) provided polymer samples with narrower distributions of molecular weights than the conventional catalysts, Ni(dppe)Cl_2 and Ni(dppp)Cl_2. In contrast, the more hindered Ni(dcpe)Cl_2 (**3**) and the less hindered Ni(dmpe)Cl_2 (**1**) were largely unreactive,

and provided low molecular weight oligomers. Despite the relatively narrow polydispersity index obtained with catalyst **2** (1.18), a close inspection of the gel permeation chromatogram revealed a predominant polymer peak with broader polydispersity and a "tail" in the low molecular weight region (Appendix 3).[24] Additionally, when other lab members repeated these reactions, they obtained broader PDIs, albeit inconsistently (Appendix 3). These results suggested that the polymerization might be predominantly chain-growth, with either a slow initiation process or an early termination reaction being responsible for the low molecular weight oligomers. Therefore, ^{31}P NMR spectroscopic studies were conducted to understand the origin of the minor amount of low molecular weight species with catalyst **2**, and the limited reactivity of catalysts **1** and **3**.

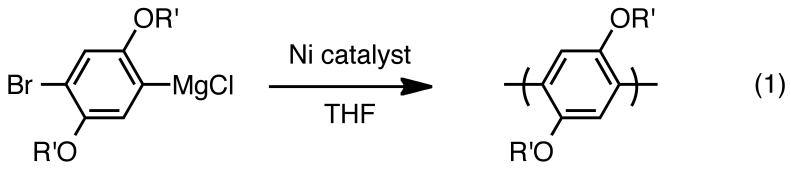

(1)

4a; R' = C_6H_{13}
4b; R' = CH_3

P1; R' = C_6H_{13}
P2; R' = CH_3

Table 4.1. Polymerization Results for Monomer **4a** using Selected Ni Catalysts at 60 °C.[a]

Nickel Complex	% Conversion	M_n (kDa)	PDI
Ni(dmpe)Cl_2 (**1**)	97	23	1.19
Ni(depe)Cl_2 (**2**)	97	23	1.13
Ni(dcpe)Cl_2 (**3**)	22	3	16
Ni(dppe)Cl_2	97	28	1.43
Ni(dppp)Cl_2	97	12	1.52

a. The conversions were measured by gas chromatography relative to an internal standard. Number-average molecular weights (M_n) and polydispersity indices (PDIs) were determined by gel permeation chromatography relative to PS

standards. The polymerizations were quenched with 5 M HCl/MeOH after 6-7 h ([Ni] = 0.0015 M; [**4a**] = 0.10 M).

Spectroscopic Studies: **General Considerations.** Although the primary goal of these spectroscopic studies was to explain the reactivity trends in the polymerizations, we anticipated that these experiments might also reveal information about the initiation sequence because of the low catalyst reactivities at room temperature. Initiation is believed to occur through two consecutive transmetalation reactions,[25] followed by reductive elimination (Scheme 4.1). The resulting Ni species enters the catalytic cycle shown in Scheme 2, presumably via intermediate **III**. It is important to note that this sequence of intermediates has not yet been observed with either Ni(dppe)Cl_2 or Ni(dppp)Cl_2 due to their high reactivities.[26,27]

Scheme 4.1. Proposed mechanism for catalyst initiation.

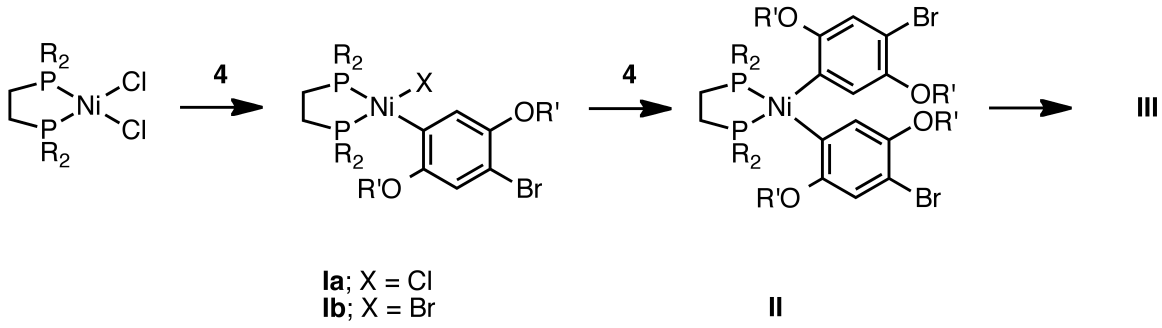

Scheme 4.2. Proposed mechanism for chain-growth polymerization.

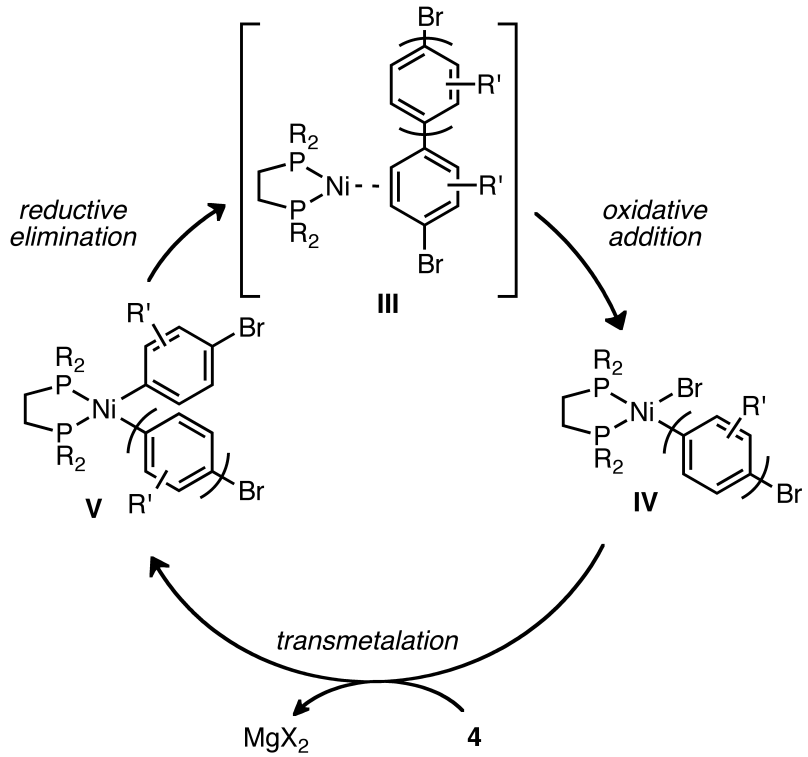

Spectroscopic Studies with Ni(depe)Cl_2 (2) and Monomer 4a. Adding several equivalents of monomer **4a** to Ni(depe)Cl_2 at room temperature resulted in the immediate, quantitative formation of a new species with a single resonance (55.3 ppm) in the ^{31}P NMR spectrum (Figure 4.1A). This species was tentatively assigned as symmetric Ni^{II} biaryl complex $\mathbf{II}_{\mathbf{depe}}$. A structurally related complex, Ni(depe)($CH_2C_6H_4$-*o*-$CH_3)_2$, was reported to have a similar chemical shift (54.8

ppm).[28,29] With additional turnovers, this complex gradually converted to a new species with two doublets (J_{PP} = 14.5 Hz) in the ^{31}P NMR spectrum (Figure 4.1B). Based on our previous studies with Ni(dppe)Cl_2[11] and the proximity of this species to complex **II$_{depe}$**, we assigned this species as unsymmetrical biaryl complex **V$_{depe}$**. As the monomer concentration decreases with polymerization, a new species appeared with two distal doublets (J_{PP} = 30.6 Hz) in the ^{31}P NMR spectrum (Figure 1C). We hypothesized that this species is complex **IV$_{depe}$** because the polymerization should stall at this complex in the absence of monomer. To provide support for this assignment, model complexes **6a**/**6b** were prepared via ligand exchange between complexes **5a**/**5b** and depe (eq 2). Interestingly, the identity of the halide ligand had a dramatic effect on the downfield resonance, with bromine-substituted complex **6b** showing a 3 ppm downfield shift relative to chlorine-substituted complex **6a** (Appendix 3). Complex **6b** gave a similar chemical shift difference (Δδ = 6.7 ppm) and coupling constant (J_{PP} = 24.3 Hz) to the species present at the end of the polymerization, supporting the assignment of complex **IV$_{depe}$** (Figure 4.1D).

It is notable that, at room temperature, complex **II$_{depe}$** persisted even after polymerization is complete. This result indicates that reductive elimination from the symmetric biaryl species (**II$_{depe}$**) is significantly slower than the unsymmetric biaryl species (**V$_{depe}$**). In other words, initiation is *slower* than propagation with Ni(depe)Cl_2; this result could account for the low molecular weight species observed in the gel permeation chromatogram. We previously[11] hypothesized that a slow initiation process might explain the improvements in M_n and PDI with adding LiCl, as reported by Yokozawa and co-workers[6e] in the polymerization of **4a** with Ni(dppp)Cl_2 and Ni(dppe)Cl_2.

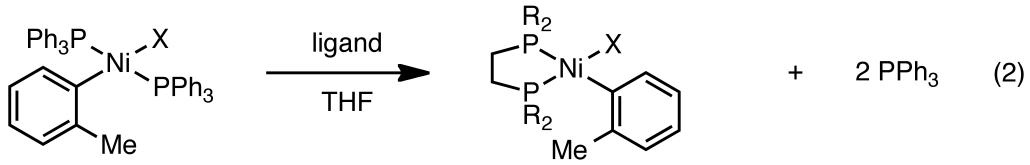

5a; X = Cl
5b; X = Br

6a; R = Et, X = Cl
6b; R = Et, X = Br
6c; R = Cy, X = Cl
6d; R = Cy, X = Br

Similar spectra were observed when these experiments were repeated at 60 °C, consistent with the fact that catalyst **2** was active for polymerization of monomer **4a** at both temperatures (Appendix 3). The predominant species observed during polymerization at 60 °C is complex $\mathbf{V_{depe}}$, which we assigned as the catalyst resting-state for the polymerization. This assignment was supported by the ^{1}H NMR spectrum that simultaneously shows signals corresponding to the polymer and monomer (Appendix 3). Once polymerization was complete, the resulting complex ($\mathbf{IV_{depe}}$) was unstable and decomposes over 24 h at room temperature and 3 h at 60 °C. During decomposition, the solution became green/black and precipitation occurred. A new peak (82.6 ppm) is observed in the ^{31}P NMR spectrum, which was assigned as Ni(depe)Br_2.[30] These results were consistent with a transarylation reaction between two equivalents of complex $\mathbf{IV_{depe}}$ to generate Ni(depe)Br_2 and Ni(depe)(polymer)$_2$, which, after reductive elimination, produced polymer and Ni^0.[31] These decomposition reactions, which are second-order in catalyst, are expected to be less prevalent under the standard polymerization conditions due to the significantly lower nickel concentrations used.[32]

In summary, initiation of catalyst **2** with monomer **4a** produced complex $\mathbf{II_{depe}}$, during propagation the catalyst resting-state was complex $\mathbf{V_{depe}}$, and once polymerization was complete the catalyst resting-state was complex $\mathbf{IV_{depe}}$ (Scheme 4.3). These results suggest that reductive elimination is rate-limiting for both initiation and propagation with catalyst **2**. The rate studies described in more detail below further support this assignment.

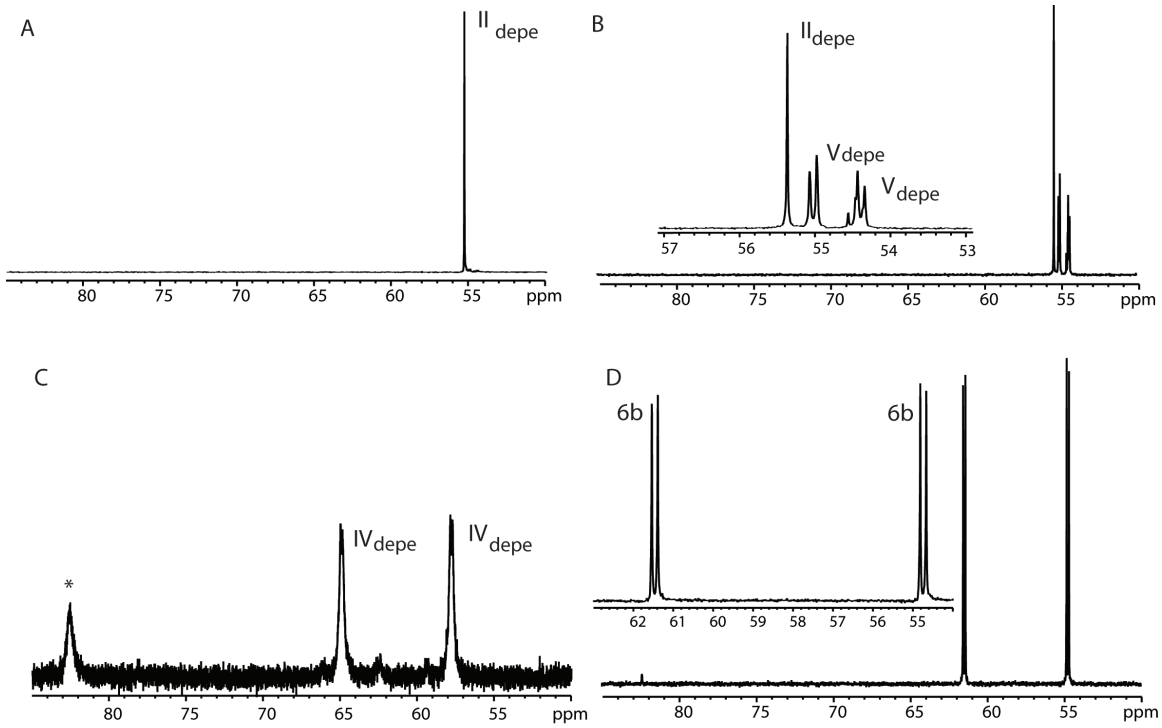

Figure 4.1. ^{31}P NMR Spectra for the reaction of monomer **4a** with catalyst **2** showing (A) the complex formed during initiation, (B) the catalyst resting state during polymerization, (C) the catalyst resting state after polymerization, and (D) complex **6b**. *Indicates Ni(depe)Br_2.

Scheme 4.3. Ni complexes observed during the reaction of monomer **4** with Ni(depe)Cl_2.

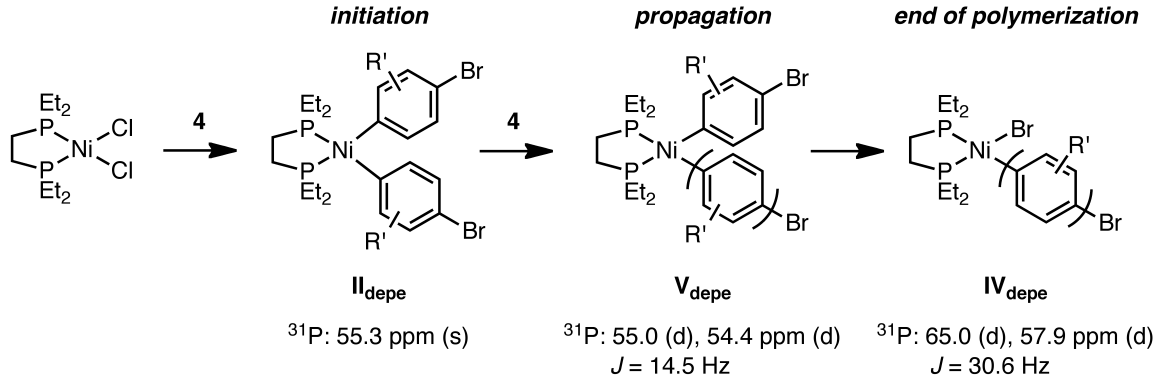

Spectroscopic Studies with Ni(dcpe)Cl_2 (3) and Monomer 4a. Adding several equivalents of monomer **4a** to Ni(dcpe)Cl_2 at room temperature led to the formation of two Ni complexes, each displaying a pair of doublets in the ^{31}P NMR

spectrum (Figure 4.2A). The minor species was assigned as complex **Ia$_{dcpe}$**, the product resulting from transmetalation of one equivalent of **4a** with Ni(dcpe)Cl_2. The major species observed was assigned as complex **Ib$_{dcpe}$**. We hypothesized that this complex formed through a halide exchange with a bromide salt (e.g., $MgBr_2$) present in the reaction mixture. To support these assignments, model complexes **6c** and **6d** were synthesized in situ by adding dcpe to complex **5a** and **5b**, respectively (eq 2). As seen in Figure 2B-C, the similarities in both the chemical shift differences and coupling constants are consistent with these assignments.

After several hours at room temperature, a new species appeared, again with a pair of doublets in the ^{31}P NMR spectrum (Figure 4.2D). Note that no polymer was observed in the corresponding ^{1}H NMR spectra during this time (Appendix 3). We tentatively assigned this complex as **IV$_{dcpe}$**. Heating the sample to 60 °C for 24 h resulted in polymerization, as evidenced by ^{1}H NMR spectroscopy. Notably, complex **Ib$_{dcpe}$** never completely disappeared. This result indicated that **Ib$_{dcpe}$** was either being regenerated during the reaction (through competing reaction pathways) or its reactivity was lower than **IV$_{dcpe}$**. During polymerization, the predominant species was assigned as complex **IV$_{dcpe}$**. Similar spectra were obtained if the experiment is repeated at 60 °C (Appendix 3).[33]

In summary, initiation of catalyst **3** with monomer **4a** led to complexes **Ia$_{dcpe}$** and **Ib$_{dcpe}$**, followed by their slow conversion to complex **IV$_{dcpe}$** at room temperature (Scheme 4.4). Once the reaction was heated to 60 °C and polymerization began, complex **IV$_{dcpe}$** remained the dominant species. These results suggested that transmetalation is rate-limiting for both initiation and propagation. The change in rate-determining step from catalyst **2** was not surprising given the significant increase in steric crowding near the Ni center, which is expected to both accelerate reductive elimination[34] and decelerate transmetalation.[35] Moreover, the continued presence of complex **Ib$_{dcpe}$** suggests that an uncontrolled pathway was intervening; we speculate that the increased steric properties of the ligand may be facilitating the breakdown of the postulated Ni^0-polymer π-complex.

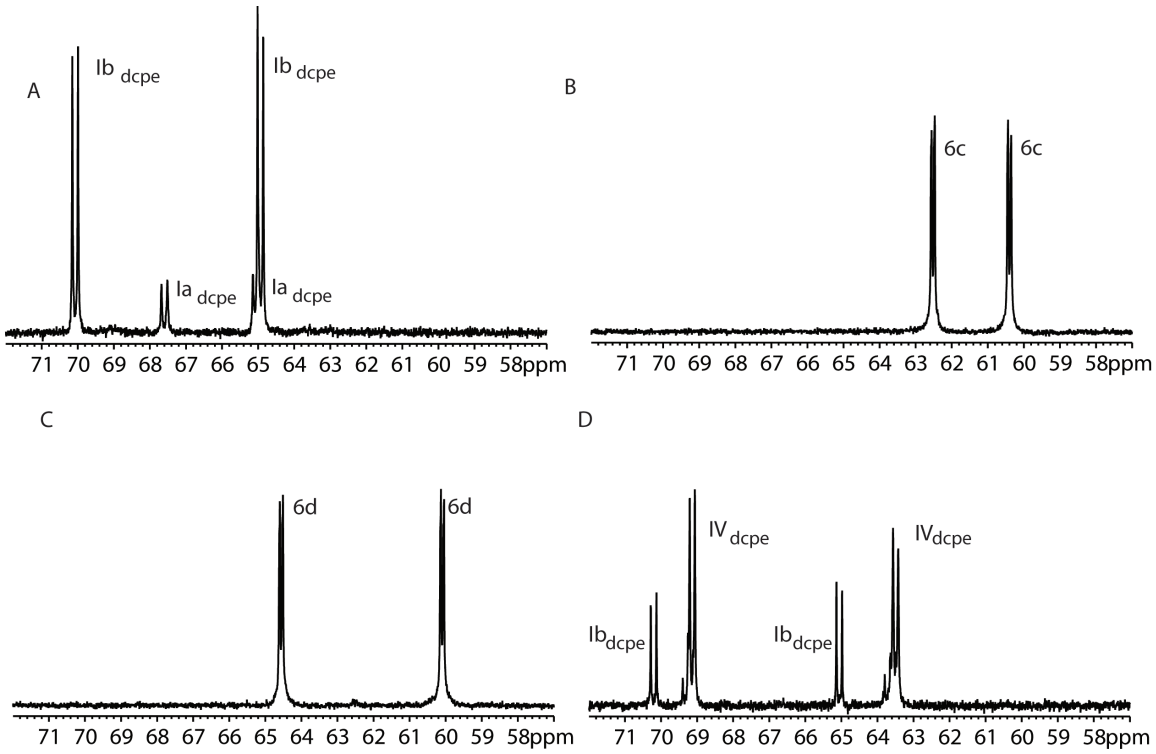

Figure 4.2. ^{31}P NMR Spectra for the reaction of monomer **4a** with catalyst **3** showing (A) the first two complexes observed during initiation, (B) complex **6c**, (C) complex **6d**, and (D) the species observed during initiation and propagation.

Scheme 4.4. Ni complexes observed during the reaction of monomer **4** with $Ni(dcpe)Cl_2$.

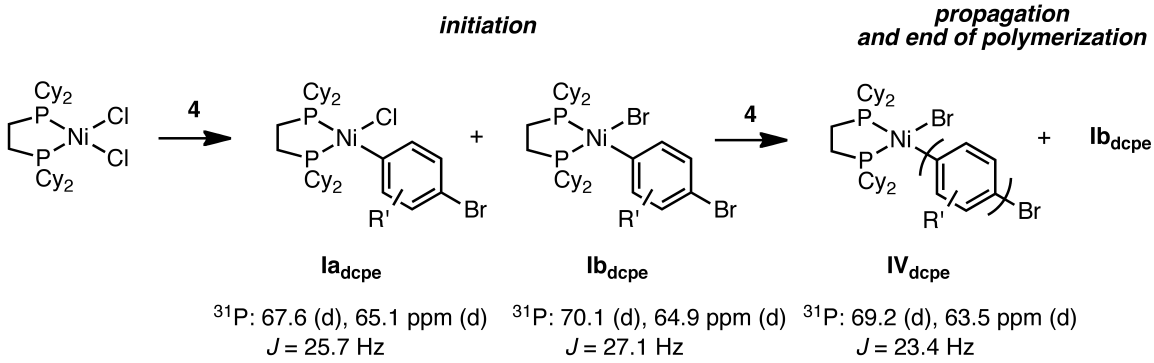

Spectroscopic Studies with $Ni(dmpe)Cl_2$ (1) and Monomer 4a. Adding several equivalents of monomer **4a** to $Ni(dmpe)Cl_2$ at room temperature led to the immediate formation of green solid in the NMR sample tube, indicating decomposition.[31] The ^{31}P NMR spectrum of the species remaining in solution showed a single new peak at 34.2 ppm (Figure 4.3A). We tentatively assigned this species as complex $\mathbf{II_{dmpe}}$ based on similarities to catalyst **2**. In addition, a structurally related complex, $Ni(dmpe)(CH_2C_6H_4\text{-}o\text{-}CH_3)_2$, was reported to have a similar chemical shift (29.7 ppm).[28] Nevertheless, we wanted to further characterize this new complex because a bischelated complex ($Ni(dmpe)_2Cl_2$) was preferentially formed during the synthesis of catalyst **1**. Specifically, the dmpe-to-arene stoichiometry was determined by ^1H NMR spectroscopy. To avoid overlap in the alkyl region, both d_8-THF and monomer **4b** were used in this experiment. Integrating the appropriate regions of the ^1H NMR spectrum provided a dmpe:monomer ratio of 1:2, which is consistent with the assignment of complex $\mathbf{II_{dmpe}}$ (Figure 4.3B). Although no polymer was observed at room temperature, heating this complex to 60 °C initiated polymerization. Coincident with the onset of polymerization, a new species with proximal doublets and a narrow coupling constant (J_{PP} = 14.8 Hz) appeared (Figure 4.3C). We assigned this as complex $\mathbf{V_{dmpe}}$ based on analogy to catalyst **2**. Notably, complex $\mathbf{II_{dmpe}}$ persisted, which is consistent with an initiation process that is *slower* than propagation. Once polymerization was complete, several species with general

structure Ni(dmpe)ArBr (**IV$_{dmpe}$**) were observed (Figure 3D), along with decomposition products (e.g., Ni(dmpe)Cl_2 and Ni(dmpe)Br_2). Based on the apparent decomposition reactions occurring both in the initial and final stages of polymerization, Ni(dmpe)Cl_2 is a less suitable polymerization catalyst than Ni(depe)Cl_2.

In summary, initiation of catalyst **1** led to formation of symmetric biaryl complex **II$_{dmpe}$**, which is inactive for polymerization at room temperature (Scheme 4.5). The lower reactivity of complex **II$_{dmpe}$** relative to **II$_{depe}$** is consistent with the notion that increased steric crowding accelerates reductive elimination with depe.[34] Heating this complex initiated polymerization, with concomitant formation of complex **V$_{dmpe}$** (Scheme 4). These results suggest that the rate-limiting step for both initiation and propagation is reductive elimination, similar to Ni(depe)Cl_2. The lower reactivity of catalyst **1** can also be explained by the irreversible loss of soluble Ni via precipitation during initiation.

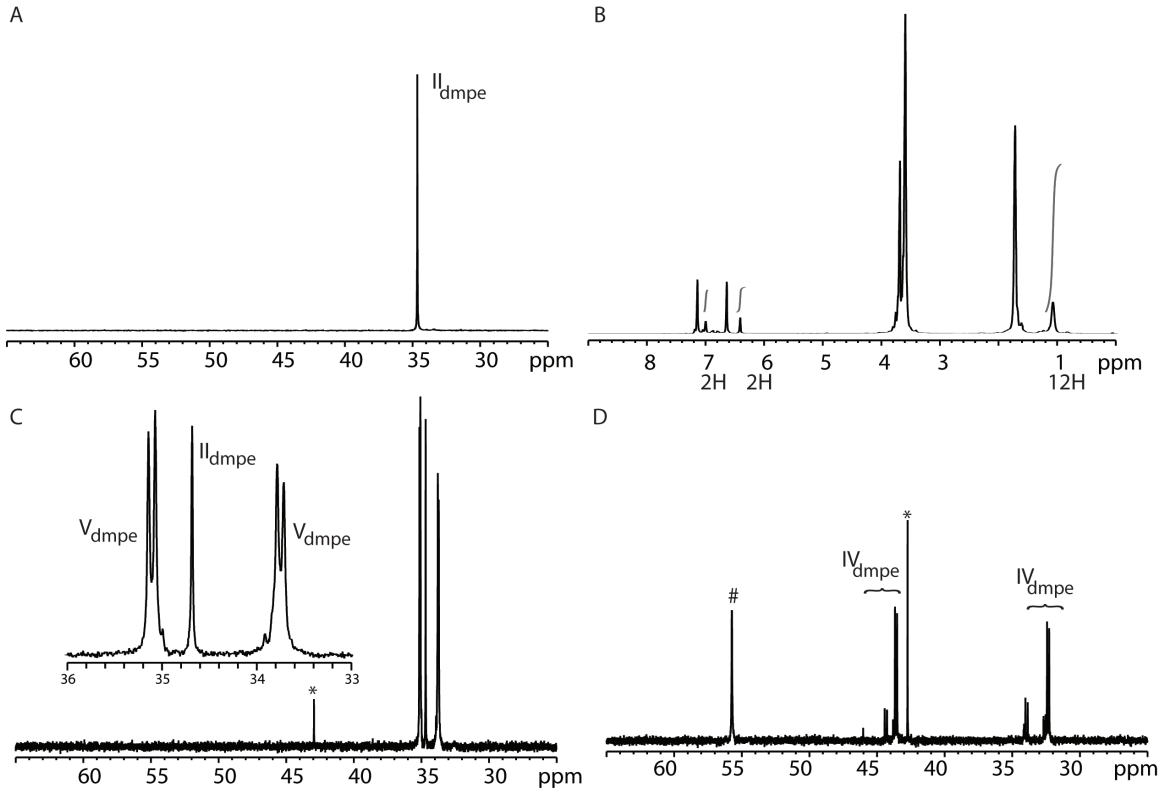

Figure 4.3. (A) ^{31}P NMR Spectrum for the reaction of monomer **4a** with catalyst **1** showing the complex observed during initiation. (B) Selected portions of the ^{1}H NMR spectrum for the reaction of monomer **4b** with catalyst **1**. (C) ^{31}P NMR Spectra for the catalyst resting state during polymerization, and (D) the catalyst resting states after polymerization. # and * refer to $Ni(dmpe)Br_2$ and $Ni(dmpe)Cl_2$, respectively.

Scheme 4.5. Ni complexes observed during the reaction of monomer **4** with Ni(dmpe)Cl_2.

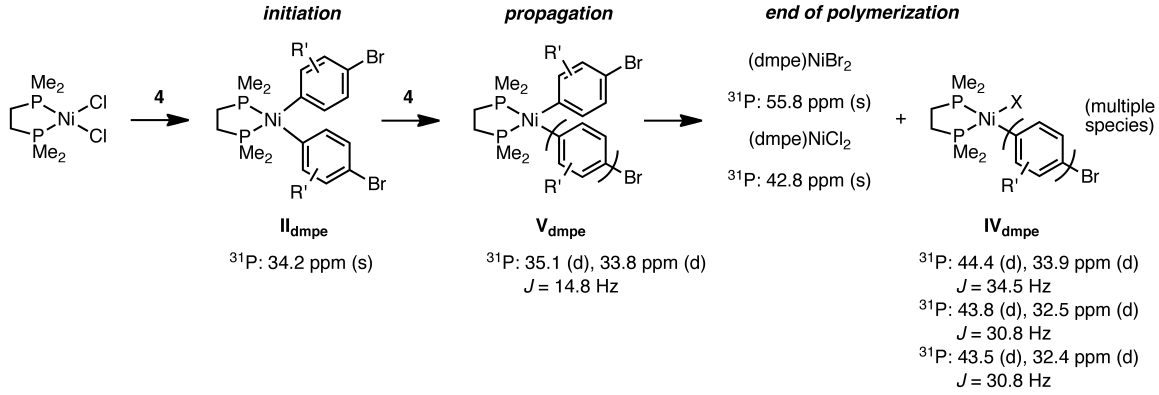

Spectroscopic Studies: Summary. Combined, the ^{31}P NMR spectroscopic studies described above provide evidence for each intermediate depicted in the initiation sequence (Scheme 4.1) as well as two of the three intermediates in the chain-growth polymerization (Scheme 4.2). A summary of the results is provided in Table 2. The lower reactivity of catalyst **1** compared to catalyst **2** can be explained by its decomposition as well as decreased steric properties. On the other hand, the lower reactivity of catalyst **3** compared to catalyst **2** can be explained by a change in rate-determining step to transmetalation and a corresponding reduction in rate due to the increased steric crowding at the metal center. Furthermore, the spectroscopic studies implicated an uncontrolled mechanism for catalyst **3**. Finally, the low molecular weight tail observed in the polymerizations with Ni(depe)Cl_2 apparently stem from a slow initiation process relative to propagation.

Table 4.2. Results of Spectroscopic Studies for Reaction of Monomer **4a** with Selected Ni Catalysts.[a]

	Initiation		Propagation	
Catalyst	**Resting-State**	**Proposed RDS**	**Resting-State**	**Proposed RDS**
$Ni(dmpe)Cl_2$	$\mathbf{II_{dmpe}}$	reductive elimination	$\mathbf{V_{dmpe}}$	reductive elimination
$Ni(depe)Cl_2$	$\mathbf{II_{depe}}$	reductive elimination	$\mathbf{V_{depe}}$	reductive elimination
$Ni(dcpe)Cl_2$	$\mathbf{Ia_{dcpe}}$ + $\mathbf{Ib_{dcpe}}$	transmetalation	$\mathbf{IV_{dcpe}}$ + $\mathbf{Ib_{dcpe}}$	transmetalation
$Ni(dppe)Cl_2$[11]	n/a	n/a	$\mathbf{V_{dppe}}$	reductive elimination
$Ni(dppp)Cl_2$[12]	n/a	n/a	$\mathbf{IV_{dppp}}$	transmetalation

a. RDS is the rate-determining step of the reaction.

Evidence for Chain-Growth Polymerization of Monomer 4a with $Ni(depe)Cl_2$ (2). Additional studies were undertaken to determine whether the polymerization of monomer **4a** using catalyst **2** was indeed chain-growth. As seen in Figure 4A, the number-average molecular weight (M_n) increased linearly with conversion, which is consistent with a chain-growth mechanism. To provide further support, complex **6a** was synthesized and used as an initiator for the polymerization of monomer **4a**. A chain-growth polymerization using initiator **6a** should lead to polymers with tolyl/H end-groups. Indeed, the MALDI-TOF-MS analysis of the crude polymer sample showed that nearly all of the polymer chains contained the tolyl/H end-groups, consistent with a chain-growth polymerization (Figure 4.4B and Appendix 3). Combined, these data suggest that

depe is an effective ligand and leads to chain-growth polymerizations of monomer **4a**. Nevertheless, the spectroscopic studies indicated that the resulting chain end is not stable indefinitely. Thus, polymerizations must be intentionally terminated (i.e., quenched) to obtain specific molecular weights.

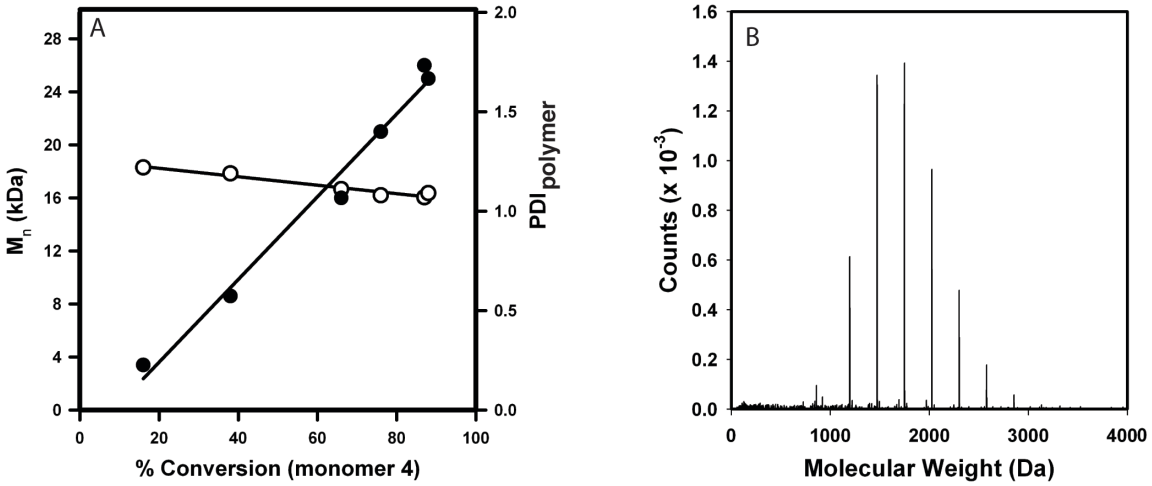

Figure 4.4. (A) Plot of M_n (●) and $PDI_{polymer}$ (○) versus conversion for the polymerization of **4a** using complex **2** at 60 °C ([Ni] = 0.0015 M; [**4a**] = 0.10 M). (B) MALDI-TOF-MS data obtained from the polymerization of **4a** using complex **6a** at 60 °C ([Ni] = 0.0015 M; [**4a**] = 0.010 M).

Rate Studies for Polymerization of Monomer 4a with Ni(depe)Cl_2 (2). To determine the influence of depe ligand on the polymerization mechanism, rate studies were performed for the Ni(depe)Cl_2-catalyzed polymerization of **4a**. The initial rates of polymerization were monitored by in situ IR analysis (see Appendix 3). As seen in Figure 5, the Ni(depe)Cl_2-catalyzed polymerization of **4a** showed a zero-order dependence on [monomer] and a first-order dependence on [catalyst]. These results were consistent with reductive elimination as the rate-determining step because this reaction does not involve the monomer (see Scheme 2). The ^{31}P NMR spectroscopic studies discussed above indicate that the catalyst resting state was complex $\mathbf{V_{depe}}$, also consistent with a rate-limiting reductive elimination.

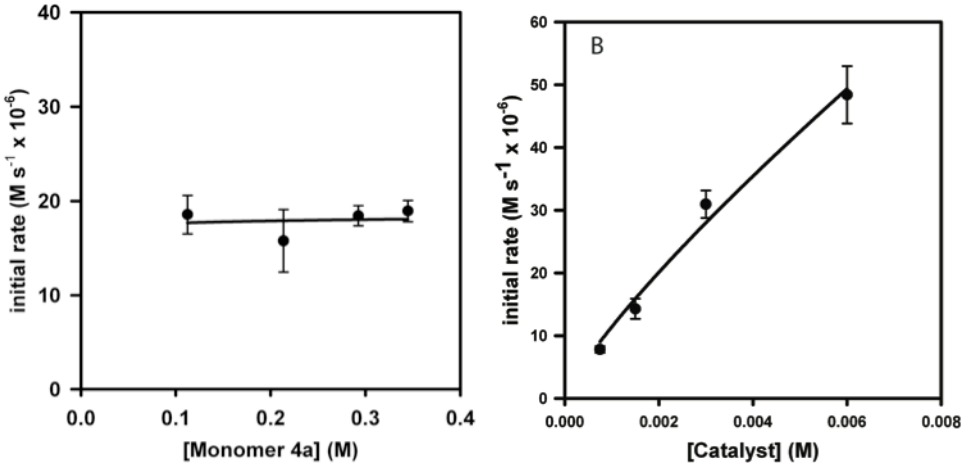

Figure 4.5. (A) Plot of the initial rate versus [monomer] for the polymerization of **4a** in THF at 50 °C ([**2**] = 0.0015 M). The curve depicts an unweighted least-squares fit to the expression initial rate = a[monomer]^n that gave a = 18 ± 3and n = -0.02 ± 0.01. (B) Plot of the initial rate versus [catalyst] for the polymerization of **4a** in THF at 50 °C ([**4a**] = 0.30 M). The curve depicts an unweighted least-squares fit to the expression initial rate = a[catalyst]^n that gave a = (3 ± 1) x 10^3 and n = 0.82 ± 0.09.

Rate Studies: Comparison of dppe versus depe. Previous mechanistic studies[11,12] revealed that ligands with different bite angles exhibited different rate-determining steps for the polymerization of monomer **4a**. We now report that ligands with the same bite angles (dppe and depe) exhibited the same rate-determining steps for polymerization.[22c,36] However, the rate of polymerization was significantly slower with depe. Because the generalized cone angles[37] and bite angles[22c,36] are similar, this result cannot be attributed to steric effects. Instead, the deceleration is likely due to the increased electron-donating ability of depe,[14] as previous studies have shown that reductive eliminations were faster from electron-poor metal centers.[38,39]

Monomer Scope for Ni(depe)Cl_2 (2). To determine whether Ni(depe)Cl_2 shows improved reactivity toward other monomers, the polymerization of monomers **7** was attempted. Complex **2** was an effective initiator for **7**, providing high molecular weight polymers (19.3 kDa) with modest polydispersities (1.20). It is notable that the gel permeation chromatograms revealed low molecular weight "tailing," consistent with a slow initiation in other hands (Appendix 3).

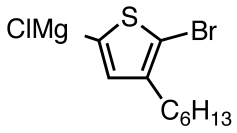

7

Conclusion

Because the ligand can tune catalyst reactivity through both steric and electronic effects, developing improved catalysts requires modifications to both aspects of the ligand scaffold. It is therefore surprising that the majority of research on these Ni-catalyzed chain-growth polymerizations has centered on two ligands (dppe and dppp). A limited number of studies have broadened the search to the structurally related diphenylphosphinoferrocene (dppf) and diphenylphosphinobutane (dppb) ligands without much success.[40] Herein, the scope of ligands investigated was broadened to include the bis(diakylphosphino)ethane-based ligands. These phosphines were chosen because of their increased electron-donating ability (relative to dppp and dppe) and variable steric properties.

Polymerization studies indicate that ligand steric properties were critical, with the least and most hindered ligands performing poorly. Spectroscopic studies revealed that these ligands are susceptible to either decomposition ($Ni(dmpe)Cl_2$) or competing reaction pathways ($Ni(dcpe)Cl_2$). In contrast, $Ni(depe)Cl_2$ provided narrower PDI samples than the other catalysts for poly(2,5-bis(hexyloxy)phenylene). For polymerization of monomer **4a**, a chain-growth mechanism was evident and the rate-limiting step was reductive elimination. Though the mechanism is similar to dppe,[11] the relative rates of polymerization were quite different. Because dppe and depe have similar generalized cone angles[37] and bite angles,[22c,36] these results suggest that ligand-based electronic properties are also important; these effects are relatively unexplored and our current efforts are elucidating their role. $Ni(depe)Cl_2$ is also found to be an effective catalyst for chain-growth polymerization of 3-hexylthiophene. Overall, these results provide a foundation for development of alternative ligand scaffolds

by elucidating the dependence of the chain-growth mechanism on the steric properties of the ligand.

References

(1) Sheina, E. E.; Liu, J.; Iovu, M. C.; Laird, D. W.; McCullough, R. D. *Macromolecules* **2004**, *37*, 3526-3528. See also: Osaka, I.; McCullough, R. D. *Acc. Chem. Res.* **2008**, *41*, 1202-1214.

(2) Yokoyama, A.; Miyakoshi, R.; Yokozawa, T. *Macromolecules* **2004**, 37, 1169-1171. Miyakoshi, R.; Yokoyama, A.; Yokozawa, T. *Macromol. Rapid Commun.* **2004**, *25*, 1663-1666. See also: Yokozawa, T.; Yokoyama, A. *Chem. Rev.* **2009**, *109*, 5595-5619.

(3) For recent examples of block copolymers prepared via this method, see: (a) Ge, J.; He, M.; Qiu, F.; Yang, Y. *Macromolecules* **2010**, *43*, 6422-6428. (b) Hollinger, J.; Jahnke, A. A.; Coombs, N.; Seferos, D. S. *J. Am. Chem. Soc.* **2010**, *132*, 8546-8547. (c) Van den Bergh, K.; Cosemans, I.; Verbiest, T.; Koeckelberghs, G. *Macromolecules* **2010**, *43*, 3794-3800. (d) Clément, S.; Meyer, F.; De Winter, J.; Coulembier, O.; Vande Velde, C. M. L.; Zeller, M.; Gerbaux, P.; Balandier, J.-Y.; Sergeyev, S.; Lazzaroni, R.; Geerts, Y.; Dubois, P. *J. Org. Chem.* **2010**, *75*, 1561-1568. (e) Zhang, Y.; Tajima, K.; Hashimoto, K. *Macromolecules* **2009**, *42*, 7008-7015. (f) Wu, P.-T.; Ren, G.; Li, C.; Mezzenga, R.; Jenekhe, S. A. *Macromolecules* **2009**, *42*, 2317-2320.

(4) Locke, J. R.; McNeil, A. J. *Macromolecules* **2010**, *43*, 8709-8710.

(5) For recent examples of chain-growth polymerization of thiophene derivatives, see: (a) Wang, C.; Kim, F. S.; Ren, G.; Xu, Y.; Pang, Y.; Jenekhe, S. A.; Jia, L. *J. Polym. Sci., Part A: Polym. Chem.* **2010**, *48*, 4681-4690. (b) Wu, S.; Sun, Y.; Huang, L.; Wang, J.; Zhou, Y.; Geng, Y.; Wang, F. *Macromolecules* **2010**, *43*, 4438-4440. (c) Benanti, T. L.; Kalaydjian, A.; Venkataraman, D. *Macromolecules* **2008**, *41*, 8312–8315. (d) Li, Y.; Xue, L.; Xia, H.; Xu, B.; Wen, S.; Tian W. *J. Poly. Sci., Part A: Polym. Chem.* **2008**, *46*, 3970-3984. (e) Ouhib, F.; Dkhissi, A.; Iratçabal, P.; Hiorns, R. C.; Khoukh, A.; Desbrières, J.; Pouchan, C.; Dagron-Lartigau, C. *J. Poly. Sci., Part A: Polym. Chem.* **2008**, *46*, 7505-7516.

(6) For chain-growth polymerization of other monomers, see: (a) Stefan, M. C.; Javier, A. E.; Osaka, I.; McCullough, R. D. *Macromolecules* **2009**, *42*, 30-32. (b) Yokoyama, A.; Kato, A.; Miyakoshi, R.; Yokozawa, T. *Macromolecules* **2008**, *41*, 7271-7273. (c) Huang, L.; Wu, S.; Qu, Y.; Geng, Y.; Wang, F. *Macromolecules* **2008**, *41*, 8944-8947. (d) Wen, L.; Duck, B. C.; Dastoor, P. C.; Rasmussen, S. C. *Macromolecules* **2008**, *41*, 4576-4578. (e) Miyakoshi, R.; Shimono, K.; Yokoyama, A.; Yokozawa, T. *J. Am. Chem. Soc.* **2006**, *128*, 16012-16013.

(7) (a) Javier, A. E.; Varshney, S. R.; McCullough, R. D. *Macromolecules* **2010**, *43*, 3233-3237. (b) Wu, S.; Bu, L.; Huang, L.; Yu, X.; Han, Y.; Geng, Y.; Wang, F. *Polymer* **2009**, *50*, 6245-6251. (c) Miyakoshi, R.; Yokoyama, A.; Yokozawa, T. *Chem. Lett.* **2008**, *37*, 1022-1023. (d) See also, ref 6b.

(8) Yokozawa has postulated that the differences in π-donor abilities of the two monomers might account for the observed dependence of cross-propagation on the order of monomer addition. For reference, see 7c.

(9) Kiriy proposes that the two monomers might exhibit different "stickiness" values that influence the near random walk of the Ni0 catalyst along the polymer chain. For reference, see: Tkachov, R.; Senkovskyy, V.; Komber, H.; Sommer, J.-U.; Kiriy, A. *J. Am. Chem. Soc.* **2010**, *132*, 7803-7810.

(10) (a) Beryozkina, T.; Senkovskyy, V.; Kaul, E.; Kiriy, A. *Macromolecules* **2008**, *41*, 7817-7823. (b) Miyakoshi, R.; Yokoyama, A.; Yokozawa, T. *J. Am. Chem. Soc.* **2005**, *127*, 17542-17547. (c) Iovu, M. C.; Sheina, E. E.; Gil, R. R.; McCullough, R. D. *Macromolecules* **2005**, *38*, 8649-8656. (d) See also, ref 9.

(11) Lanni, E. L.; McNeil, A. J. *J. Am. Chem. Soc.* **2009**, *131*, 16573-16579.

(12) Lanni, E. L.; **McNeil, A. J.** *Macromolecules* **2010**, *43*, 8039-8044.

(13) Ni0-arene π-complexes have previously been implicated as intermediates in oxidative addition reactions. For examples, see (a) Li, T.; García, J. J.; Brennessel, W. W.; Jones, W. D. *Organometallics* **2010**, *29*, 2430-2445. (b) Johnson, S. A.; Taylor, E. T.; Cruise, S. J. *Organometallics* **2009**, *28*, 3842-3855. (c) Yoshikai, N.; Matsuda, H.; Nakamura, E. *J. Am. Chem. Soc.* **2008**, *130*, 15258-15259. (d) Zenkina, O. V.; Karton, A.; Freeman, D.; Shimon, L. J. W.; Martin, J. M. L.; van der Boom, M. E. *Inorg. Chem*. **2008**, *47*, 5114-5121. (e) Ateşin, T. A.; Li, T.; Lachaize, S.; García, J. J.; Jones, W. D. *Organometallics* **2008**, *27*, 3811-3817. (f) Johnson, S. A.; Huff, C. W.; Mustafa, F.; Saliba, M. *J. Am. Chem. Soc.* **2008**, *130*, 17278-17280. (g) Reinhold, M.; McGrady, J. E.; Perutz, R. N. *J. Am. Chem. Soc.* **2004**, *126*, 5268-5276. (h) García, J. J.; Brunkan, N. M.; Jones, W. D. *J. Am. Chem. Soc.* **2002**, *124*, 9547-9555. (i) Braun, T.; Cronin, L.; Higgitt, C. L.; McGrady, J. E.; Perutz, R. N.; Reinhold, M. *New J. Chem*. **2001**, *25*, 19-21. (j) Bach, I.; Pörschke, K.-R.; Goddard, R.; Kopiske, C.; Krüger, C.; Rufińska, A.; Seevogel, K. *Organometallics* **1996**, *15*, 4959-4966.

(14) Depe is estimated to be more electron-donating than dppe and dppp based on the CO stretching frequencies in related complexes $Ni(CO)_3L$ where L is either PEt_3 (2061.7 cm-1) or $PEtPh_2$ (2066.7 cm-1). For reference, see: Tolman, C. A. *J. Am. Chem. Soc.* **1970**, *92*, 2953-2956. A more recent report using *cis*-Mo[diphosphine]$(CO)_4$ provides a CO stretching frequency for depe (2012 cm^{-1}) and dppe (2021.4 cm^{-1}). For reference, see: ref 38a.

(15) Electron-donating ligands were previously shown to increase olefin-binding affinities in related Ni0-olefin π-complexes. For reference, see: Tolman, C. A.; Seidel, W. C.; Gosser, L. W. *Organometallics* **1983**, *2*, 1391-1396.

(16) To date, studies probing the influence of steric properties in the polymerization have focused largely on steric properties of monomers and the aryl-functionalized initiators. For recent examples, see: (a) Tkachov, R.; Senkovskyy, V.; Komber, H.; Kiriy, A. *Macromolecules* **2011**, DOI: 10.1021/ma102724y. (b) Doubina, N.; Paniagua, S. A.; Soldatova, A. V.; Jen. A. K. Y.; Marder, S. R.; Luscombe, C. K. *Macromolecules* **2011**, *44*, 512-520. (c) Boyd, S. D.; Jen, A. K.-Y.; Luscombe, C. K. *Macromolecules* **2009**, *42*, 9387-9389. (d) Doubina, N.; Ho, A.; Jen, A. K.-Y.; Luscombe, C. K. *Macromolecules* **2009**, *42*, 7670-7677.

(17) Syntheses were adapted from: Angulo, I. M.; Bouwman, E.; Lutz, M.; Mul, W. P.; Spek, A. L. *Inorg. Chem*. **2001**, *40*, 2073-2082.

(18) Tolman, C. A. *Chem. Rev.* **1977**, *77*, 313-348.

(19) Immirzi, A.; Musco, A. *Inorg. Chim. Acta* **1977**, *25*, L41-L42.

(20) Niksch, T.; Görls, H.; Weigand, W. *Eur. J. Inorg. Chem*. **2010**, 95-105.

(21) Casey, C. P.; Whiteker, G. T. *Isr. J. Chem.* **1990**, *20*, 299-303.

(22) For leading references on bite-angle effects in cross-coupling reactions, see: (a) Gillespie, J. A.; Dodds, D. L.; Kamer, P. C. J. *Dalton Trans.* **2010**, *39*, 2751-2764. (b) Birkholz, M.-N.; Freixa, Z.; van Leeuwen, P. W. N. M. *Chem. Soc. Rev.* **2009**, *38*, 1099-1118. (c) van Leeuwen, P. W. N. M.; Kamer, P. C. J.; Reek, J. N. H.; Dierkes, P. *Chem. Rev.* **2000**, *100*, 2741-2769. (d) Dierkes, P.; van Leeuwen, P. W. N. M. *Dalton Trans.* **1999**, 1519-1529.

(23) Monomers **4a**, **4b**, **7**, and **8** were prepared in situ via Grignard metathesis reaction with iPrMgCl. For leading references, see: (a) Shi, L.; Chu, Y.; Knochel, P.; Mayr, H. *Org. Lett.* **2009**, *11*, 3502-3505. (b) Shi, L.; Chu, Y.; Knochel, P.; Mayr, H. *J. Org. Chem.* **2009**, *74*, 2760-2764.

(24) Note that although the polymer peak was consistently narrow, the overall PDIs (including the tail) would fluctuate between 1.3 and 2.3 with Ni(depe)Cl_2. We were unable to trace these fluctuations to any specific variable (i.e., catalyst batch, age of i-PrMgCl, student, etc).

(25) Using hindered Grignard reagents, Kiriy and coworkers recently observed the product of a single transmetalation reaction with Ni(dppe)Cl_2 and Ni(dppp)Cl_2. For reference, see: Senkovskyy, V.; Sommer, M.; Tkachov, R.; Komber, H.; Huck, W. T. S.; Kiriy, A. *Macromolecules* **2010**, *43*, 10157-10161.

(26) Lamps and Catala reported polymerization rate profiles with two distinct regions and suggested that the first region (~10% conversion of monomer) corresponded to initiation and oligomer formation. For reference, see: Lamps, J.-P.; Catala, J.-M. *Macromolecules* **2009**, *42*, 7282-7284.

(27) In our previous studies with Ni(dppe)Cl_2 (ref 11) we tentatively assigned a singlet in the ^{31}P NMR spectrum (48.5 ppm) which inconsistently appeared as Ni(dppe)$_2X_2$. Based on the data presented in this manuscript, it is also possible that it corresponds to the Ni(dppe)(aryl)$_2$ which forms during initiation.

(28) Boutry, O.; Nicasio, M. C.; Paneque, M.; Carmona, E.; Gutiérrez, E.; Ruiz, C. *J. Organomet. Chem.* **1993**, *444*, 245-250.

(29) A related biaryl complex, (depe)Pt(2,2′-biphenyl), has been reported with a chemical shift of 54.7 ppm in the ^{31}P NMR spectrum. For reference, see: Edelbach, B. L.; Lachicotte, R. J.; Jones, W. D. *J. Am. Chem. Soc.* **1998**, *120*, 2843-2853.

(30) Ni(depe)Br_2 is reported to have a chemical shift of 83.5 ppm in 1:1 $CDCl_3$:$CHCl_3$. For reference, see: Jarrett, P. S.; Sadler, P. J. *Inorg. Chem*. **1991**, *30*, 2098-2104.

(31) A similar reaction was observed in the synthesis of phenyl-functionalized Ni initiators with PPh_3 as the ligand. For reference, see: Smeets, A.; Van den Bergh, K.; De Winter, J.; Gerbaux, P.; Verbiest, T.; Koeckelberghs, G. *Macromolecules* **2009**, *42*, 7638-7641. See also: Tsou, T. T.; Kochi, J. K. *J. Am. Chem. Soc.* **1979**, *101*, 7547-7560.

(32) The ^{31}P NMR spectroscopy experiments were performed at higher concentrations of nickel ([Ni] = 0.03 M) compared to the lab-scale polymerizations ([Ni] = 0.0015 M).

(33) Though not understood at this time, the downfield resonances are substantially broadened at these elevated temperatures (see Supporting Information).

(34) For examples of phosphine ligand-based steric effects in reductive eliminations, see: (a) Yamashita, M.; Hartwig, J. F. *J. Am. Chem. Soc.* **2004**, *126*, 5344-5345. (b) Shelby, Q.; Kataoka, N.; Mann, G.; Hartwig, J. *J. Am. Chem. Soc.* **2000**, *122*, 10718-10719. (c) Mann, G.; Incarvito, C.; Rheingold, A. L.; Hartwig, J. F. *J. Am. Chem. Soc.* **1999**, *121*, 3224-3225. (d) Ref 38f.

(35) For recent examples of phosphine ligand-based steric effects in transmetalation reactions, see: (a) Ariafard, A.; Yates, B. F. *J. Am. Chem. Soc.* **2009**, *131*, 13891-13991. (b) Clarke, M. L.; Heydt, M. *Organometallics* **2005**, *24*, 6475-6478.

(36) Raebiger, J. W.; Miedaner, A.; Curtis, C. J.; Miller, S. M.; Anderson, O. P.; DuBois, D. L. *J. Am. Chem. Soc.* **2004**, *126*, 5502-5514.

(37) The generalized equivalent cone angles for dppe (177°) and depe (175°) are similar. See ref 20.

(38) For leading references on phosphine ligand-based electronic effects in reductive eliminations, see: (a) Korenaga, T.; Abe, K.; Ko, A.; Maenishi, R.; Sakai, T. *Organometallics* **2010**, *29*, 4025-4035. (b) Ariafard, A.; Yates, B. F. *J. Organomet. Chem.* **2009**, *694*, 2075-2084. (c) Hartwig, J. F. *Inorg. Chem.* **2007**, *46*, 1936-1947. (d) Ananikov, V. P.; Musaev, D. G.; Morokuma, K. *Eur. J. Inorg. Chem.* **2007**, 5390-5399. (e) Culkin, D. A.; Hartwig, J. F. *Organometallics* **2004**, *23*, 3398-3416. (f) Mann, G.; Shelby, Q.; Roy, A. H.; Hartwig, J. F. *Organometallics* **2003**, *22*, 2775-2789. (g) Yamashita, M.; Cuevas Vicario, J. V.; Hartwig, J. F. *J. Am. Chem. Soc.* **2003**, *125*, 16347-16360. (h) Hamann, B. C.; Hartwig, J. F. *J. Am. Chem. Soc.* **1998**, *120*, 3694-3703.

(39) Hartwig, J. F. Reductive Elimination. *Organotransition Metal Chemistry*; University Science Books: Sausalito, CA, 2010; pp 321-348.

(40) For a recent example, see: Miyakoshi, R.; Yokoyama, A.; Yokozawa, T. *J. Polym. Sci., Part A: Polym. Chem.* **2008**, *46*, 753-765.

Chapter 5[1]

Conclusion and Future Directions

The discovery of a chain-growth method represents a major advance in the synthesis of π-conjugated polymers, but highly specific conditions have limited its scope and utility. Because the mechanistic influence of each reagent remains unclear, it has become common practice to screen a variety of reaction conditions. As ligands and additives are optimized independently for each monomer, the synthesis of even simple block copolymers becomes challenging. The requirement for specialized reaction conditions suggests that the desired chain-growth pathway is competing with others, including chain-transfer and termination. Catalyst decomposition is also a concern; Luscombe[1] and Kiriy[2] independently reported that monomers lacking substituents ortho to the halogen are less effective for chain-growth. Kiriy hypothesized that the substituent stabilizes the Ni(II)aryl halide species from undergoing bimolecular disproportionation. Major advances in this field will only be obtained when all competing pathways are identified and the role of each reagent in determining the reaction outcome is understood. Some progress toward this goal has been made; for example, our group demonstrated that LiCl, an additive reported to be essential for the Ni(dppe)Cl_2-catalyzed chain-growth polymerization of (2,5-bishexyloxy)phenylene,[3] was unnecessary if the catalyst is pre-initiated with 5-7 equiv of monomer. These results suggest that LiCl plays a role in initiation but not propagation.[4] On the other hand, our group showed that LiCl can have a rate-accelerating or rate-decelerating effect depending on its concentration in the Ni(dppp)Cl_2-catalyzed polymerizations.[5] Thus, the role of additives is not

---

[1] Excerpted from the manuscript version of McNeil, A. J.; Lanni, E. L. "New Conjugated Polymers and Synthetic Methods." In *Synthesis of Polymers*; Hawker, C.; Junji, S.; Schlüter, D., Eds. Wiley-VCH: Weinheim Germany. *In press.*

universal but instead depends on the catalyst structure and rate-determining step of the reaction. As a result, more rate and spectroscopic studies are needed to obtain a complete mechanistic understanding of the Ni-catalyzed chain-growth polymerization. To that end, future work in our group is focused on understanding the electronic effect of different substituent's on the phosphine ligand in each elementary step of the reaction. We are also continuing to look for firm evidence of the postulated nickel-aryl π-complex through competition experiments. Finally, members of the group have begun to explore the ability of other ligand scaffolds, such as *N*-heterocyclic carbenes, and metals to successfully synthesize conjugated polymers.

Conclusion and Outlook

The remarkable discovery of a chain-growth method for preparing π-conjugated polymers has sparked renewed interest in their synthesis and application, as well as provided access to new polymers and composite materials. Even the simplest new materials – all-conjugated thiophene block copolymers – have shown unique solubilities[6] optical properties,[7] solution aggregates,[8] and phase separation behavior in thin films.[9] However, work in this area has been hindered by the difficulties in obtaining chain-growth conditions for each specific copolymer system. Therefore, the primary focus over the next decade should be in three main directions: (1) Gaining a mechanistic understanding and improving the synthetic method. (2) Applying the chain-growth method to prepare polymers with more complex architectures (e.g., graft, star, and hyperbranched copolymers). (3) Preparing well-defined materials to probe structure-property relationships. The results reported herein suggest that this method is poised to produce new, well-defined materials that will have a significant impact on future applications of π-conjugated polymers.

---

(1) S. D. Boyd, A. K.-Y. Jen, and C. K. Luscombe, *Macromolecules*, **42**, 9387 (2009).

(2) Beryozkina, T.; Senkovskyy, V.; Kaul, E.; Kiriy, A. *Macromolecules* **2008**, *41*, 7817.

(3) Miyakoshi, R.; Shimono, K.; Yokoyama, A.; Yokozawa, T. *J. Am. Chem. Soc*. **2006**, *128*, 16012.

(4) Lanni, E. L.; McNeil, A. J. *J. Am. Chem. Soc.* **2009**, *131*, 16573.

(5) Lanni, E. L.; McNeil, A. J. *Macromolecules* **2010**, *43*, 8039.

(6) Yokozawa, T.; Adachi, I.; Miyakoshi, R.; Yokoyama, A. *High Perform. Polym*. **2007**, *19*, 684.

(7) Ohshimizu, K.; Ueda, M. *Macromolecules* **2008**, *41*, 5289.

(8) Van den Bergh, K.; Cosemans, I.; Verbiest, T.; Koeckelberghs, G.; *Macromolecules* **2010**, *43*, 3794.

(9) Zhang, Y.; Tajima, K.; Hashimoto, K.; *Macromolecules* **2009**, *42*, 7008.

Appendix 1

Appendix to Chapter 2: Mechanistic Studies on Ni(dppe)Cl_2-catalyzed Chain-Growth Polymerizations: Evidence for Rate-Determining Reductive Elimination.

I. Materials

Flash chromatography was performed on SiliCycle silica gel (40-63 μm) and thin layer chromatography was performed on Merck TLC plates pre-coated with silica gel 60 F254. *i*-PrMgCl (2M in THF) was purchased in 100 mL quantities from Aldrich and Ni(dppe)Cl_2 was purchased from Strem. All other reagent grade materials and solvents were purchased from Aldrich, Acros, EMD, or Fisher and used without further purification unless otherwise noted. THF was dried and deoxygenated using an Innovative Technology (IT) solvent purification system composed of activated alumina, copper catalyst, and molecular sieves. *N*-bromosuccinimide was recrystallized from hot water and dried over P_2O_5. Tridecane was distilled from sodium/benzophenone. Benzene was distilled from calcium hydride. Compounds **1**, **2a**, **2b**, **S2**, **S6** and **S7** were prepared from modified procedures reported by Yokozawa et al.[1,2] Mg-anthracene,[3] and compounds **4**,[4] **5**,[5] **6**,[5] **7**,[6] **8**,[7] **S1**,[8] **S3**,[9] **S4**,[10] **S5**,[11] and **S8**[12] were prepared from modified literature procedures (see Synthetic Procedures for full details).

II. General Experimental

NMR Spectroscopy: Unless otherwise noted, ^{1}H, ^{13}C, and ^{31}P NMR spectra for all compounds were acquired in $CDCl_3$ on a Varian MR400 or a Varian Inova 400 Spectrometer operating at 400, 100, and 161 MHz, respectively. For ^{1}H and ^{13}C NMR spectra the chemical shift data are reported in units of δ (ppm) relative to tetramethylsilane (TMS) and referenced with residual solvent. ^{31}P NMR spectra were referenced to external H_3PO_4 (85% aq). Multiplicities are reported as follows: singlet (s), doublet (d), doublet of doublets (dd), multiplet (m), and broad resonance (br). Unless otherwise indicated, the ^{1}H, ^{31}P and ^{13}C NMR spectra were recorded at room temperature. Note that integrations for protons on the alkyl chains of some compounds are high due to insufficient relaxation time.

IR Spectroscopy: Samples were recorded using a Mettler Toledo ReactIR iC10 fitted with a Mercury Cadmium Telluride (MCT) detector, and AgX 9.5 mm x 1.5 mm probe with a SiComp tip. Unless otherwise indicated, spectra were processed using icIR 4.0 software and raw absorbances were exported into Microsoft Excel or Sigma Plot 10 for analysis.

Mass Spectrometry: HRMS data were obtained on a Micromass AutoSpec Ultima Magnetic Sector mass spectrometer.

Gel-Permeation Chromatography: Polymer molecular weights were determined by comparison with polystyrene standards (Varian, EasiCal PS-2 MW 580-377,400) on a Waters 1515 HPLC instrument equipped with Waters Styragel® (7.8 x 300 mm) THF HR 0.5, THF HR 1, and THF HR 4 type columns in sequence and analyzed with Waters 2487 dual absorbance detector (254 and 350 nm). Samples were dissolved in THF (with mild heating), and passed through a 0.2 μm PTFE filter prior to analysis.

Gas Chromatography: Gas chromatography was carried out using a Shimadzu GC 2010 using a Shimadzu SHRX5 (crossbound 5% diphenyl – 95% dimethyl polysiloxane; 15 m, 0.25 mmID, 0.25 μm df) column.

Titrations: For **2a** and **2b**: an accurately weighed sample of salicylaldehyde phenylhydrazone[13] (typically between 290 - 310 mg) was dissolved in 5.00 mL of THF. A 0.20 mL aliquot of this solution was stirred at rt while ArMgCl was added dropwise using a 250 μL syringe. The initial solution is yellow and turns bright orange at the end-point. For **6**: a solution of 25 μL of tridecane in 1.0 mL of the Grignard solution was quenched with methanol. An aliquot of this solution was withdrawn, diluted with $CHCl_3$, analyzed by GC and the concentration determined using a calibration curve (see page S36).

Statistical Analysis: Reported quantitative data represents the average of 2-3 experiments and the error bars represent the standard deviation in these measurements. In cases where the error bars were greater than 10% of the average value, the experiments were repeated an additional 2-3 times and these values were included in the average and standard deviation calculations.

III. Synthetic Procedures

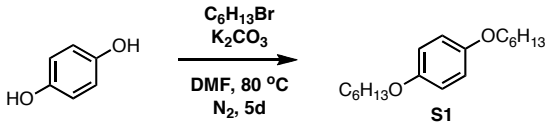

S1. A 500 mL flask was equipped with a stir bar. Sequentially, hydroquinone (20 g, 0.2 mol, 1.0 equiv), anhydrous DMF (120 mL), potassium carbonate (63 g, 0.45 mol, 2.5 equiv), and 1-bromohexane (63 mL, 0.45 mol, 2.5 equiv) were added to the flask. The reaction mixture was stirred vigorously under N_2 at 80 °C for 5 d. After cooling to rt, the reaction mixture was poured into water (400 mL). The mixture was extracted with hexanes (3 x 200 mL). The organic layer was washed with water (2 x 200 mL) and brine (1 x 200 mL), then dried over anhydrous $MgSO_4$, filtered, and concentrated in vacuo. The resulting oil was passed through silica gel using neat CH_2Cl_2 as the eluent. Finally, recrystallization from hot methanol gave 44 g of **S1** as a white, crystalline solid (88% yield). HRMS (EI): Calcd. for $C_{18}H_{30}O_2$, 278.2246 [M+]; found, 278.2251.

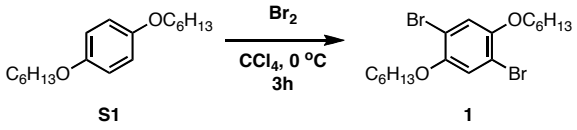

1. A 500 mL flask was equipped with a stir bar. Sequentially, **S1** (22 g, 0.79 mol, 1.0 equiv) and CCl_4 (90 mL) were added to the flask. The reaction mixture was cooled to 0 °C in an ice/water bath and fitted with an addition funnel. Bromine (10 mL, 0.20 mol, 2.5 equiv) was added dropwise under N_2 and the pressure was vented through an aq solution of 10% Na_2SO_3 (~150 mL). After 3 h, the reaction was quenched with an aq saturated solution of Na_2SO_3 and vigorously stirred until colorless. The aqueous mixture was extracted with CH_2Cl_2 (3 x 100 mL) and

the combined organic layers were washed with water (2 x 100 mL) and brine (1 x 100 mL), then dried over $MgSO_4$, filtered, and concentrated in vacuo. The residue was recrystallized from CH_2Cl_2-ethanol to give 27 g (80% yield) of **1** as white crystals. HRMS (EI): Calcd. for $C_{18}H_{28}Br_2O_2$, 434.0456 [M+]; found, 434.0451.

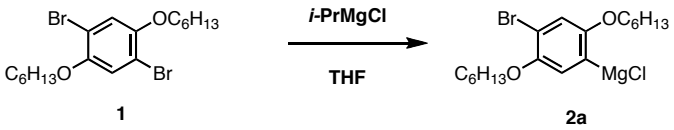

1 **2a**

2a. All actions were performed in a glovebox under N_2 atmosphere. A 200 mL flask was equipped with a stir bar. Sequentially, **1** (14.4 g, 33.0 mmol, 1.00 equiv), THF (35 mL), and *i*-PrMgCl (15 mL, 30 mmol, 0.9 equiv) were added to the flask. The reaction mixture was stirred at rt overnight.

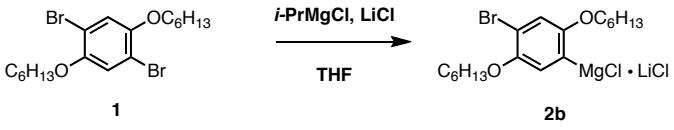

1 **2b**

2b. All actions were performed in a glovebox under N_2 atmosphere. A 200 mL flask was equipped with a stir bar. Sequentially, **1** (14.4 g, 33.0 mmol, 1.00 equiv), THF (35 mL), LiCl (1.3 g, 30 mmol, 0.90 equiv) and *i*-PrMgCl (15 mL, 30 mmol, 0.90 equiv) were added to the flask. The reaction mixture was stirred at rt overnight.

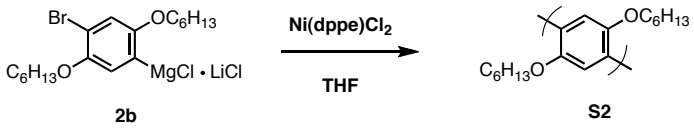

2b **S2**

S2. In the glovebox an oven-dried 50 mL Schlenk flask containing a stir bar was charged with THF (6.6 mL) and **2b** (2.4 mL, 0.96 mmol, 0.40 M solution, 1.0 equiv). The flask was removed from the box, placed under N_2 and cooled to 0 ^oC. After 5 min, the pre-initiated catalyst solution (1 mL, 0.015 mmol, 0.015 M solution, 0.015 equiv) was injected. After 3 h the reaction was quenched with HCl (5 mL, 5 M) then extracted with $CHCl_3$ (3 x 5 mL). The combined organic layers were washed with water (2 x 5 mL) and brine (1 x 5 mL), dried over $MgSO_4$, filtered, and concentrated in vacuo. The resulting solid was washed with methanol to give 162 mg of **S2** as a white solid (60% yield)

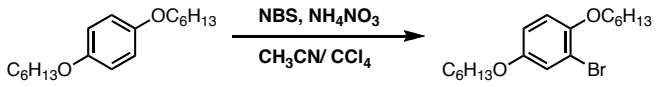

S1 **S3**

S3. A 4 mL vial was equipped with a stir bar. Sequentially, **S1** (0.50 g, 1.8 mmol, 1.0 equiv), acetonitrile (2.0 mL), CCl_4 (0.25 mL), *N*-bromosuccinimide (0.32 g, 1.8 mmol, 1.0 equiv), and NH_4NO_3 (14 mg, 0.2 mmol, 0.2 equiv) were added and the mixture allowed to stir at rt. After ~18 h, the reaction mixture was poured into water (10 mL). The aqueous mixture was extracted with EtOAc (3 x 10 mL) and the combined organic layers were washed with water (2 x 10 mL) and brine (1 x 10 mL), then dried over $MgSO_4$, filtered, and concentrated in vacuo. The resulting oil was purified on silica gel, using 10-20% toluene in hexanes as the eluent to give 225 mg of **S3** as a clear colorless oil (35% yield). HRMS (EI): Calcd. for $C_{18}H_{29}BrO_2$, 356.1351 [M+]; found 356.1346.

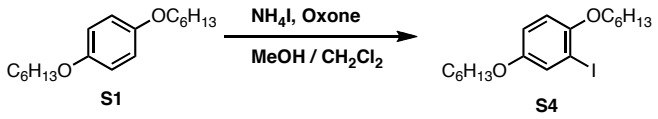

S4. A 100 mL flask was equipped with a stir bar. Sequentially, **S1** (0.55 g, 2.0 mmol, 1.0 equiv), methanol (9 mL), dichloromethane (2 mL), ammonium iodide (0.32 g, 2.2 mmol, 1.1 equiv) and Oxone® (1.3 g, 2.2 mmol, 1.1 equiv) were added to the flask. The dark orange reaction mixture was stirred vigorously under N_2 at rt until complete conversion was observed by GC analysis and the mixture had turned pale orange (~ 36 h). The remaining Oxone® was quenched with 10% aq Na_2SO_3. The aqueous mixture was extracted with CH_2Cl_2 (3 x 20 mL) and the combined organic layers were washed with water (2 x 20 mL) and brine (1 x 20 mL), then dried over $MgSO_4$, filtered, and concentrated in vacuo. The resulting oil was purified on silica gel, using 10-20% toluene in hexanes as the eluent to give 350 mg **S4** as a clear colorless oil (48% yield). HRMS (EI): Calcd. for $C_{18}H_{29}IO_2$, 404.1212 [M+]; found, 404.1210.

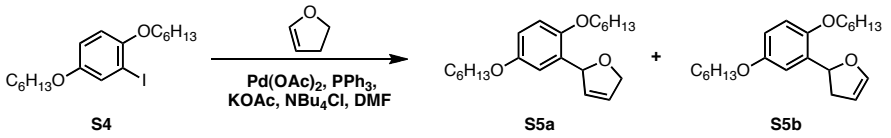

S5. An oven-dried 25 mL Schlenk tube was cooled under N_2 atmosphere and equipped with a stir bar. Sequentially, $Pd(OAc)_2$ (4 mg, 0.02 mmol, 0.04 equiv), tetrabutylammonium chloride (0.17 g, 0.76 mmol, 1.5 equiv), potassium acetate (0.22 g, 2.3 mmol, 4.6 equiv), and triphenyl phosphine (5 mg, 0.02 mmol, 0.04 equiv) were added to the tube. The tube was placed under vacuum and then refilled with N_2. After two additional cycles, **S4** (0.20 g, 0.50 mmol, 1.0 equiv), DMF (1.5 mL) and 2,3-dihydrofuran (0.29 mL, 3.8 mmol, 7.6 equiv) were added

by syringe. The tube was sealed and the reaction mixture was stirred vigorously overnight at 80 °C. After cooling to rt, the reaction mixture was washed with saturated aq NH_4Cl (2 x 10 mL) and water (1 x 10 mL). The aqueous mixture was extracted with Et_2O (3 x 10 mL) and the combined organic layers were washed with brine (1 x 10 mL) then dried over anhydrous $MgSO_4$, filtered, and concentrated in vacuo. The resulting oil was purified on silica gel using 5% ether in hexanes as the eluent to give 64 mg **S5a** (24% yield) and 63 mg **S5b** (24% yield) as clear colorless oils. **S5a**: HRMS (ESI): Calcd. for $C_{22}H_{24}O_3$, 369.2406 [M +Na]+; found, 369.2394. **S5b**: HRMS (ESI): Calcd. for $C_{22}H_{24}O_3$, 369.2406 [M +Na]+; found, 369.2394.

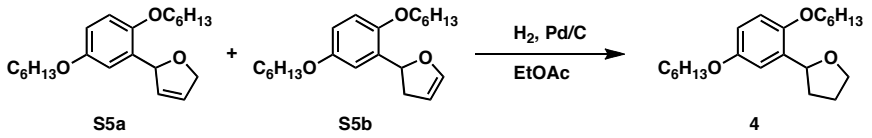

S5a S5b 4

---

4. A 50 mL oven-dried flask was cooled under N_2 atmosphere and equipped with a stir bar. Sequentially, **S5a** and **S5b** (0.21 mg combined, 0.6 mmol, 1 equiv) and 10% Pd/C (63 mg, 0.06 mmol Pd, 0.05 equiv) were added to the flask. Initially, H_2 from a balloon was bubbled through the mixture (10 min), and then the reaction was allowed to stir under H_2 atmosphere. After 1 h, the reaction mixture was filtered through Celite and concentrated in vacuo to give 0.2 g of **4** (quant.) as a clear colorless oil. HRMS (ESI): Calcd. for $C_{22}H_{36}O_3$, 371.2562 [M+Na]+; found, 371.2547.

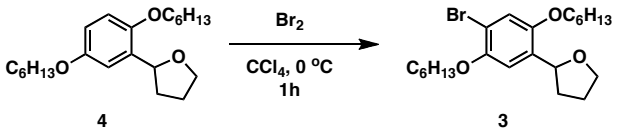

4 3

---

3. A 10 mL flask was equipped with a stir bar and an ice bath. Sequentially, **4** (60 mg, 0.16 mmol, 1 equiv), CCl_4 (1 mL) and Br_2 (10 µL, 0.16 mmol, 1 equiv) were

added to the flask which was then sealed. After 1h the reaction was quenched with aq saturated Na_2SO_3 (5 mL). The aqueous mixture was extracted with CH_2Cl_2 (3 x 5 mL) and the combined organic layers were washed with water (2 x 5 mL) and brine (1 x 5 mL), then dried over $MgSO_4$, filtered, and concentrated in vacuo. The resulting oil was purified on silica gel using 5% ether in hexanes as the eluent to give **3** as a white solid. HRMS (ESI): Calcd. for $C_{22}H_{35}BrO_3$, 449.1667 [M+Na]+; found, 449.1663.

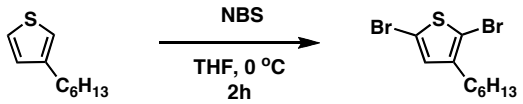

5

---

5. A 100 mL flask was equipped with a stir bar and an ice bath. Sequentially, 3-hexylthiophene (5.0 g, 30 mmol, 1.0 equiv), THF (60 mL) and *N*-bromosuccinimide (13.2 g, 74.3 mmol, 2.50 equiv) were added to the flask. The flask was then then placed under N_2. After 2h the reaction was quenched with aq saturated sodium carbonate (25 mL). The aqueous mixture was extracted with hexanes (3 x 25 mL) and the combined organic layers were washed with water (2 x 25 mL) and brine (1 x 25 mL), then dried over $MgSO_4$, filtered, and concentrated in vacuo. The resulting oil was purified by distillation (85 ^oC, 0.03 torr) followed by filtration through silica gel using hexanes as the eluent to give 7.9 g **5** as a clear oil (80% yield). HRMS (EI): Calcd. for $C_{10}H_{14}Br_2S$ [M+] 323.9183; found, 323.9176.

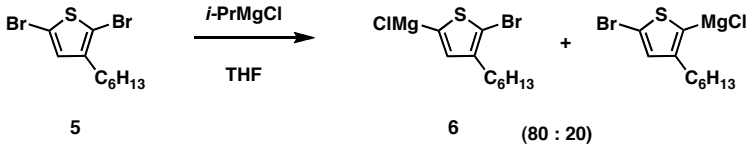

5 6 (80 : 20)

6. All actions were performed in a glovebox under N_2 atmosphere. A 25 mL Schlenk tube was equipped with a stir bar. Sequentially, **5** (2.4 g, 7.4 mmol, 1.0 equiv), THF (21 mL), and *i*-PrMgCl (3.7 mL, 7.4 mmol, 1.0 equiv) were added to the tube. The reaction mixture was stirred for 1h.

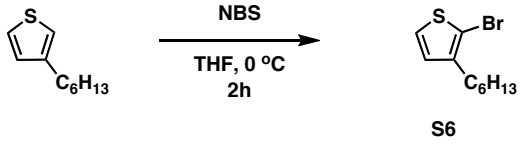

S6

S6. A 100 mL flask was equipped with a stir bar and an ice bath. Sequentially, 3-hexylthiophene (0.30 g, 1.8 mmol, 1.0 equiv), THF (10 mL) and *N*-bromosuccinimide (0.32 g, 1.8 mmol, 1.0 equiv) were added to the flask which was then placed under N_2. After 2h the reaction was quenched with aq saturated sodium carbonate (10 mL). The aqueous mixture was extracted with hexanes (3 x 10 mL) and the combined organic layers were washed with water (2 x 10 mL) and brine (1 x 10 mL), then dried over $MgSO_4$, filtered, and concentrated in vacuo. The resulting oil was purified by distillation (65 °C, 0.02 torr) followed by filtration through silica gel using hexanes as the eluent to give 5.2 g **S6** as a clear oil (70% yield). HRMS (EI): Calcd. for $C_{10}H_{15}BrS$ [M+] 246.0078; found, 246.0081.

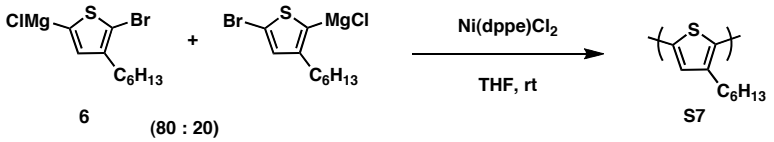

S7. In the glovebox an oven-dried 20 mL vial was equipped with a stir bar and charged with **6** (1.0 mL, 0.20 mmol, 1.0 equiv) and THF (3.5 mL). The pre-initiated catalyst solution (0.50 mL, 0.0013 mmol, 0.0063 equiv) was added. After 1 h the reaction was quenched with HCl (5 mL, 5 M) then extracted with $CHCl_3$ (3 x 5 mL). The combined organic layers were washed with water (2 x 5 mL) and brine (1 x 5 mL) and concentrated in vacuo. The resulting solid was washed with methanol to give 30 mg of **S7** as a dark purple solid (quant.).

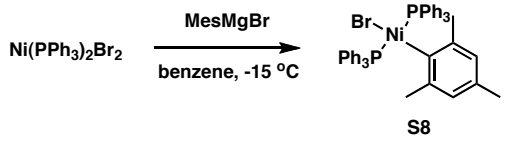

S8. In the glovebox an oven-dried 25 mL Schlenk flask was equipped with a stir bar and charged with $Ni(PPh_3)_2Br_2$ (0.44 g, 0.60 mmol, 1.0 equiv) and benzene (5 mL). The flask was removed from the box, placed under N_2 and cooled in a brine/ice bath over ~5 min. A solution of mesitylmagnesium bromide (1.1 mL, 0.82 mmol, 1.4 equiv) was added by syringe and the mixture was allowed to stir at -15 °C for 20 min. The mixture was warmed to rt and quenched with water (5 mL) then extracted with benzene (3 x 10 mL). The combined organic layers were washed with water (2 x 10 mL) and brine (1 x 10 mL), dried over $MgSO_4$, filtered, and concentrated in vacuo. The resulting solid was recrystallized from toluene/ hexanes to give 0.30 g of **S8** as an orange solid (65% yield). The product is air stable.

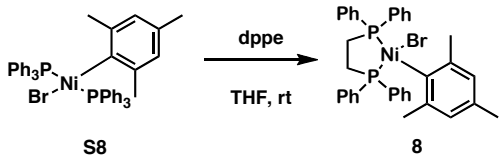

S8 8

---

8. In the glovebox an oven-dried 20 mL vial was equipped with a stir bar and charged with **S8** (0.10 g, 0.13 mmol, 1.0 equiv) and THF (5 mL). Dppe (51 mg, 0.13 mmol, 1.0 equiv) was added and the mixture stirred at room temperature for 5 min. The THF was removed under vacuuum and the resulting solid was recrystallized twice from toluene/hexanes to give 30 mg of **8** as an red-orange solid (35% yield). The product is air stable. HRMS (EI): Calcd. for $C_{35}H_{35}BrNiP_2$ [M+] 654.0751; found, 654.0748.

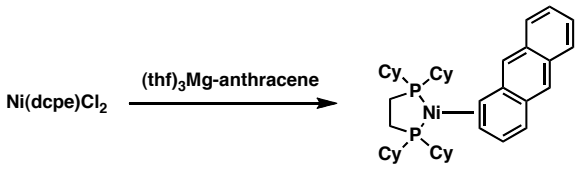

7

---

7. In the glovebox an oven-dried 8 mL vial was equipped with a stir bar and charged with Ni(dcpe)Cl_2 (75 mg, 0.14 mmol, 1.0 equiv) and THF (3 mL). A separate vial was charged with $(thf)_3$Mg-anthracene[3] (57 mg, 0.14 mmol, 1.0 equiv) and THF (3 mL). Both vials were cooled to -40 ^oC in the glovebox freezer. The vials were removed from the freezer and the $(thf)_3$Mg-anthracene solution was added to the Ni(dcpe)Cl_2 suspension with stirring. The brick red suspension became a homogenous dark red-purple solution. The solvent was removed under vacuum, the solids were extracted with hexanes and the solution was filtered. Removal of the hexanes under vacuum gave 30 mg **7** as a dark purple solid (30% yield, crude). The product is air sensitive.

IV. NMR Spectra

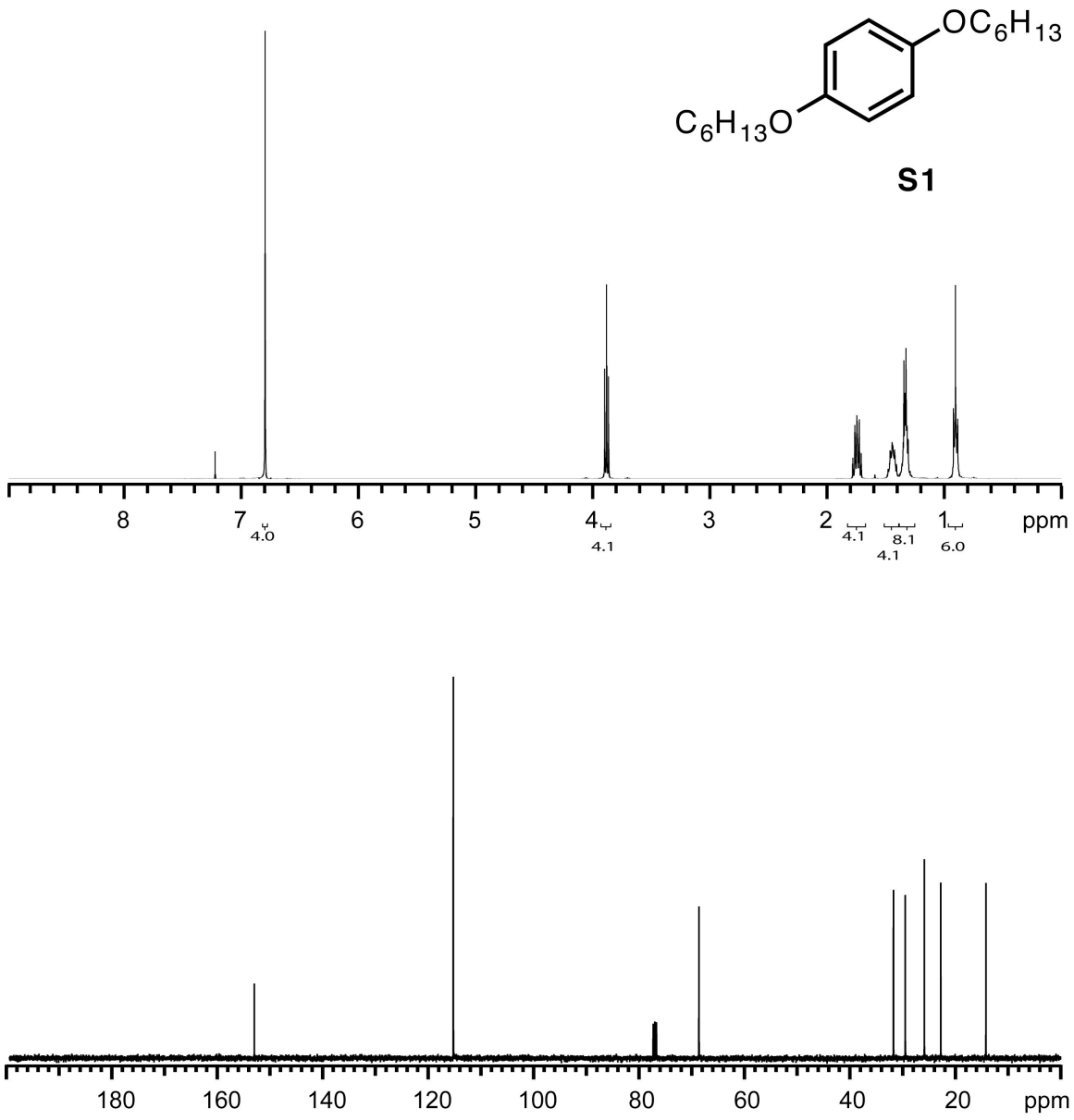

Figure S1. ^{1}H and ^{13}C NMR Spectra of S1.
^{1}H NMR (400 MHz, $CDCl_3$) δ 6.81 (s, 4H), 3.89 (t, *J* = 6.8 Hz, 4H), 1.75 (m, 4H), 1.44 (m, 4H), 1.33 (m, 8H), 0.90 (m, 6H). ^{13}C NMR (100 MHz, $CDCl_3$) δ 153.41, 115.57, 68.84, 31.84, 29.60, 25.96, 22.83, 14.24.

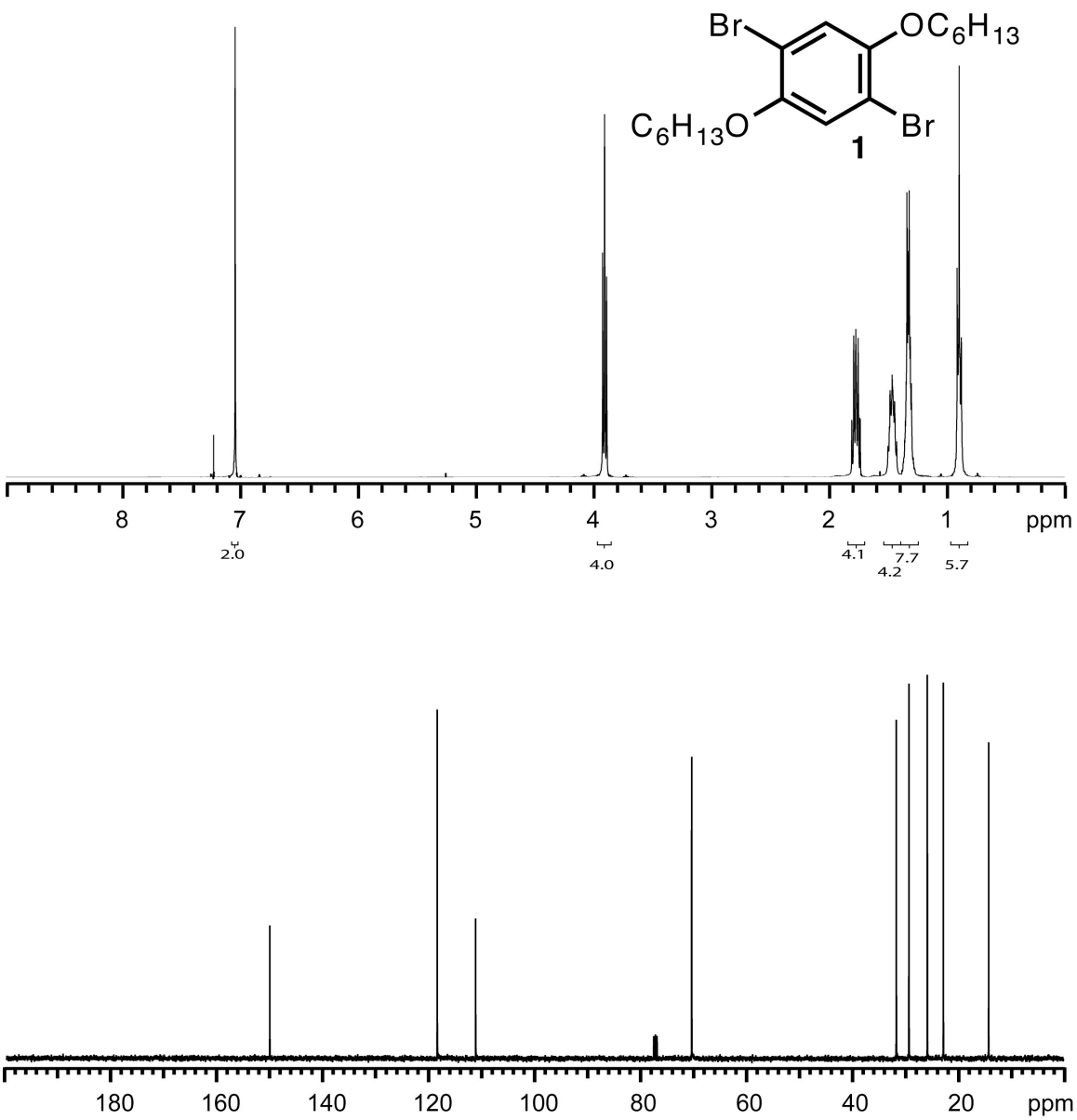

Figure S2. ^{1}H and ^{13}C NMR Spectra of 1.
^{1}H NMR (400 MHz, $CDCl_3$) δ 7.06 (s, 2H), 3.91 (t, *J* = 6.4 Hz, 4H), 1.77 (m, 4H), 1.45 (m, 4H), 1.33 (m, 8H) 0.89 (m, 6H). ^{13}C NMR (100 MHz, $CDCl_3$) δ 150.20, 118.51, 111.24, 70.36, 31.65, 29.25, 25.78, 22.74, 14.17.

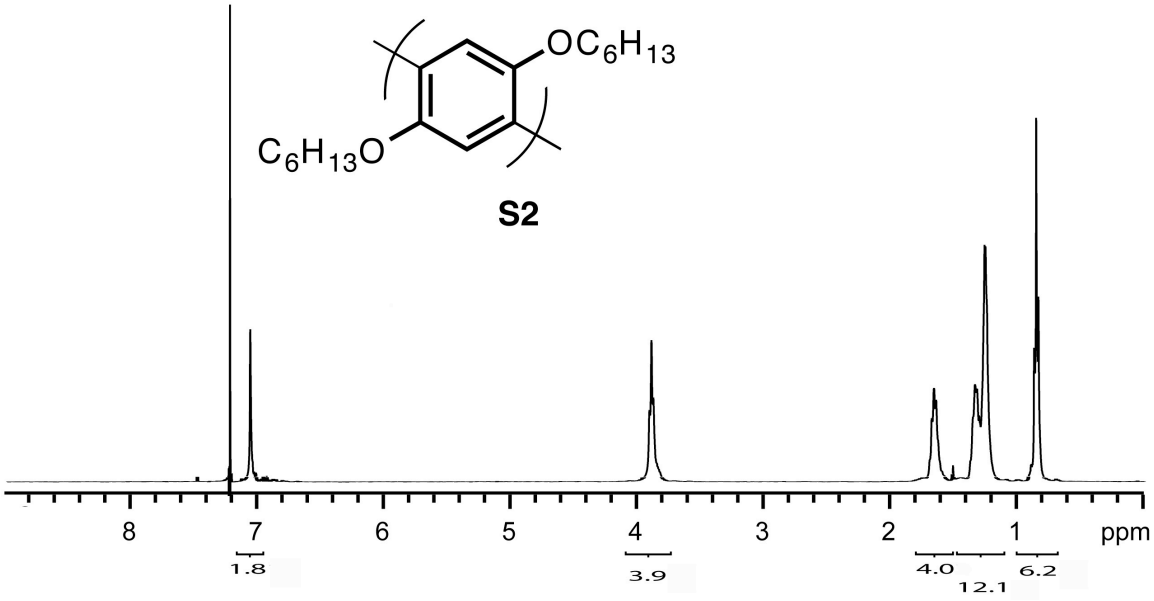

Figure S3. ^{1}H NMR Spectrum of S2.
^{1}H NMR (400 MHz, $CDCl_3$) δ 7.1 (br s, 2H), 3.9 (br m, 4H), 1.7 (br m, 4H), 1.35-1.25 (br m, 12 H), 0.90 (br m, 6H).

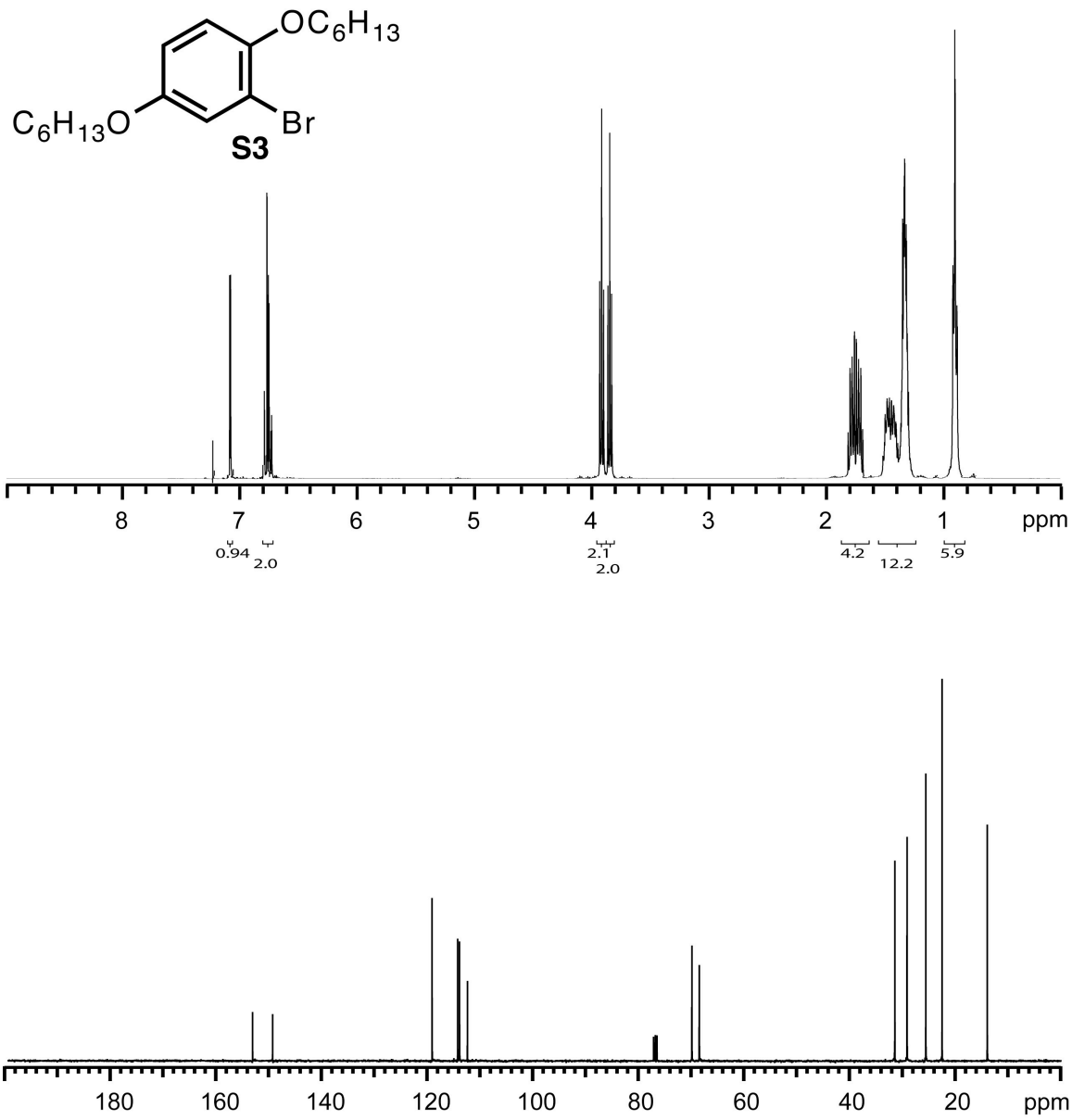

Figure S4. ^{1}H and ^{13}C NMR Spectra of S3.
^{1}H NMR (400 MHz, $CDCl_3$) δ 7.10 (d, *J* = 2 Hz, 1H), 6.80 (d, *J* = 8 Hz, 1H), 6.76 (dd, *J* = 2, 8 Hz, 1H), 3.93 (t, *J* = 6.8 Hz, 2H), 3.86 (t, *J* = 6.8 Hz, 2H), 1.82-1.64 (m, 4H), 1.52-1.29 (m, 12H), 0.93-0.91 (m, 6H). ^{13}C NMR (100 MHz, $CDCl_3$) δ 153.73, 149.92, 119.63, 114.78, 114.42, 112.915, 70.29, 68.89, 31.75, 31.73, 29.41, 25.85, 22.77, 14.18.*
* Some carbons on the hexyl chains are unresolved.

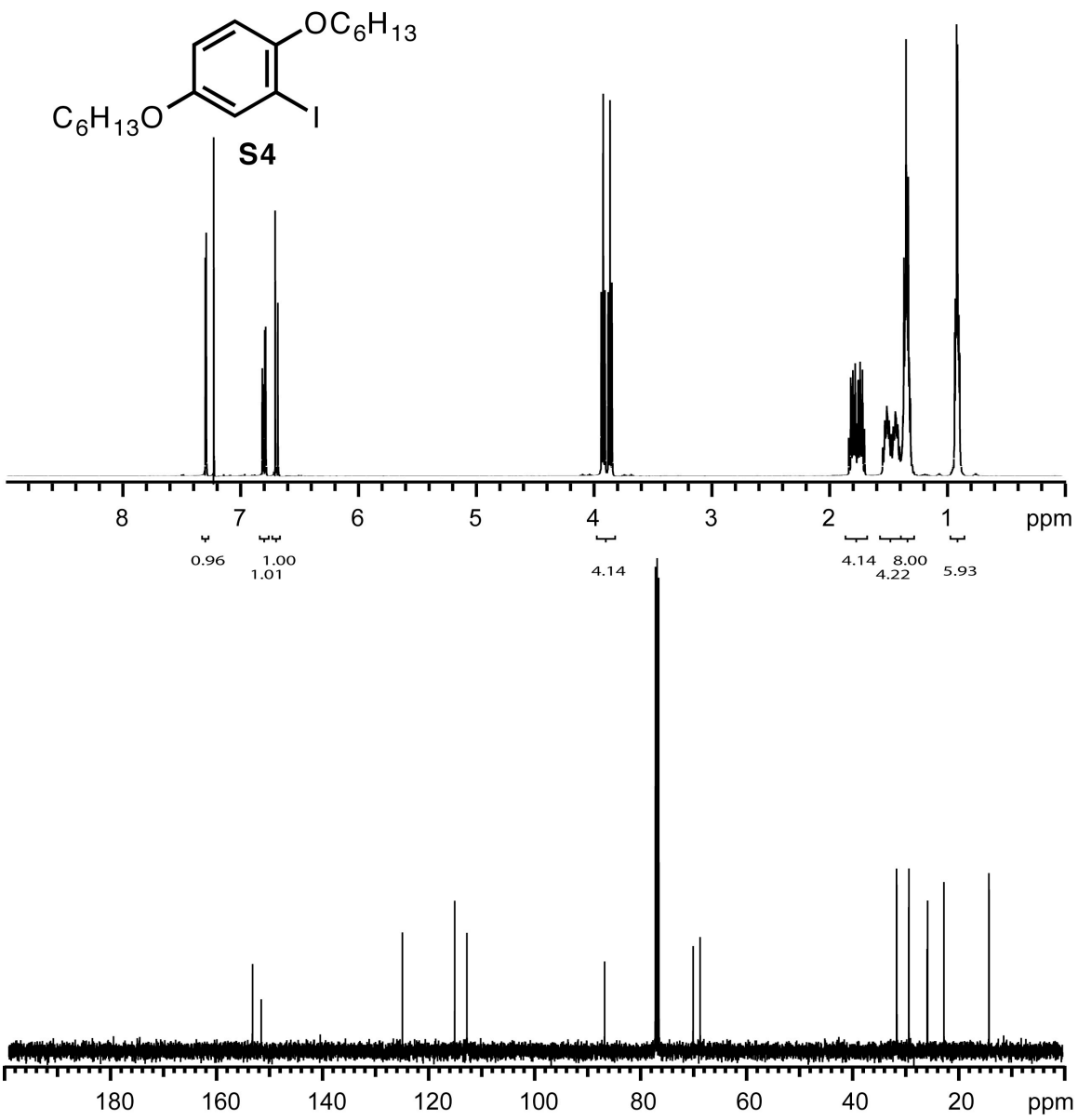

Figure S5. ^{1}H and ^{13}C NMR Spectra of S4.
^{1}H NMR (400 MHz, $CDCl_3$) δ 7.30 (d, *J* = 4 Hz, 1H), 6.81 (dd, *J* = 4, 12 Hz, 1H), 6.70 (d, *J* = 12 Hz, 1H), 3.92 (t, *J* = 8.8 Hz, 2H), 3.86 (t, *J* = 9.2 Hz, 2H), 1.82-1.67 (m, 4H), 1.51-1.42 (m, 12H), 0.91 (m, 6H). ^{13}C NMR (100 MHz, $CDCl_3$) δ 153.77, 152.13, 125.31, 115.40, 113.09, 86.97, 70.16, 68.82, 31.55, 31.51, 29.24, 29.22, 25.76, 25.66, 22.57, 14.02, 14.01.*
*Some carbons on the hexyl chains are unresolved.

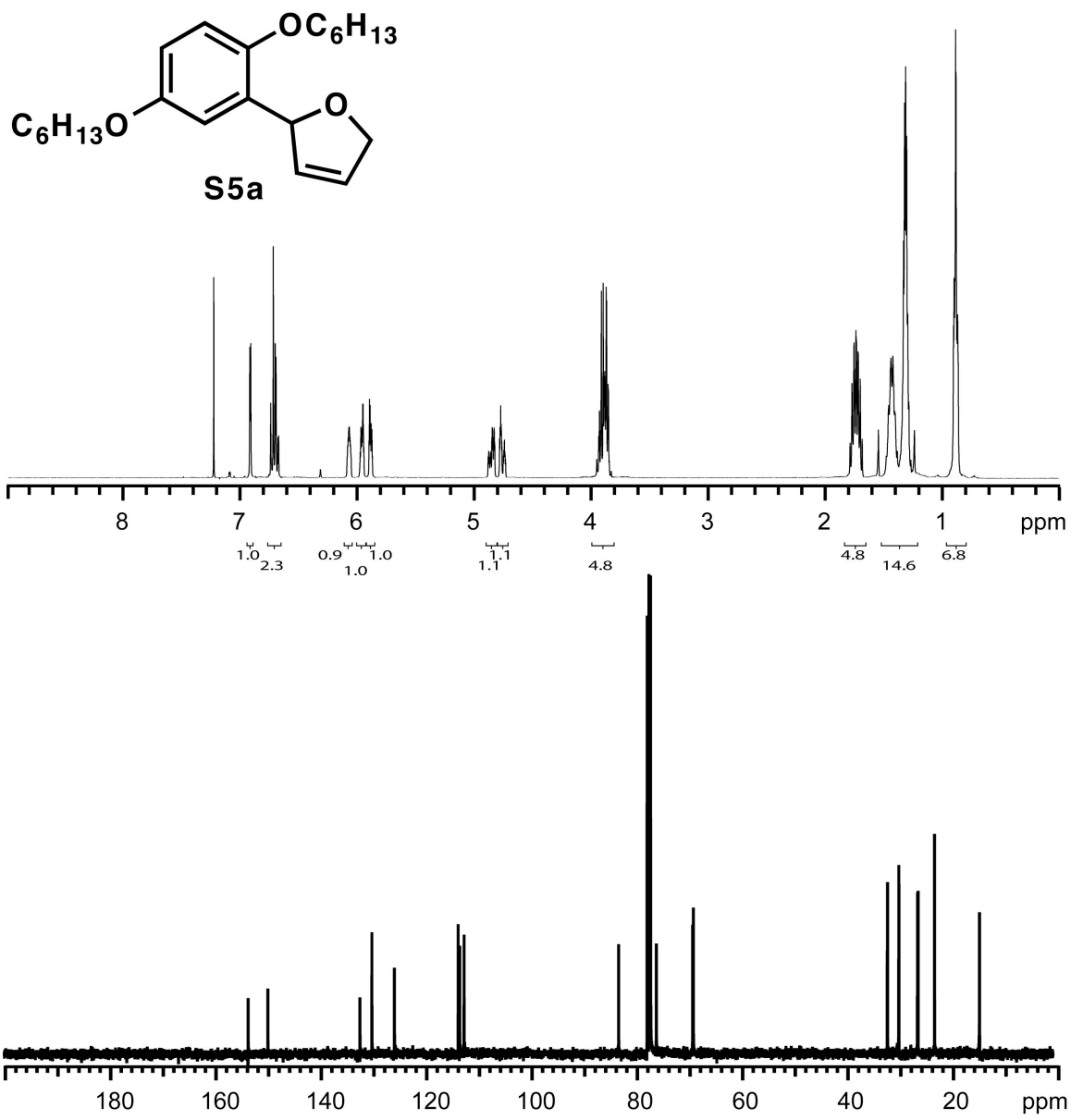

Figure S6. ^{1}H and ^{13}C NMR Spectra of S5a.

^{1}H NMR (400 MHz, $CDCl_3$) δ 6.96 (d, *J* = 3 Hz, 1H), 6.77 (d, *J* = 9 Hz, 1H), 6.73 (dd, *J* = 3, 9 Hz, 1H), 6.11 (m, 1H), 6.00 (m, 1H), 5.92 (m, 1H), 4.92-4.77 (m, 2H), 3.99-3.86 (m, 4H), 1.82-1.71 (m, 4H), 1.58-1.27 (m, 12H), 0.91 (m, 6H). ^{13}C NMR (100 MHz, $CDCl_3$) δ 153.31, 149.54, 132.03, 129.76, 125.46, 113.31, 113.03, 112.19, 82.76, 75.59, 68.66, 68.53, 31.61, 31.56, 29.40, 29.39, 25.85, 25.74, 22.60, 14.04.*

* Some carbons on the hexyl chains are unresolved.

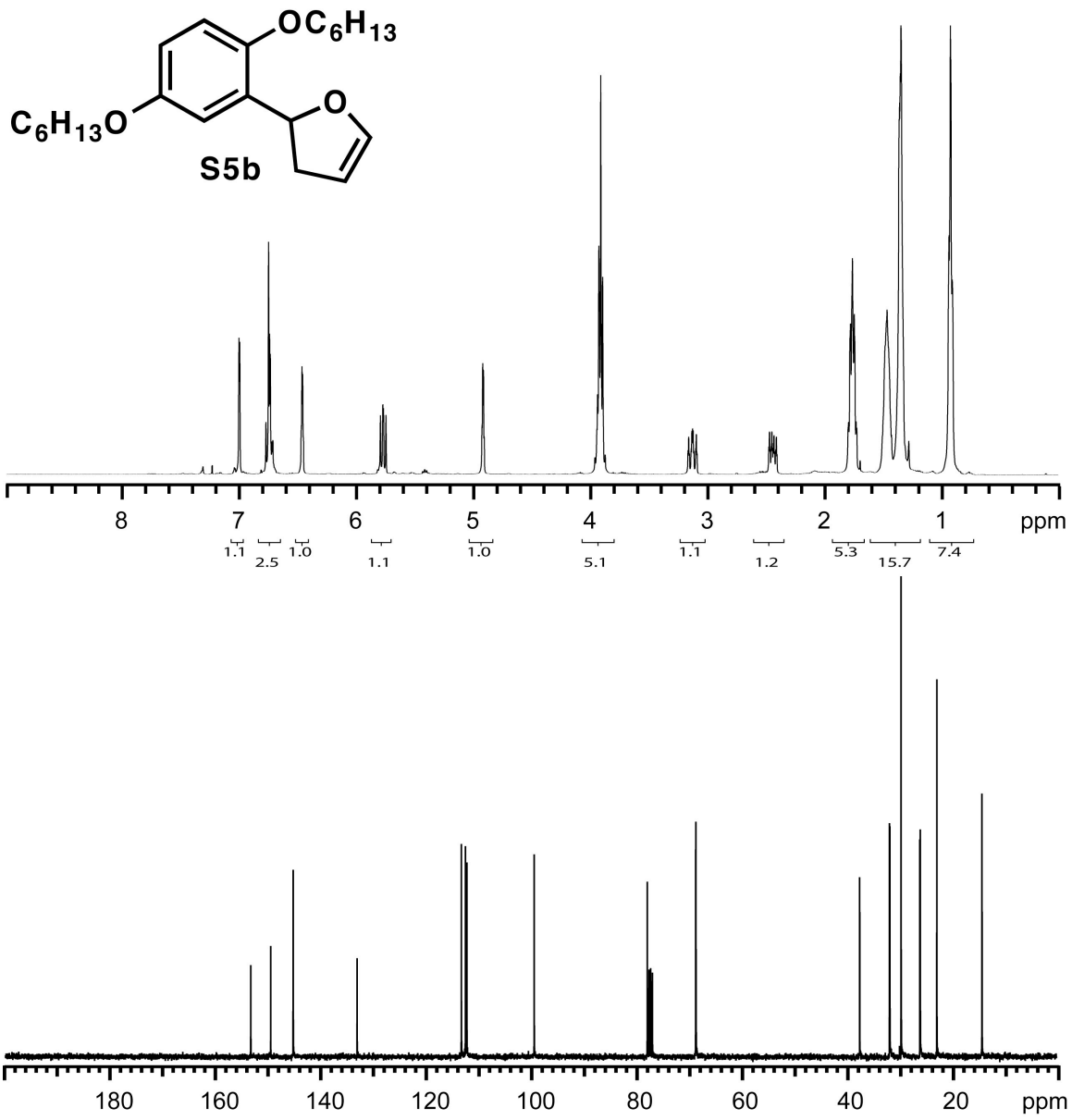

Figure S7. ^{1}H and ^{13}C NMR Spectra of S5b.
^{1}H NMR (400 MHz, CDCl3) δ 6.99 (d, *J* = 3 Hz, 1H), 6.78 (d, *J* = 9 Hz, 1H), 6.74 (dd, *J* = 3, 9 Hz, 1H), 6.47 (dd, *J* = 2, 4.8 Hz, 1H), 5.76 (dd, *J* = 8.0, 10.4 Hz, 1H), 4.93 (dd, *J* = 2, 4.8 Hz, 1H), 3.97-3.88 (m, 4H), 3.12 (m, 1H), 2.44 (m, 1H), 1.80-1.72 (m, 4H), 1.50-1.26 (m, 12H), 0.91 (m, 6H). ^{13}C NMR (100 MHz, $CDCl_3$) δ 153.09, 149.28, 145.02, 132.85, 113.02, 112.25, 111.98, 99.16, 76.68, 68.42, 68.39, 37.23, 31.57, 31.50, 29.35, 25.78, 25.71, 22.55, 13.96.*
*Some carbons on the hexyl chains are unresolved.

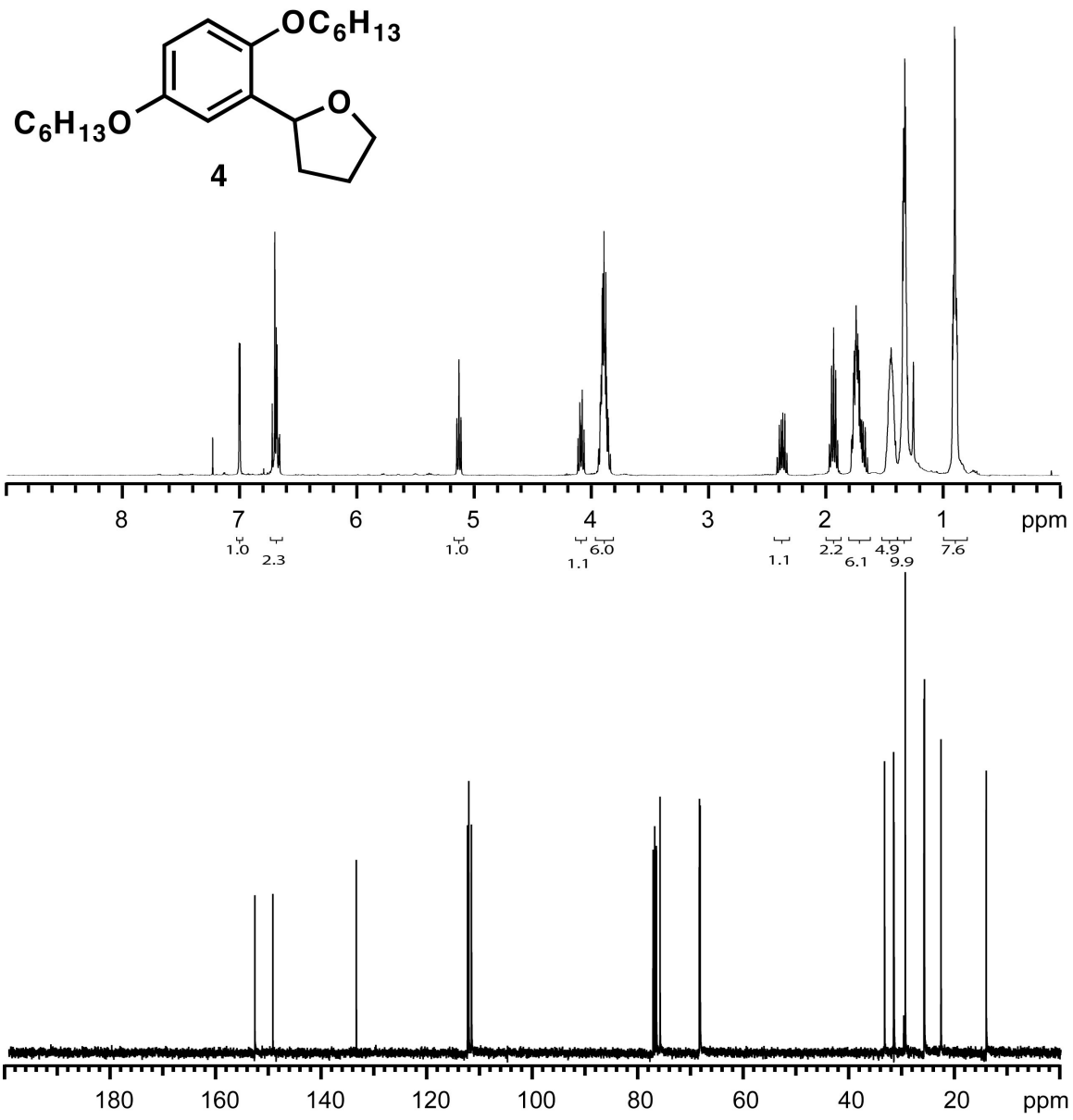

Figure S8. ^{1}H and ^{13}C NMR Spectra of 4.
^{1}H NMR (400 MHz, $CDCl_3$) δ 7.01 (d, *J* = 3 Hz, 1H), 6.72 (d, *J* = 9 Hz, 1H), 6.68 (dd, *J* = 3, 9 Hz, 1H), 5.13 (m, 1H), 4.09 (m, 1H), 3.94-3.84 (m, 5H), 2.47 (m, 1H), 1.93 (m, 2H), 1.74-1.64 (m, 5H), 1.47-1.40 (m, 4H), 1.37-1.28 (m, 8H), 0.90 (m, 6H). ^{13}C NMR (100 MHz, $CDCl_3$) δ 153.24, 149.82, 133.94, 112.82, 112.57, 112.05, 76.21, 68.74, 68.72, 68.6, 33.54, 31.75, 31.54, 29.61, 26.06, 26.04, 25.95, 22.82, 22.80, 14.24, 14.22.

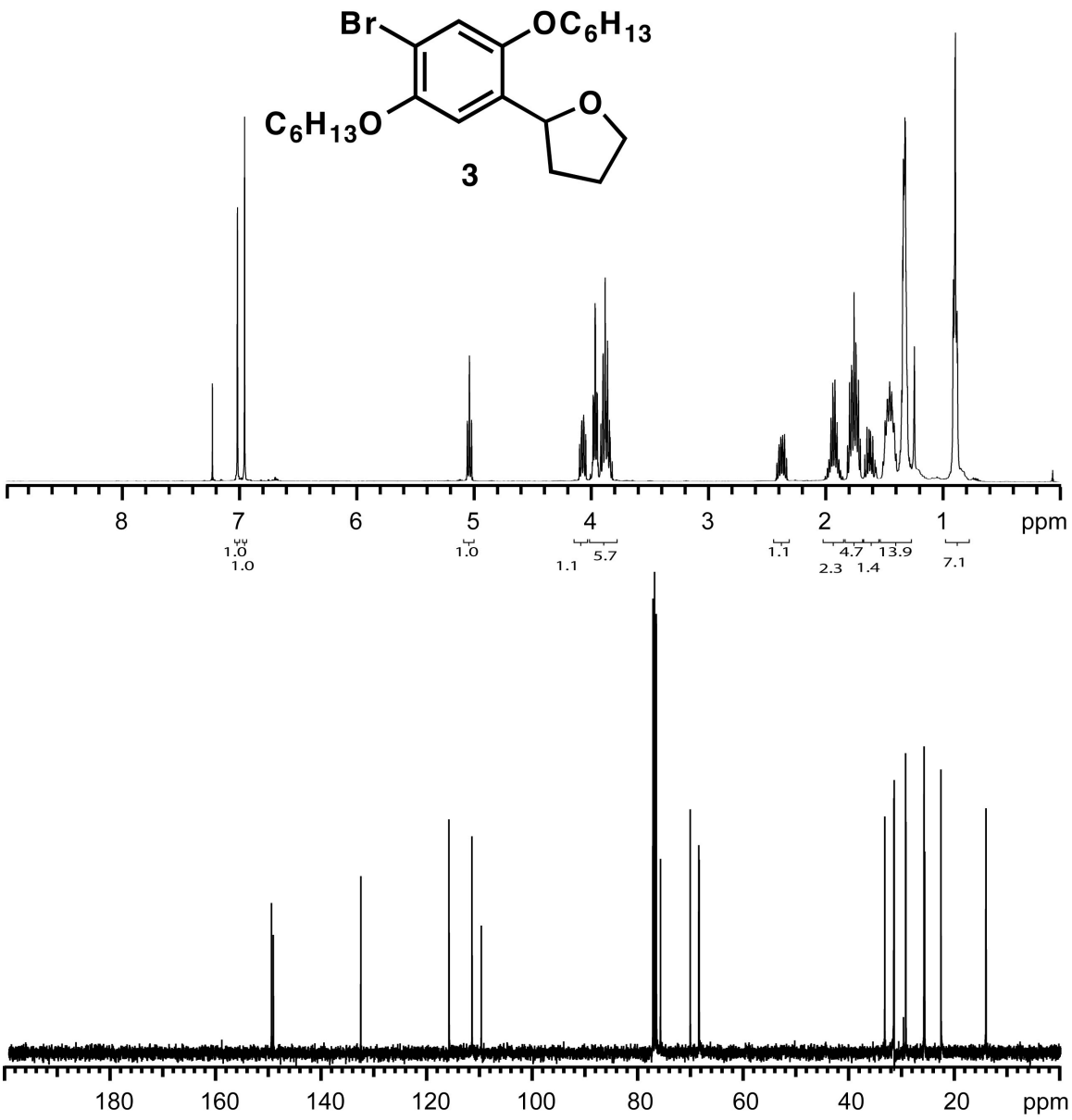

Figure S9. ^{1}H and ^{13}C NMR Spectra of 3.
^{1}H NMR (400 MHz, $CDCl_3$) δ 7.06 (s, 1H), 6.99 (s, 1H), 5.07 (m, 1H), 4.10 (m, 1H), 3.95-3.85 (m, 5H), 2.40 (m, 1H), 2.02-1.88 (m, 2H), 1.84-1.73 (m, 4H), 1.69-1.60 (m, 1H), 1.53-1.29 (m, 12H), 0.92 (m, 6H). ^{13}C NMR (100 MHz, $CDCl_3$) δ 149.82, 149.47, 132.86, 116.09, 111.73, 109.94, 75.89, 70.22, 68.61, 68.53, 33.26, 31.53, 31.47, 29.28, 29.23, 25.80, 25.76, 25.66, 22.58, 22.56, 14.01, 14.00.

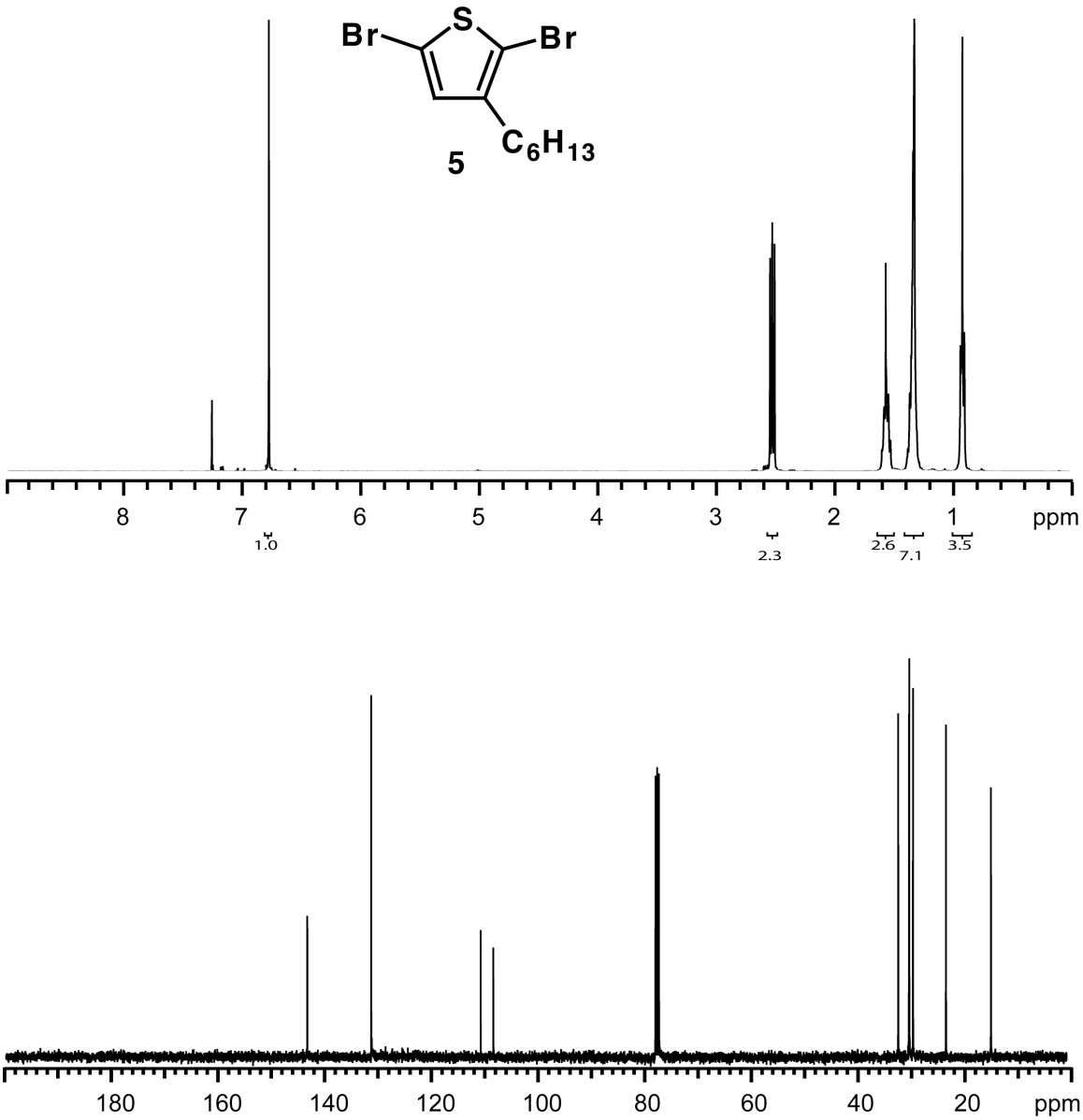

Figure S10. ^{1}H and ^{13}C NMR Spectra of 5.
^{1}H NMR (400 MHz, $CDCl_3$) δ 6.79 (s, 1H), 2.51 (t, *J* = 7.6 Hz, 2H), 1.55 (m, 2H), 1.33 (m, 6H), 0.90 (m, 3H). ^{13}C NMR (100 MHz, $CDCl_3$) δ 142.97, 130.93, 110.28, 107.90, 31.55, 29.54, 29.46, 28.77, 22.56, 14.07.

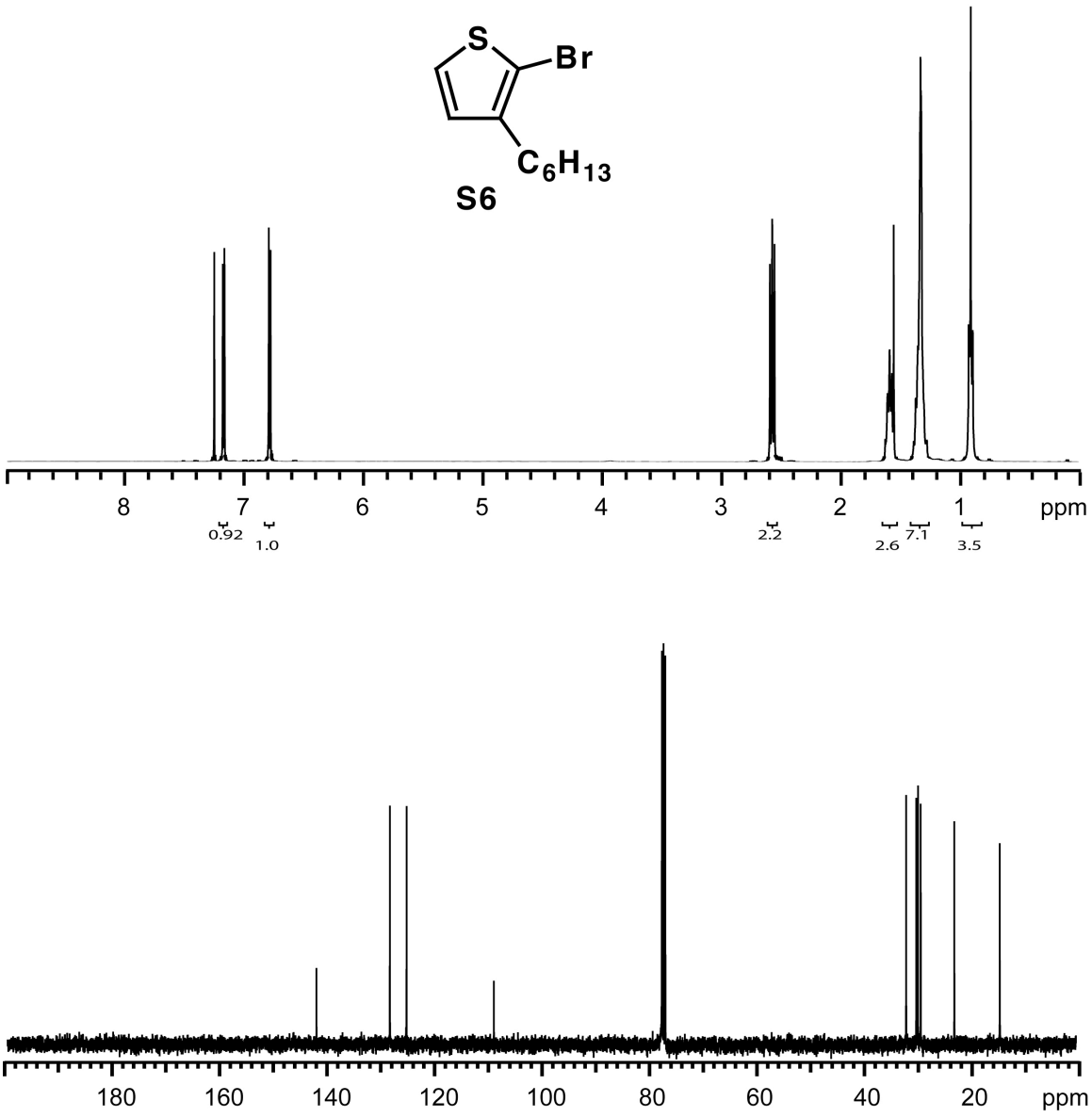

Figure S11. ^{1}H and ^{13}C NMR Spectra of S6.
^{1}H NMR (400 MHz, $CDCl_3$) δ 7.19 (d, *J* = 5.6 Hz, 1H), 6.80 (d, *J* = 5.6 Hz, 1H), 2.57 (t, *J* = 7.6 Hz, 2H), 1.58 (m, 2H), 1.32 (m, 6H), 0.90 (m, 3H). ^{13}C NMR (100 MHz, $CDCl_3$) δ 141.96, 128.22, 125.11, 108.76, 31.61, 29.69, 29.38, 28.88, 22.58, 14.07.

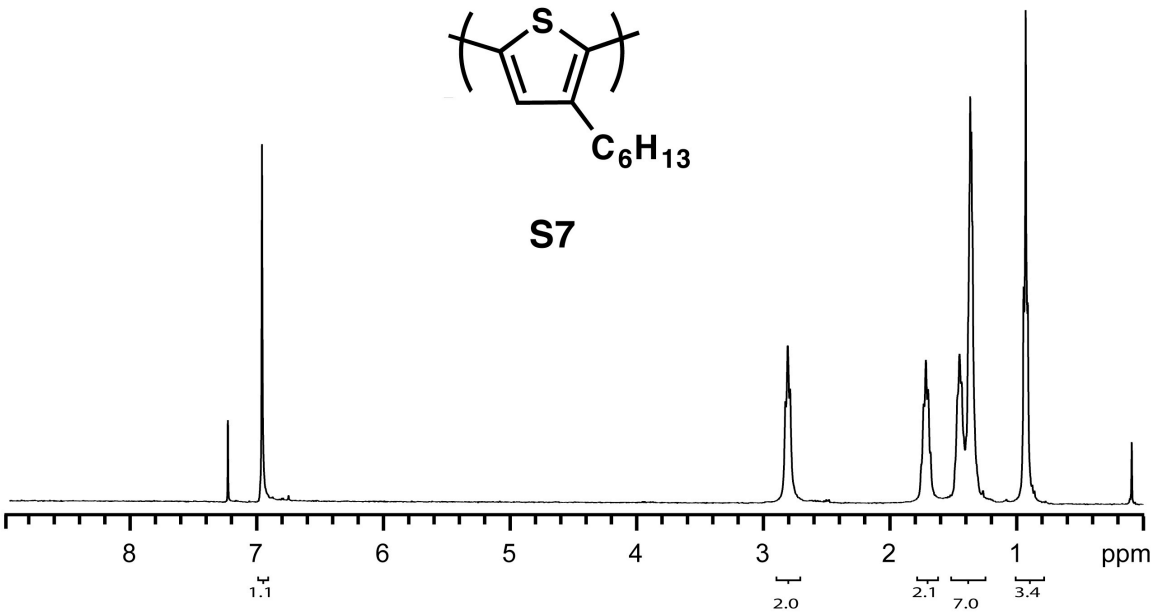

Figure S12. ^{1}H Spectra of S7.
^{1}H NMR (400 MHz, $CDCl_3$) δ 7.00 (s, 1H), 2.82 (br m, 2H), 1.73 (br m, 2H), 1.45-1.37 (br m, 6 H), 0.93 (br m, 3H).

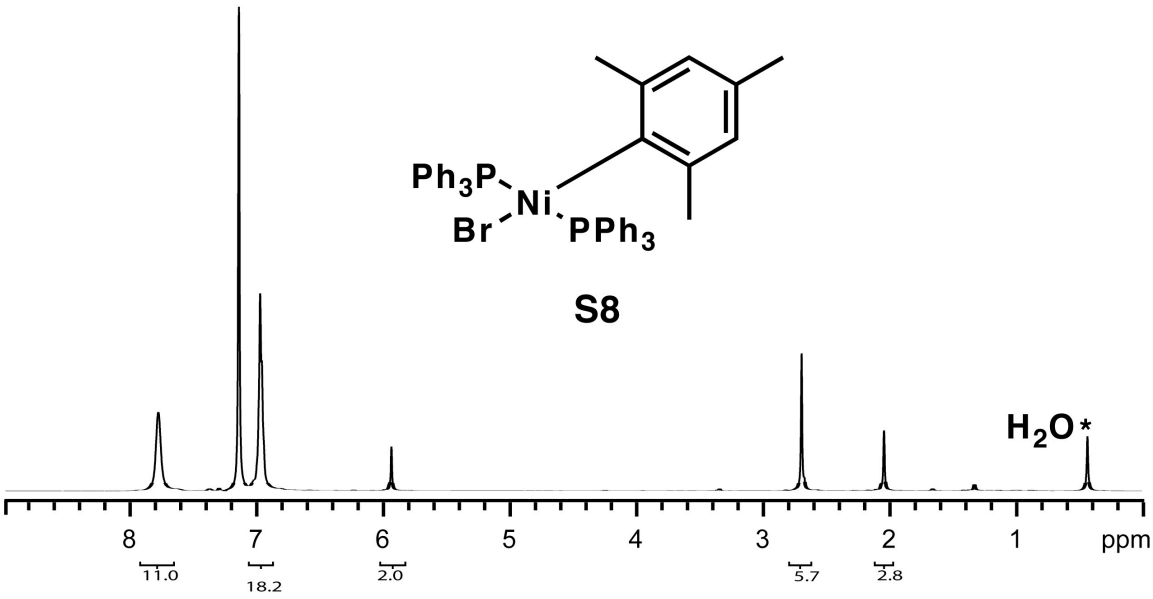

Figure S13. ^{1}H Spectra of S8.
^{1}H NMR (500 MHz, C_6D_6) δ 7.8 (br s, 12H), 6.98 (m, 18H), 5.95 (s, 2H), 2.69 (s, 6H), 2.04 (s, 3H). ^{31}P NMR (161 MHz, C_6D_6) δ 20.32.

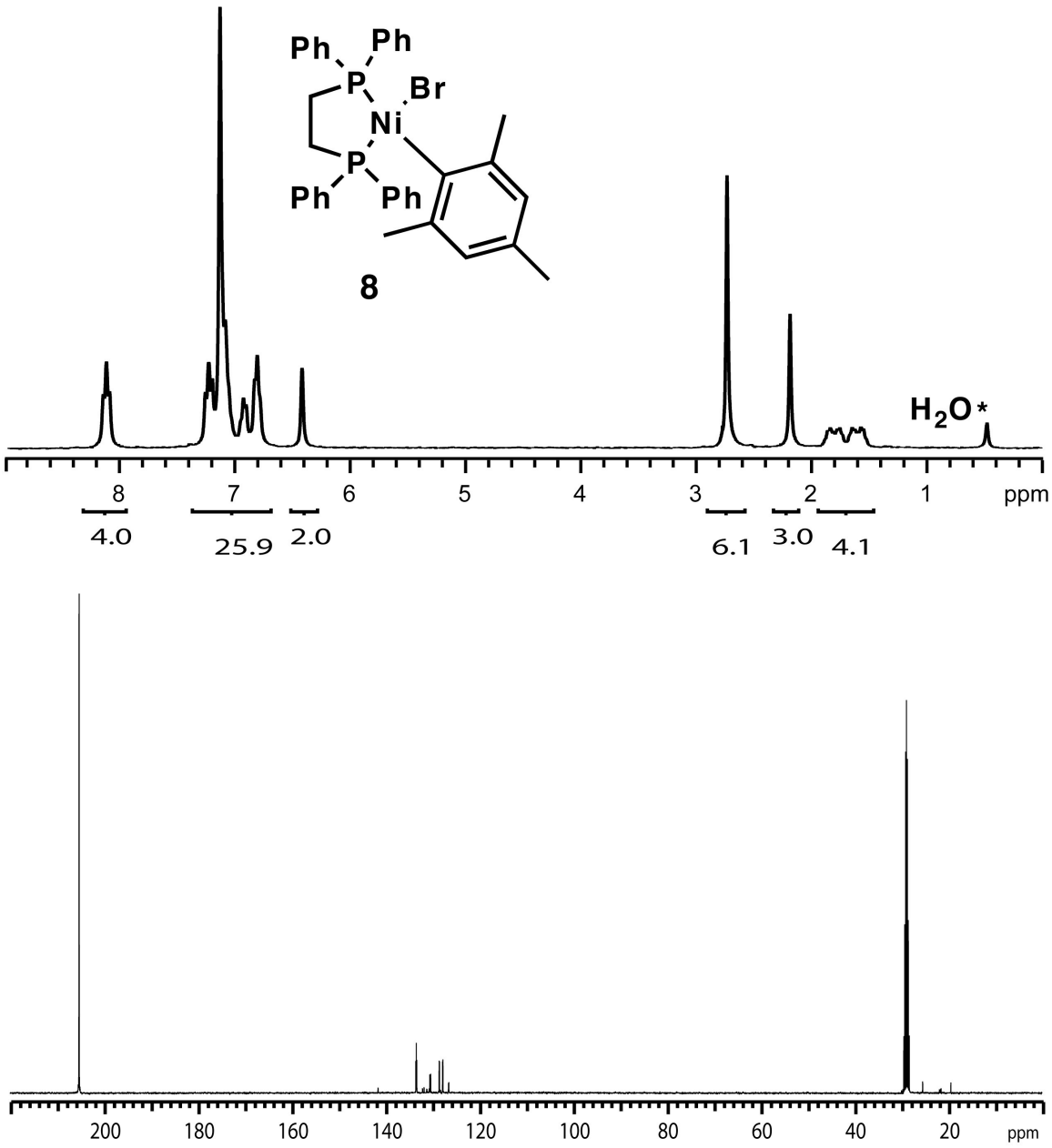

Figure S14. ^{1}H and ^{13}C NMR Spectra of 8

^{1}H NMR (300 MHz, C_6D_6) δ 8.15 (m, 4H), 7.29-6.34 (m, 16H), 6.45 (br s, 2H), 2.74 (br s, 6H), 2.19 (br s, 3H), 1.84-1.55 (m, 4H). ^{13}C NMR (100 MHz, acetone-d_6) δ 141.57 (t, J_{C-P} = 3 Hz), 133.11 (t, J_{C-P} = 10 Hz), 131.93 (t, J_{C-P} = 34 Hz), 130.91 (dd, J_{C-P} = 30.4, 2 Hz), 130.45 (dd, J_{C-P} = 16.3, 3 Hz), 128.19 (dd, J_{C-P} =9, 72 Hz), 126.51 (dd, J_{C-P} = 2, 7 Hz), 25.50, 21.88 (d, J_{C-P} = 11 Hz), 21.62 (d, J_{C-P} = 11 Hz), 19.48.^{31}P NMR (161 MHz, THF) δ 54.0 (d, J = 15 Hz), 31.7 (d, J = 15 Hz).

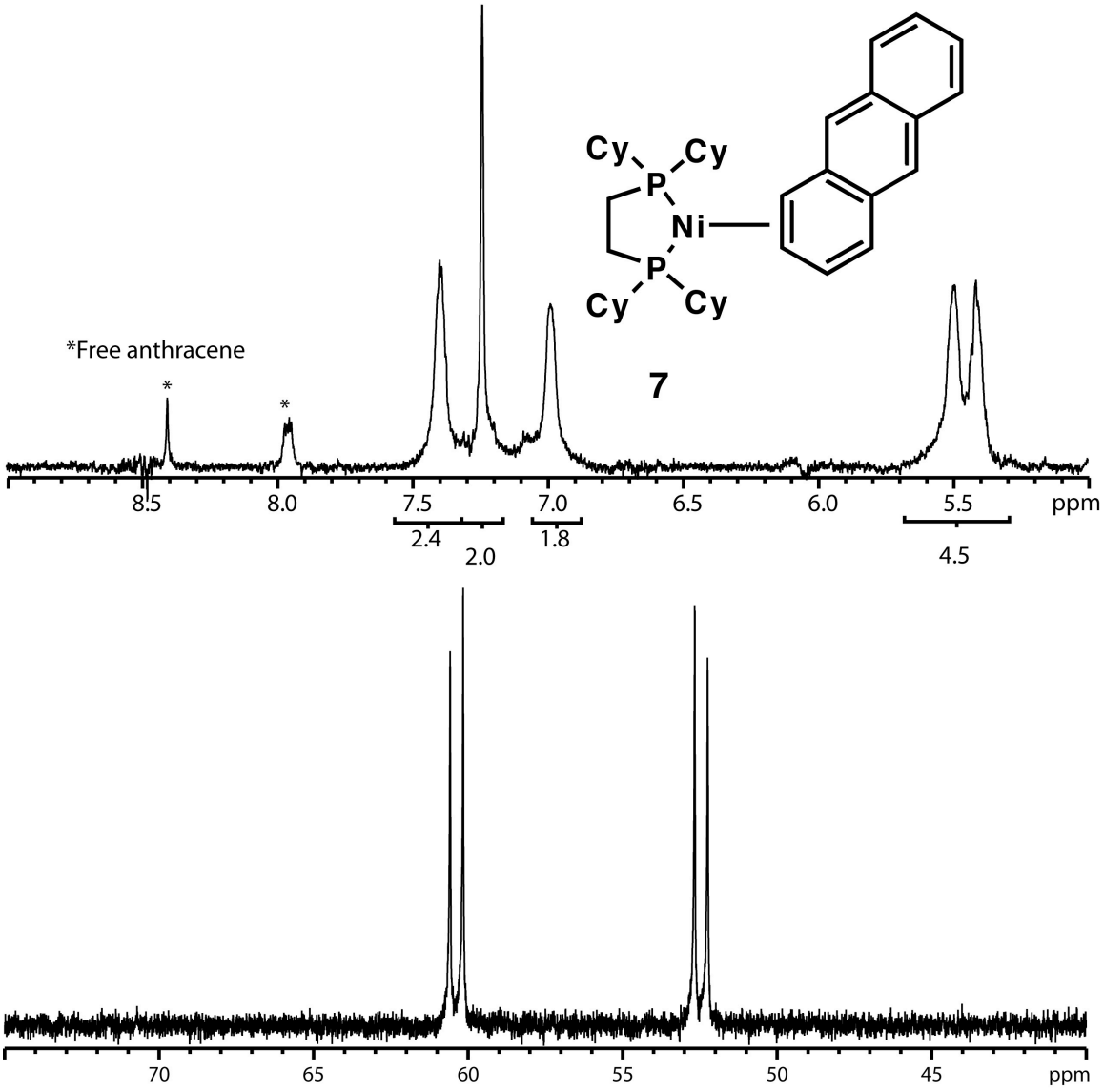

Figure S15. ^{1}H and ^{31}P NMR Spectra of 7.
^{1}H NMR (400 MHz, THF) δ 7.40 (br s, 2H), 7.24 (br s, 2H), 6.99 (br s, 2H), 5.49-5.41 (br m, 4H). ^{31}P NMR (161 MHz, THF) δ 60.35 (d, *J* = 68 Hz), 52.44 (d, *J* = 68 Hz).

V. Determination of GRIM Reaction By-Products

Each potential by-product was independently synthesized (see Synthetic Procedures), individually spiked into a sample of **2b** and analyzed by ^{1}H NMR spectroscopy. The figures below show representative examples.

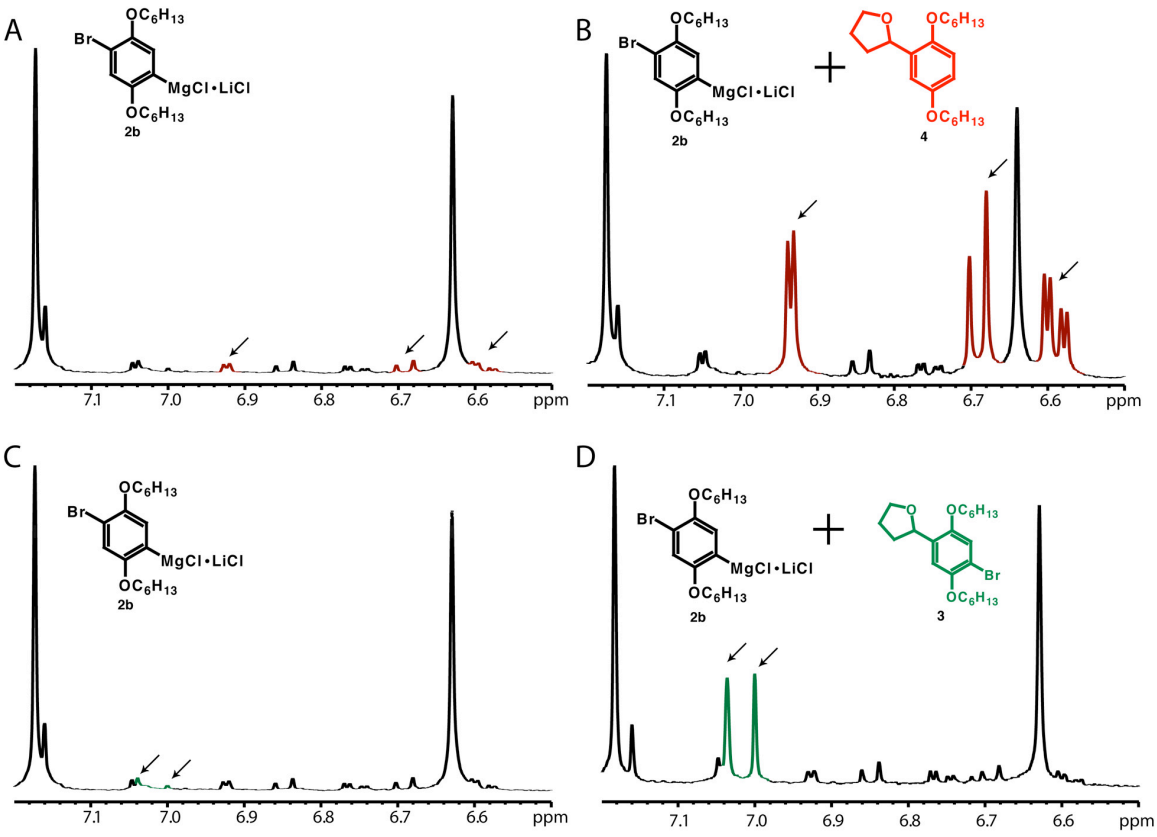

Figure S16. (A)^{1}H NMR spectrum showing **2b**. (B) ^{1}H NMR spectrum showing **2b** spiked with **4**. (C) ^{1}H NMR spectrum showing **2b**. (D) ^{1}H NMR spectrum showing **2b** spiked with **3**.

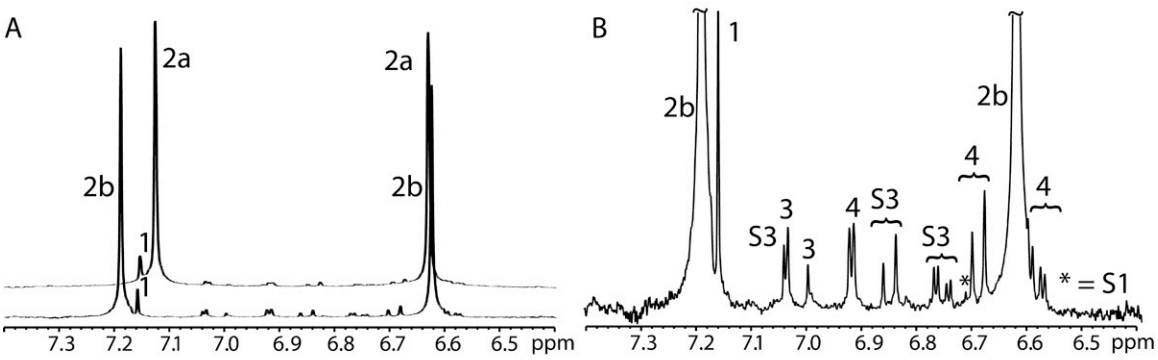

Figure S17. (A) Overlaid ^{1}H NMR spectra of **2a** and **2b.** (B) ^{1}H NMR spectrum showing a summary of the spiking experiment results.

VI. Representative IR spectrum and GC Chromatogram.

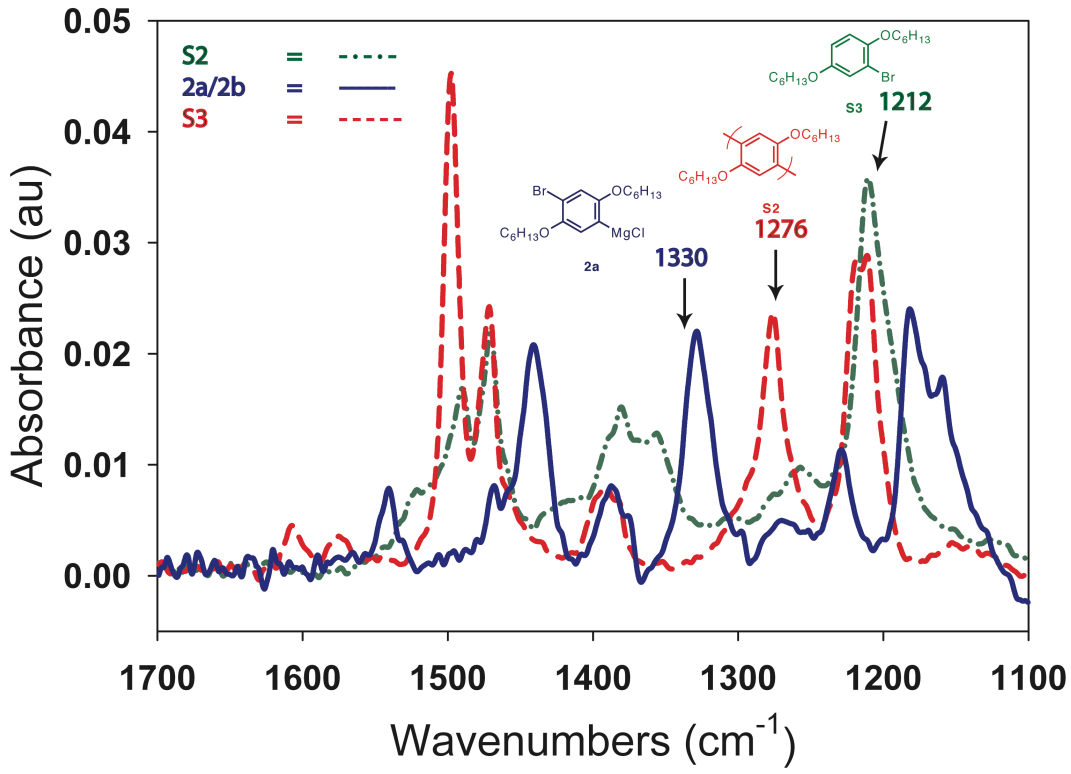

Figure S18. IR spectral overlay of **2b**, **S2** and **S3**.

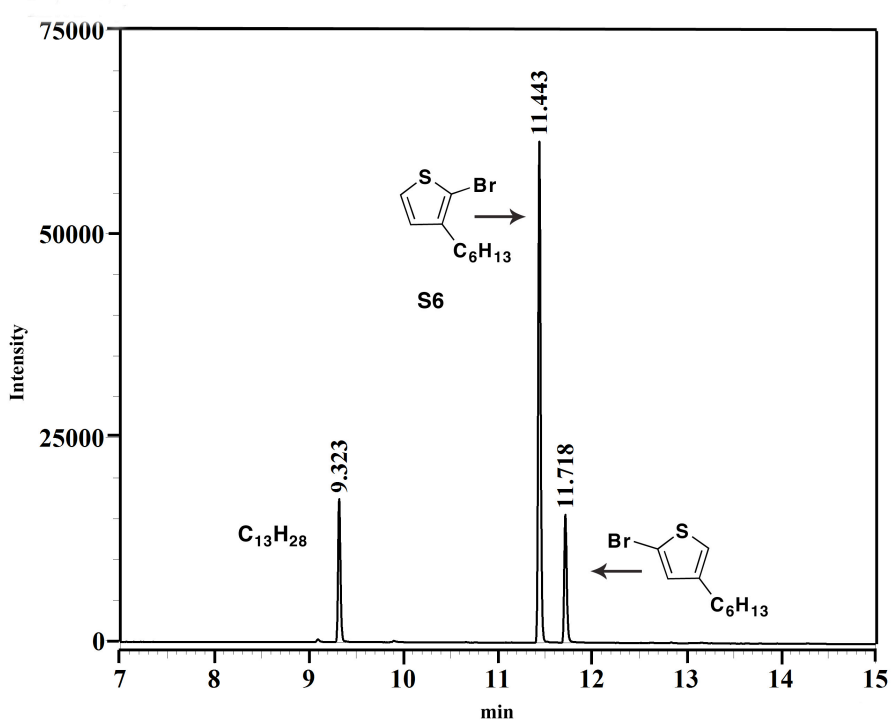

Figure S19. Representative GC trace.

VII. GRIM rate studies

General procedure for GRIM rate studies

All preparative manipulations were performed under N_2 atmosphere in a glovebox. Glassware was dried in a 130 °C oven for a minimum of 1 h prior to use and *i*-PrMgCl was titrated using the method of Love and Jones.[13] Standard solutions in THF of **1** (0.5 M), *i*-PrMgCl (1.0 M) and *i*-PrMgCl•LiCl (1.0 M) were used to facilitate consistent addition of reagents. For each reaction: 200 µL of **1** (0.1 mmol) and 700 µL of THF were combined in an NMR tube, 100 µL of *i*-PrMgCl solution (0.1 mmol) was added for a total volume of 1 mL (0.1 M). Consumption of starting material over 10% conversion was followed by ^{1}H NMR spectroscopy at 25 °C.

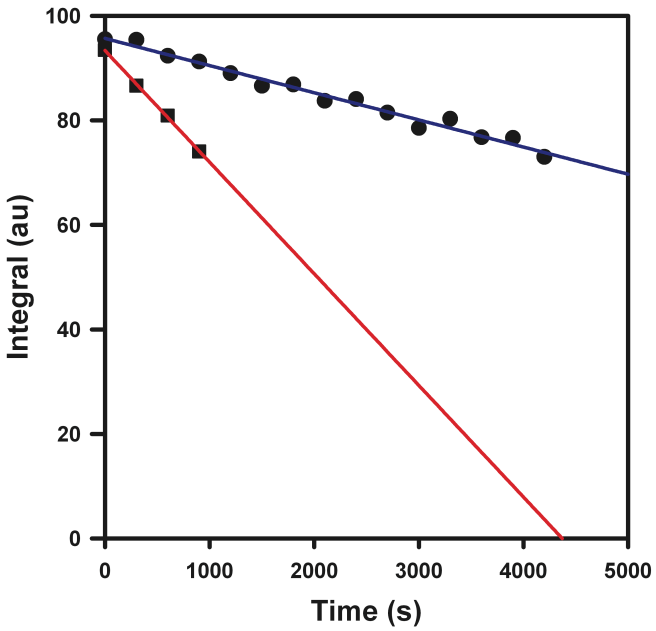

Figure S20. Plot of initial conversion versus time for the Grignard metathesis of **1** in the presence (squares) and absence (circles) of 1 equiv LiCl.

Table S1. Data from the plot in Figure S20.

Conditions	Initial rate (s^{-1})
without LiCl (**2a**)	5.1 ± 0.2 x 10^{-3}
with LiCl (**2b**)	21 ± 2 x 10^{-3}

VIII. Calibration Curves

General procedure for generating a calibration curve utilizing the ReactIR:

The IR probe was inserted through an O-ring sealed 14/20 ground glass adapter (custom made) into an oven-dried 50 mL 2-neck flask containing a stir bar. The other neck was equipped with a three-way adapter fitted with a septum for injections and an N_2 line. The oven-dried flask was cooled under vacuum and then refilled with N_2. Following two more cycles of evacuation and refilling, the flask was charged with THF and cooled to 0 ^oC over ~5 min. After recording a background spectrum, **2a** or **2b** was added by syringe and allowed to equilibrate for at least 5 min and then the spectra were recorded.

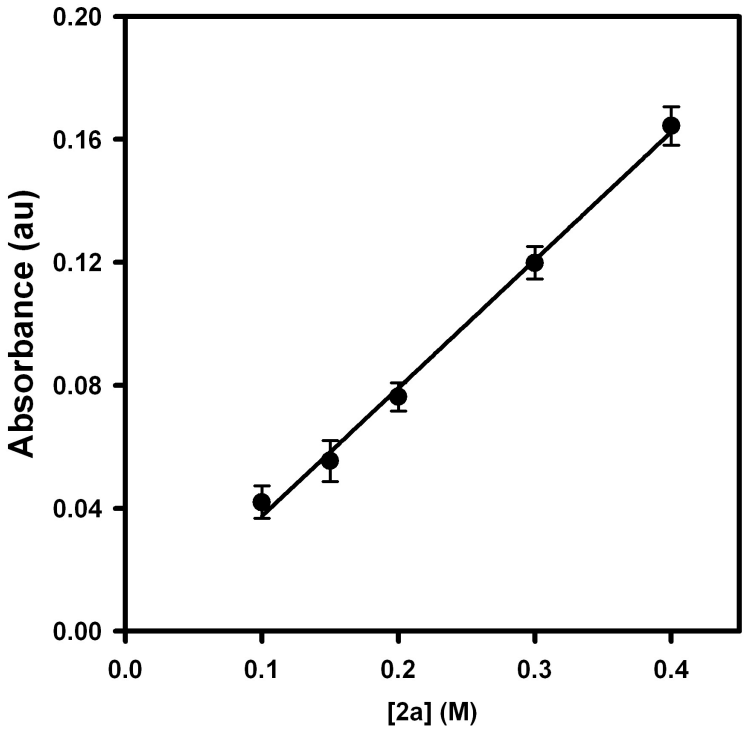

Figure S21. Plot of absorbance versus [**2a**] fitted to y = *m*x + *b* where *m* = 0.42 ± 0.02 and *b* = -0.004 ± 0.004.

Table S2. Data for the plot in Figure S21.

[**2a**] (M)	Absorbance (au)
0.1	$4.2 \pm 0.5 \times 10^{-2}$
0.15	$5.5 \pm 0.7 \times 10^{-2}$
0.2	$7.6 \pm 0.5 \times 10^{-2}$
0.3	$12 \pm 1 \times 10^{-2}$
0.4	$16 \pm 1 \times 10^{-2}$

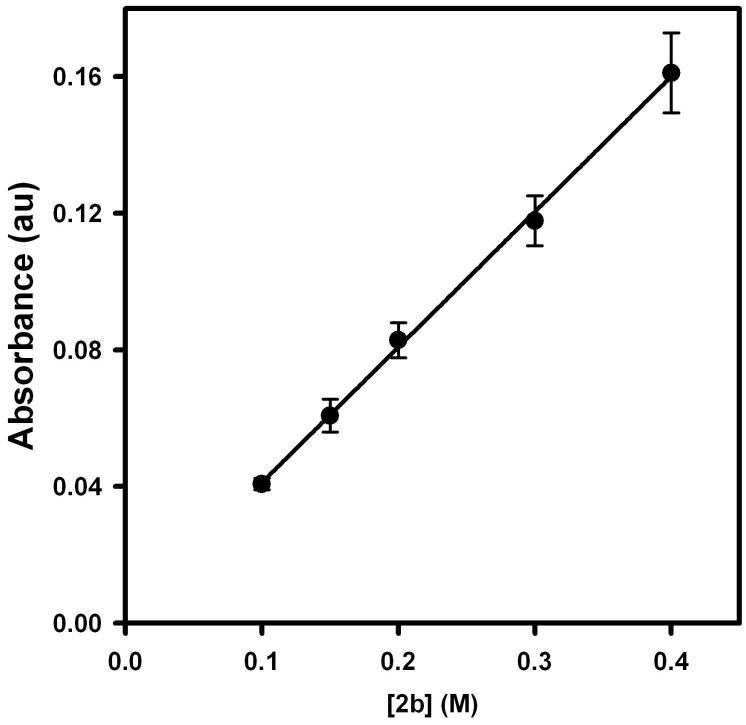

Figure S22. Plot of absorbance versus [**2b**] fitted to y = mx + b where m = 0.396 ± 0.002 and b = 0.001 ± 0.002.

Table S3. Data for the plot in Figure S22.

[**2b**] (M)	Absorbance (au)
0.1	$4.1 \pm 0.1 \times 10^{-2}$
0.15	$6.1 \pm 0.5 \times 10^{-2}$
0.2	$8.3 \pm 0.5 \times 10^{-2}$
0.3	$11.8 \pm 0.5 \times 10^{-2}$
0.4	$16 \pm 1 \times 10^{-2}$

Procedure for generating a calibration curve utilizing the GC:

Solutions containing a constant concentration of tridecane (0.00257 M) and varying concentrations of 2-bromo-3-hexylthiophene (0.00581, 0.00348, 0.00232, 0.00116, and 0.000581 M) were prepared in chloroform. Each was analyzed by GC and the response factor **F** calculated by fitting the data to the following equation:

$$\frac{\text{Area of thiophene signal}}{\text{Concentration of thiophene}} = \mathbf{F}\left(\frac{\text{Area of tridecane signal}}{\text{Concentration of tridecane}}\right)$$

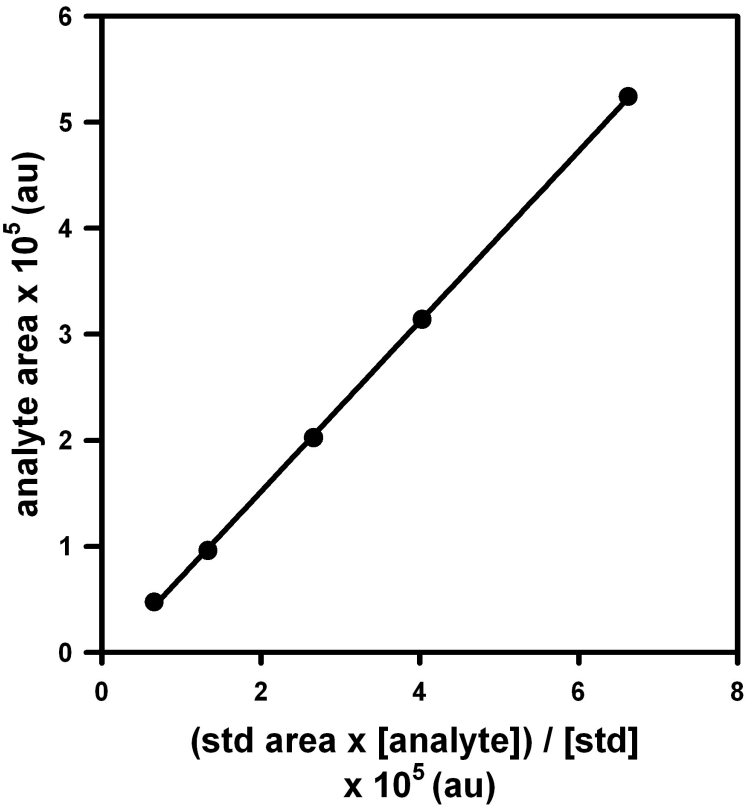

Figure S23. Plot of analyte area versus (std area x [**S6**]) / [std] fitted to y = *m*x + *b* where *m* = 0.803 ± 0.006 and *b* = -9.1 x 10^3 ± 2.3 x 10^3.

Table S4. Data for the plot in Figure S23.

[**S6**]	area **S6** (analyte)	area tridecane (std)	(std area x [**S6**]) / [std]
5.80 x 10^{-4}	4.74 x 10^5	2.91 x 10^5	6.59 x 10^4
1.16 x 10^{-3}	9.59 x 10^5	2.94 x 10^5	1.33 x 10^5
2.23 x 10^{-3}	2.02 x 10^5	2.95 x 10^5	2.66 x 10^5
3.48 x 10^{-3}	3.14 x 10^5	2.97 x 10^5	4.03 x 10^5
5.80 x 10^{-3}	5.24 x 10^5	2.93 x 10^5	6.62 x 10^5

IX. Representative Procedure for Preparing the Catalyst Solution.

All actions were performed in a glovebox under N_2 atmosphere. A 20 mL vial was equipped with a stir bar. Sequentially, Ni(dppe)Cl_2 (55 mg, 0.11 mmol, 1.0 equiv) THF (6 mL), and **2b** (1.0 mL, 0.52 M, 5 equiv) were added to the flask. The reaction mixture was stirred for 10 min until homogeneous.

X. M_n and PDI versus conversion

Representative procedure for obtaining plots of M_n and PDI versus conversion utilizing the ReactIR:

The IR probe was inserted through an O-ring sealed 14/20 ground glass adapter (custom made) into an oven-dried 50 mL 2-neck flask containing a stir bar. The other neck was equipped with a three-way adapter fitted with a septum for injections and an N_2 line. The oven-dried flask was cooled under vacuum and then refilled with N_2. Following two more cycles of evacuation and refilling, the flask was charged with THF (1.0 mL) and cooled at 0 ^oC over ~ 5 min. After recording a background spectrum, **2b** (8.0 mL, 0.23 M, 1.0 equiv) was added by syringe and allowed to equilibrate for at least 5 min to 0 ^oC. After 5 min, the pre-initiated catalyst solution (1.0 mL, 0.015 M, 0.0075 equiv) was injected and spectra were recorded every 30 s over the entire reaction. To account for mixing and temperature equilibration, spectra recorded in the first 30 s of the reaction were discarded. Aliquots (~ 0.5 mL) were withdrawn through the three way adapter via syringe and immediately quenched with 5 M HCl (~ 1 mL). Each aliquot was then extracted with CH_2Cl_2 (with mild heating if polymer had precipitated), dried over $MgSO_4$ and filtered, then concentrated. The samples were dissolved in THF (with heating), and passed through a 0.2 μm PTFE filter for GPC analysis.

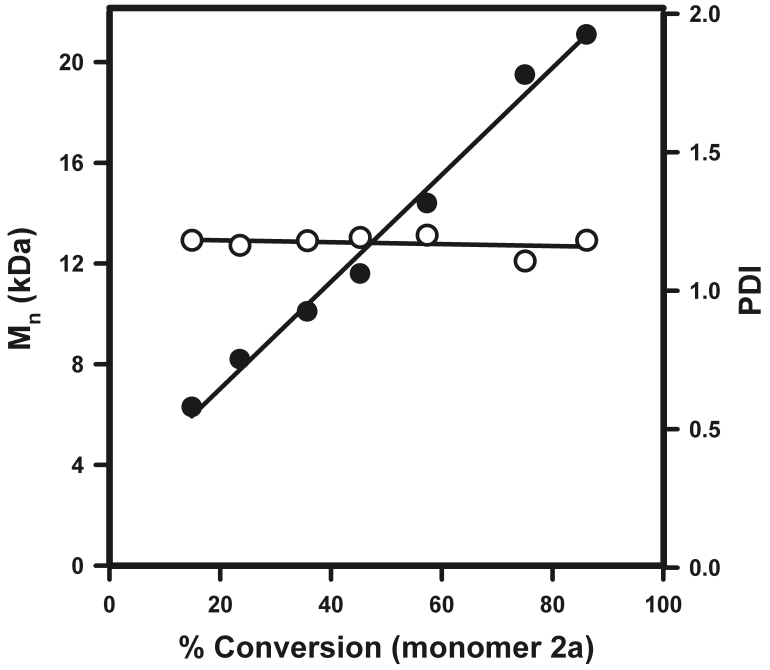

Figure S24. Plot of M_n and PDI versus conversion for **2a** (temp = 0 °C, [Ni(dppe)Cl_2] = 0.0015 M, [**2a**] = 0.1 M). Note that 0% conversion corresponds to the quenched pre-initiated catalyst solution.

Table S5. Data for the plot in Figure S24.

% Conversion (**2a**)	M_n (kDa)	PDI
15	6.3	1.18
24	8.2	1.16
36	10	1.18
45	12	1.19
57	14	1.21
75	19	1.11
86	21	1.18

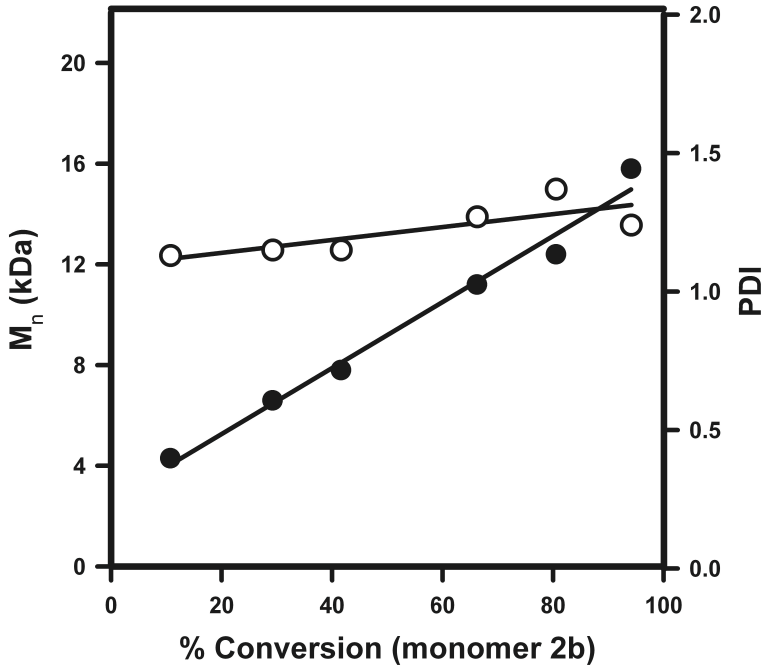

Figure S25. Plot of M_n and PDI versus conversion for **2b** (temp = 0 °C, [Ni(dppe)Cl_2] = 0.0015 M, [**2b**] = 0.2 M) Note that 0% conversion corresponds to the quenched pre-initiated catalyst solution.

Table S6. Data for the plot in Figure S25.

% Conversion (**2b**)	M_n (kDa)	PDI
11	4.3	1.13
29	6.6	1.15
41	7.8	1.15
66	11	1.27
81	12	1.37
94	16	1.24

Representative procedure for obtaining plots of M_n and PDI versus conversion utilizing GC:

An oven-dried 10 mL flask equipped with a stir bar and a rubber septum was cooled under vacuum and then refilled with N_2. Following two more cycles of evacuation and refilling the flask was charged with tridecane (0.1 mL), THF (7.0) and **6** (2.0 mL, 0.25 M, 1.0 equiv) and cooled to 0 ^oC over 2 min. After 2 min the pre-initiated catalyst solution (1.0 mL, 0.0025 M, 0.0050 equiv) was injected. Aliquots (~ 0.5 mL) were withdrawn through the septum and immediately quenched with 5 M HCl (~ 1 mL). Each aliquot was then extracted with $CHCl_3$ (with mild heating if polymer had precipitated) and a portion analyzed by GC. The remainder was dried over $MgSO_4$, filtered, and then concentrated. The samples were dissolved in THF (with heating) and passed through a 0.2 μm PTFE filter for GPC analysis.

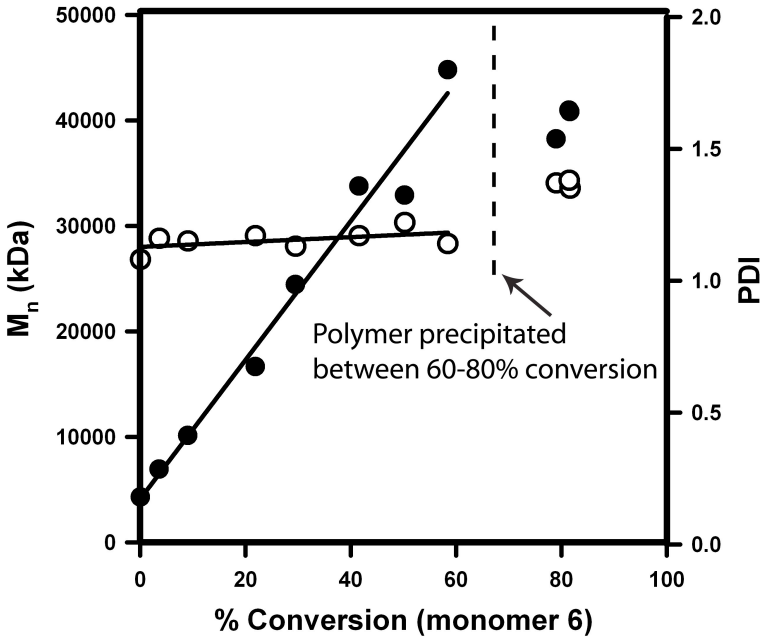

Figure S26. Plot of M_n and PDI versus conversion for **6** (temp = 0 °C, [**6**] = 0.05 M, [Ni(dppe)Cl_2] = 0.00025 M). Note that 0% conversion corresponds to an aliquot taken immediately after the catalyst was added.

Table S7. Data for the plot in Figure S26.

% Conversion (**6**)	M_n (kDa)	PDI
0	4.3	1.08
4	6.9	1.16
9	10	1.15
22	17	1.17
29	24	1.13
42	34	1.17
50	33	1.22
58	45	1.14
79	38	1.37
82	41	1.35
81	41	1.38

XI. Polymerization Rate Studies

General procedure for polymerization rate studies utilizing the ReactIR:

The IR probe was inserted through an O-ring sealed 14/20 ground glass adapter (custom made) into an oven-dried 50 mL 2-neck flask containing a Teflon magnetic stir bar. The other neck was equipped with a three-way adapter fitted with a septum for injections and an N_2 line. The flask was cooled under vacuum and then refilled with N_2. Following two more cycles of evacuation and refilling, the flask was charged with THF and cooled to 0 ^oC over ~5 min. After recording a background spectrum, ArMgCl (see Synthetic Procedures) was added by syringe and allowed to equilibrate for at least 5 min to 0 ^oC. After 5 min, the pre-initiated catalyst solution was injected and spectra were recorded every 30 s over the first 10% conversion. To account for mixing and temperature equilibration, spectra recorded in the first 60 s of the reaction were discarded. The data were converted to concentrations using the appropriate calibration curves (see above).

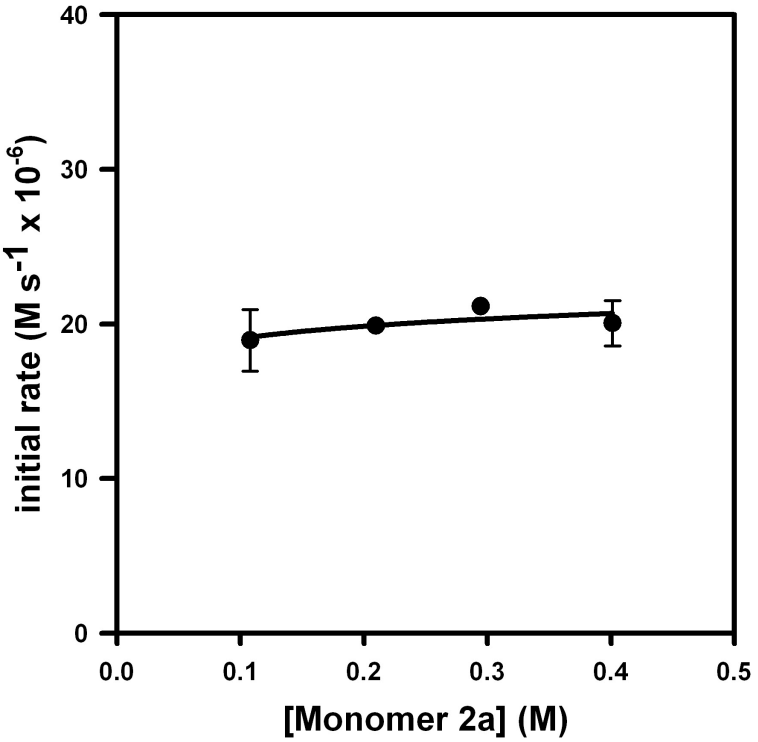

Figure S27. Plot of initial rate versus [monomer] for the polymerization of **2a**. (temp = 0 °C, [Ni(dppe)Cl_2] = 0.0015 M) fitted to y = ax^b, where a = 22 ± 1 and b = 0.06 ± 0.04.

Table S8. Table of data for the plot in Figure S27.

[**2a**] (M)	initial rate (M s^{-1})
0.1	20 ± 1 x 10^{-6}
0.2	19.9 ± 0.1 x 10^{-6}
0.3	21.1 ± 0.1 x 10^{-6}
0.4	19 ± 2 x 10^{-6}

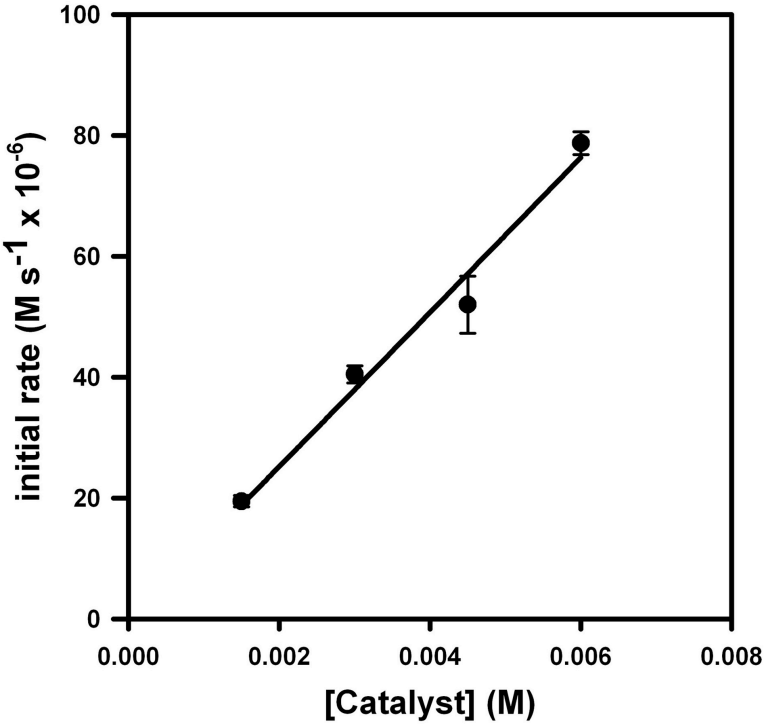

Figure S28. Plot of initial rate versus [catalyst] for the polymerization of **2a** (temp = 0 ^{o}C, [**2a**] = 0.20 M), fitted to y = ax^b, where a = 1.3 ± 0.1 x 10^4 and b = 1.01 ± 0.01.

Table S9. Table of data for the plot in Figure S28.

[Cat.] (M)	initial rate (M s^{-1})
0.0015	19.4 ± 0.9 x 10^{-6}
0.003	41 ± 2 x 10^{-6}
0.0045	52 ± 5 x 10^{-6}
0.006	78 ± 2 x 10^{-6}

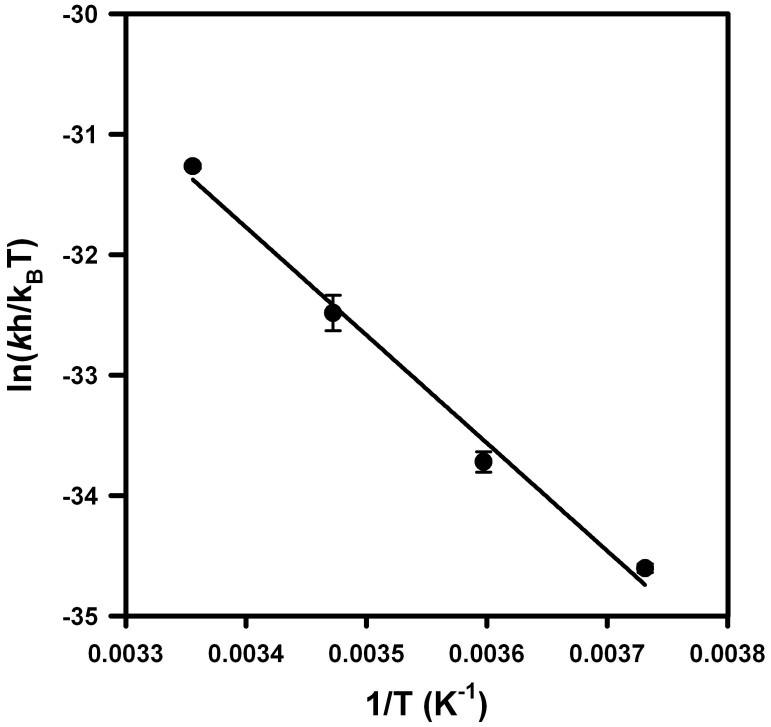

Figure S29. Plot of ln(kh/k_bT) versus 1/T for the polymerization of **2a** (temp= 0 ^{o}C, [**2a**] = 0.20 M, [Ni(dppe)Cl_2] = 0.001M) fitted to y =mx + b, where m = -8.9 ± 6 x 10^3 and b = -1 ± 2, providing an $\Delta H^{‡}$ of 18 ± 1 kcal/mol and a $\Delta S^{‡}$ of -3 ± 5 cal·mol^{-1}·K^{-1}.

Table S10. Data for the plot in Figure S29.

Temp (^{o}C)	initial rate (M s^{-1})	k	ln(kh/k_BT)
25	16.4 ± 0.3 x 10^{-5}	16.4 ± 0.3 x 10^{-2}	-31.26 ± 0.02
15	4.7 ± 0.7 x 10^{-5}	4.7 ± 0.7 x 10^{-2}	-32.4 ± 0.2
5	12 ± 1 x 10^{-6}	12 ± 1 x 10^{-3}	-33.72 ± 0.08
-5	53 ± 2 x 10^{-7}	53 ± 2 x 10^{-4}	-34.60 ± 0.04

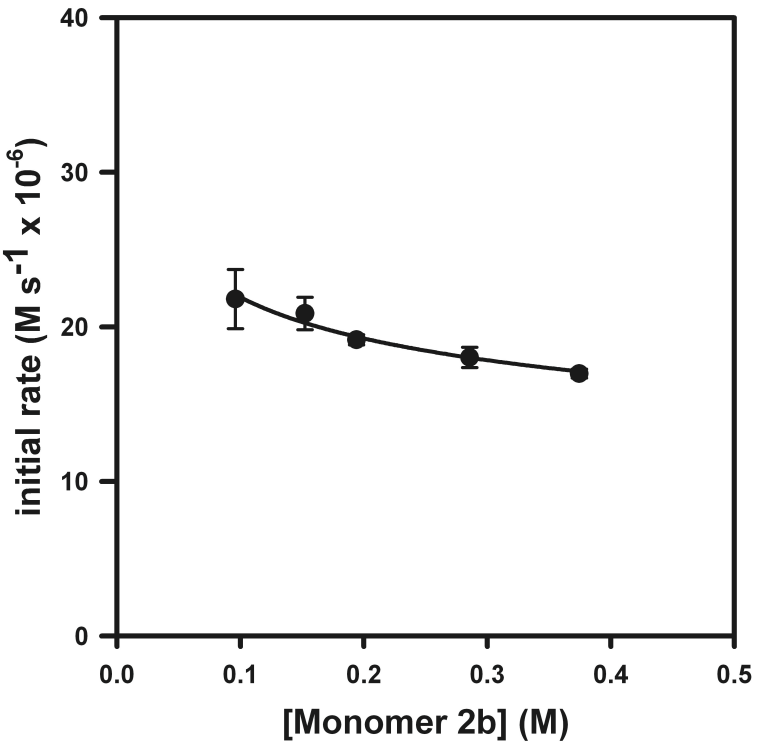

Figure S30. Plot of initial rate versus [monomer] for the polymerization of **2b** (temp = 0 °C, [Ni(dppe)Cl_2] = 0.0015 M) fitted to $y = ax^b$, where a = 14.2 ± 0.5 and b = -0.19 ± 0.02.

Table S11. Data for the plot in Figure S30.

[**2b**] (M)	initial rate (M s^{-1})
0.1	22 ± 2 x 10^{-6}
0.15	21 ± 1 x 10^{-6}
0.19	19.2 ± 0.3 x 10^{-6}
0.29	18.0 ± 0.6 x 10^{-6}
0.37	17 ± 2 x 10^{-6}

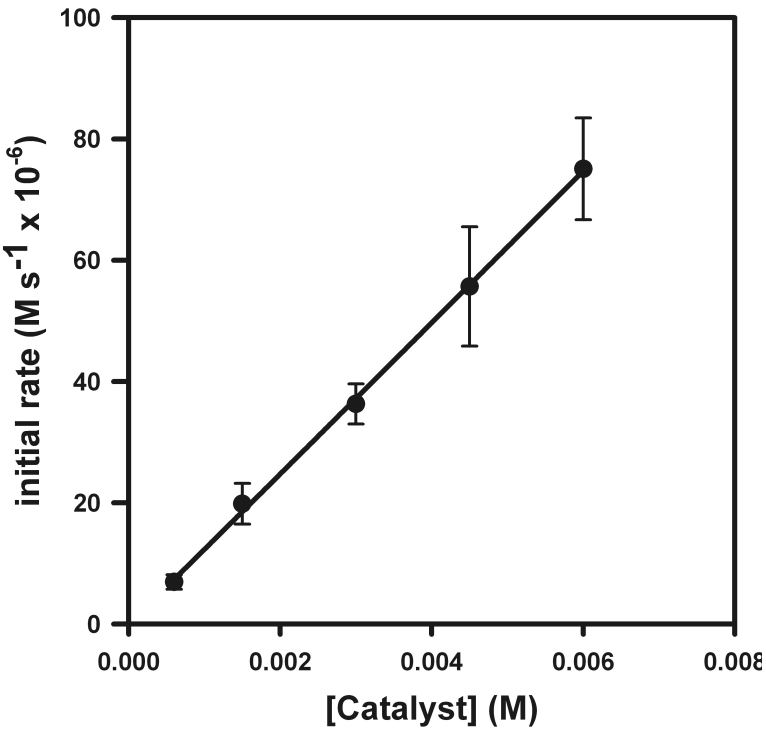

Figure S31. Plot of initial rate versus [catalyst] for the polymerization of **2b** (temp = 0 °C, [**2b**] = 0.20 M) fitted to $y = ax^b$, where $a = 1.3 \pm 0.2 \times 10^4$ and $b = 1.01 \pm 0.03$

Table S12. Data for the plot in Figure S31.

[Cat.] (M)	initial rate (M s^{-1})
0.0006	$7 \pm 1 \times 10^{-6}$
0.0015	$19 \pm 3 \times 10^{-6}$
0.003	$36 \pm 3 \times 10^{-6}$
0.0045	$55 \pm 10 \times 10^{-6}$
0.006	$75 \pm 8 \times 10^{-6}$

Changes to the general procedure to determine the order in LiCl:

A solution of **2a** was prepared and titrated as described above. After titration 1.0 equiv LiCl was added and the solution stirred until homogeneous. Separately a 0.6 M solution of LiCl in THF was prepared in the glovebox. A 2-neck flask was cooled under vacuum and then refilled with N_2. Following two more cycles of evacuation and refilling, the flask was charged with THF and the appropriate amount of LiCl solution and cooled to 0 ^oC over ~5 min. After recording a background spectrum, ArMgCl (see Synthetic Procedures) was added by syringe and allowed to equilibrate for at least 5 min.

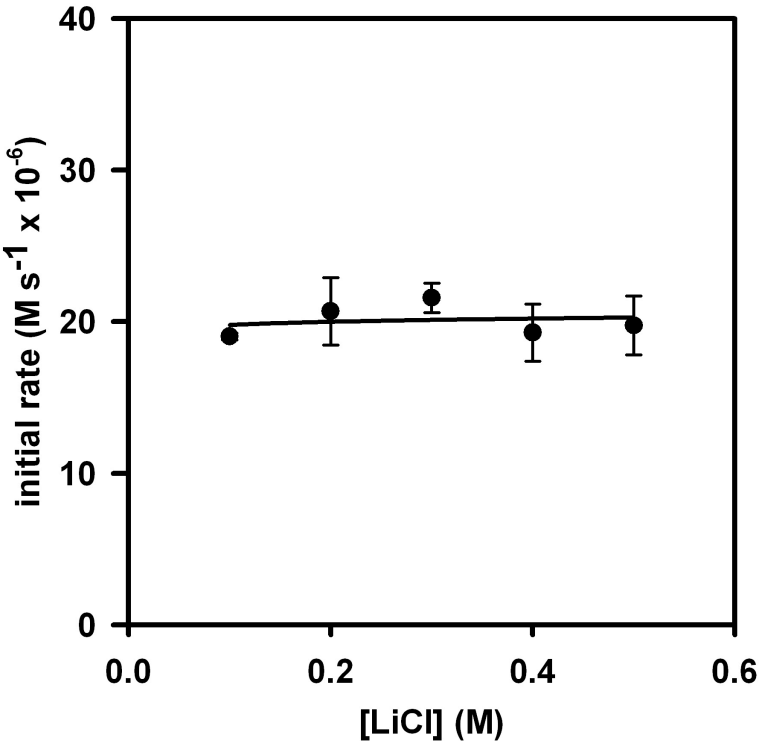

Figure S32. Plot of initial rate versus [LiCl] for the polymerization of **2b** (temp = 0 ^{o}C, [**2b**] = 0.20 M, [Ni(dppe)Cl_2] = 0.0015 M) fitted to y = ax^b, where a = 20 ± 1 and b = 0.02 ± 0.05.

Table S13. Table of data for the plot in Figure S32.

[LiCl] (M)	initial rate (M s^{-1})
0.1	19.0 ± 0.2 x 10^{-6}
0.2	21 ± 2 x 10^{-6}
0.3	21 ± 1 x 10^{-6}
0.4	19 ± 2 x 10^{-6}
0.5	19 ± 2 x 10^{-6}

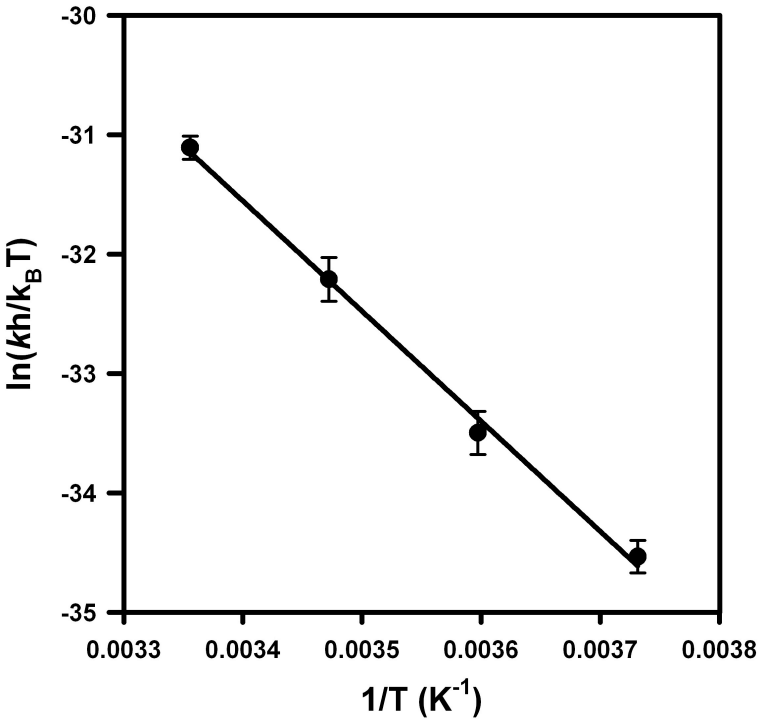

Figure S33. Plot of ln(kh/k_BT) versus 1/T for the polymerization of **2b** ([**2b**] = 0.20 M, [Ni(dppe)Cl_2] = 0.001 M) fitted to y = mx + b where m = -9.0 ± 0.4 x 10^3 and b = 0 ± 1, providing a $\Delta H^{\ddagger}$ of 18.4 ± 0.7 kcal/mol and a $\Delta S^{\ddagger}$ of -0 ± 3 cal·mol^{-1}·K^{-1}.

Table S14. Data for the plot in Figure S33.

Temp (^{o}C)	initial rate (M s^{-1})	k	ln(kh/k_BT)
25	19 ± 2 x 10^{-5}	19 ± 2 x 10^{-2}	-31.6 ± 0.1
15	6 ± 1 x 10^{-5}	6 ± 1 x 10^{-2}	-32.2 ± 0.2
5	16 ± 2 x 10^{-6}	16 ± 2 x 10^{-3}	-33.5 ± 0.2
-5	56 ± 7 x 10^{-7}	56 ± 7 x 10^{-4}	-34.5 ± 0.1

General procedure for polymerization rate studies utilizing GC:

An oven-dried 10 mL flask equipped with a stir bar and a rubber septum was cooled under vacuum and then refilled with N_2. Following two more cycles of evacuation and refilling the flask was charged with tridecane (25 μL), THF and **6** and cooled to 0 ^oC over 2 min. After 2 min the pre-initiated catalyst solution was injected. Aliquots (~ 0.025 mL) were withdrawn through the septum and immediately quenched with methanol (~ 0.5 mL). Each aliquot was then diluted with $CHCl_3$ and analyzed by GC.

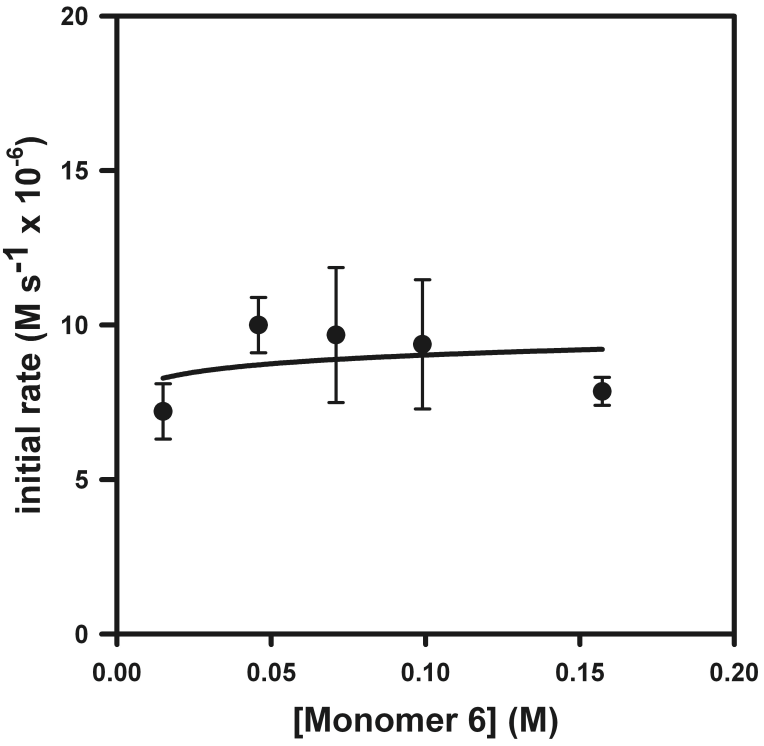

Figure S34. Plot of initial rate versus [monomer] for the polymerization of **6** (temp = 0 °C, [Ni(dppe)Cl_2] = 0.00025 M) fitted to y = ax^b, where a = 10 ± 3 and b = 0.05 ± 0.09.

Table S15. Table of data for the plot in Figure S34.

[**6**] (M)	initial rate (M s^{-1})
0.015	7 ± 1 x 10^{-6}
0.046	10 ± 1 x 10^{-6}
0.071	10 ± 2 x 10^{-6}
0.099	9 ± 2 x 10^{-6}
0.16	7.9 ± 0.5 x 10^{-6}

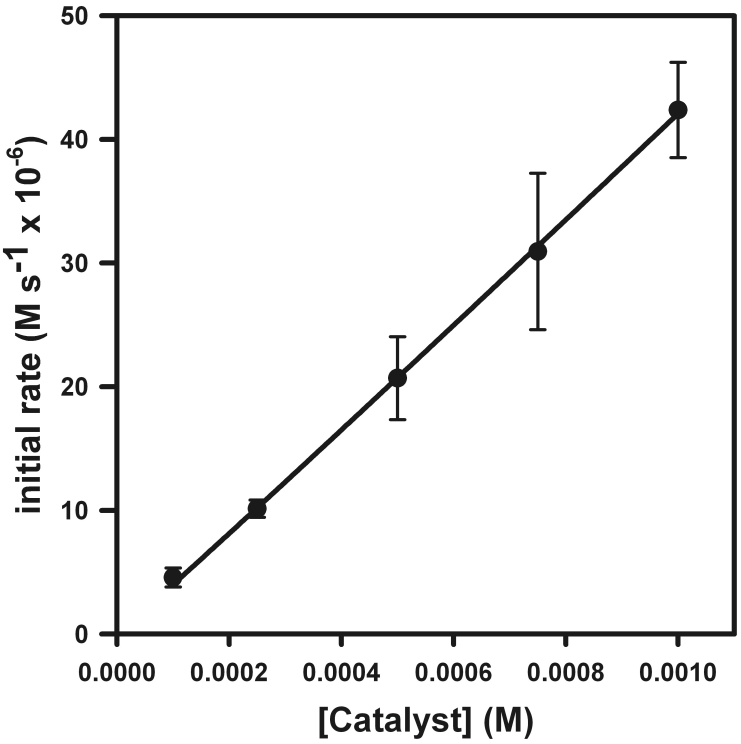

Figure S35. Plot of initial rate versus [catalyst] for the polymerization of **6** (temp = 0 °C, [**6**] = 0.10 M) fitted to $y = ax^b$, where $a = 4.9 \pm 0.8 \times 10^4$ and $b = 1.02 \pm 0.02$

Table S16. Data for the plot in Figure S35.

[Cat.] (M)	initial rate (M s^{-1})
0.0001	$4.5 \pm 0.8 \times 10^{-6}$
0.00025	$10.1 \pm 0.7 \times 10^{-6}$
0.0005	$21 \pm 3 \times 10^{-6}$
0.00075	$31 \pm 6 \times 10^{-6}$
0.001	$42 \pm 4 \times 10^{-6}$

XII. Spectroscopic Studies

General Procedure for Performing Spectroscopic Studies

Complexes **IIa**, **IIb** and **V**

All actions were performed in a glovebox under N_2 atmosphere. A 20 mL vial was equipped with a stir bar. Sequentially, Ni(dppe)Cl_2 (1 equiv), THF, and **2** or **6** (0.15-0.2 M, 15 equiv) were added to the vial to prepare a ~0.015 M solution of the Ni species. The reaction mixture was stirred for 10 min until homogeneous.

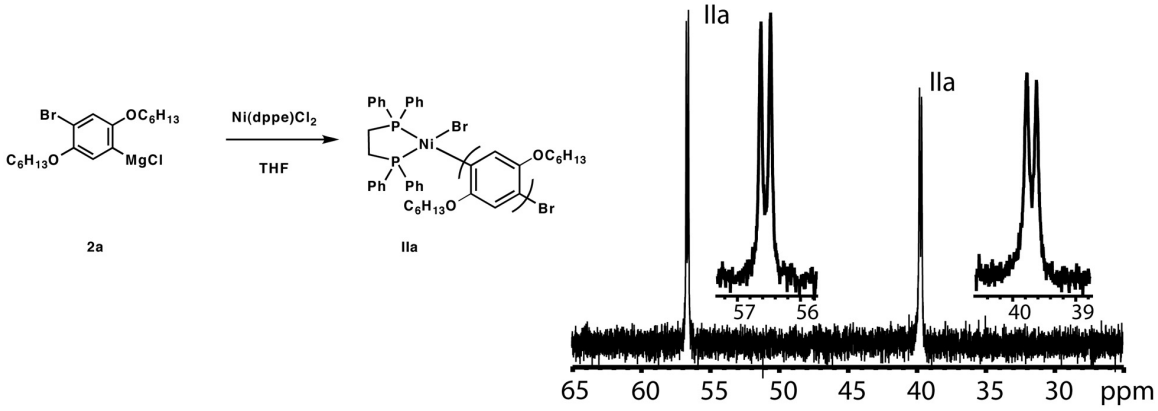

Figure S36. ^{31}P NMR (161 MHz, THF) δ 56.6 (d, *J* = 25 Hz), 39.7 (d, *J* = 25 Hz).

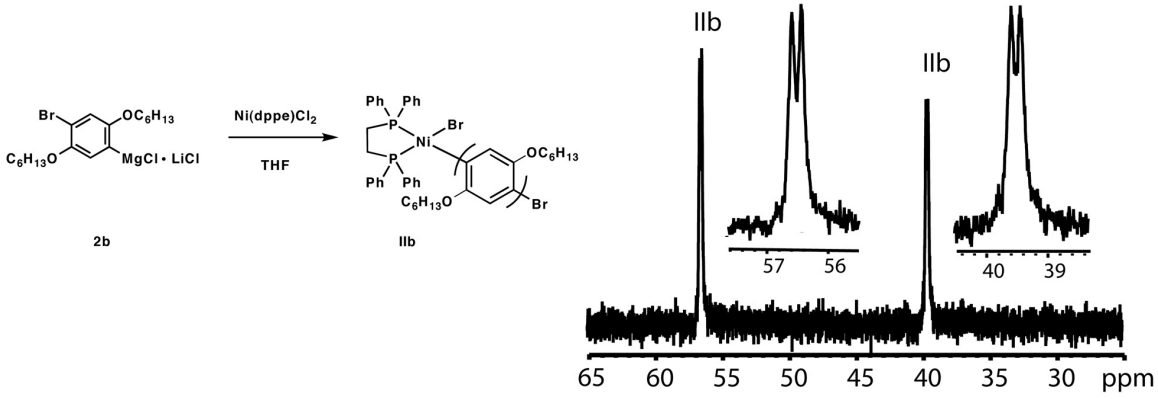

Figure S37. ^{31}P NMR (161 MHz, THF) δ 56.5 (d, *J* = 24 Hz), 39.6 (d, *J* = 24 Hz).

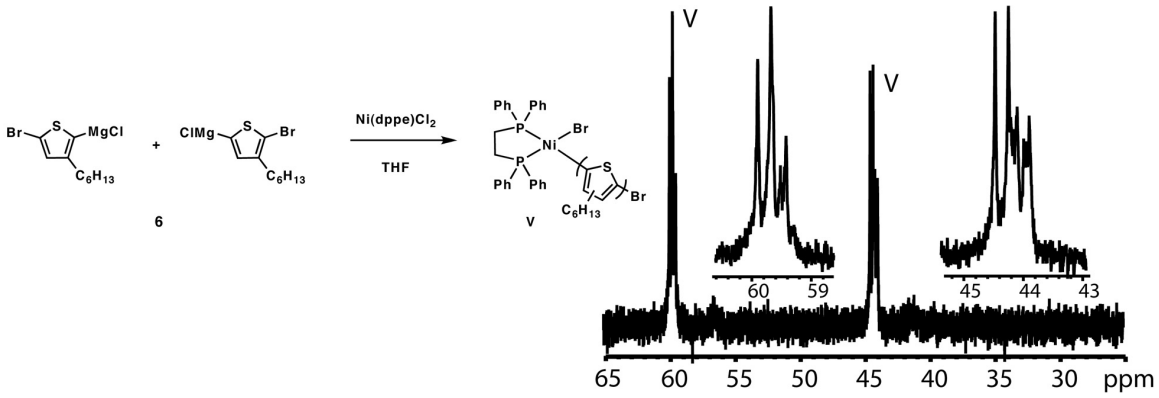

Figure S38. ^{31}P NMR (161 MHz, THF) δ 59.8 (d, *J* = 36 Hz), 44.4 (d, *J* = 36 Hz).

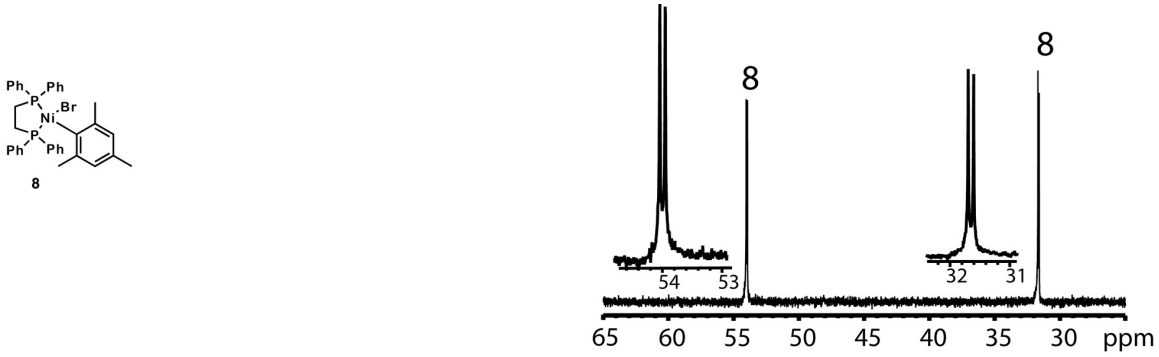

Figure S39. ^{31}P NMR (161 MHz, THF) δ 54.0 (d, *J* = 15 Hz), 31.7 (d, *J* = 15 Hz)

Complexes **IIIa**, **IIIb**, and **VI**

All actions were performed in a glovebox under N_2 atmosphere. A 20 mL vial was equipped with a stir bar. Sequentially, Ni(dppe)Cl_2 (1 equiv), THF, and **2** or **6** (0.15-0.2 M, 10 equiv) were added to the vial to prepare an ~0.03 M solution of the Ni species. The reaction mixture was stirred for 10 min until homogeneous. The Ni solution was loaded into a 1 mL syringe. Separately, 0.5-1 mL of a 0.15-0.2 M solution of **2** or **6** was loaded into a NMR tube sealed with a rubber septum. The NMR tube was removed from the glovebox and cooled in a brine-ice solution. Immediately before acquiring the spectrum the Ni solution (0.25-0.5 mL)

was injected into the NMR tube which was then rapidly inverted. The sample was loaded into the NMR spectrometer cooled to the appropriate temperature.

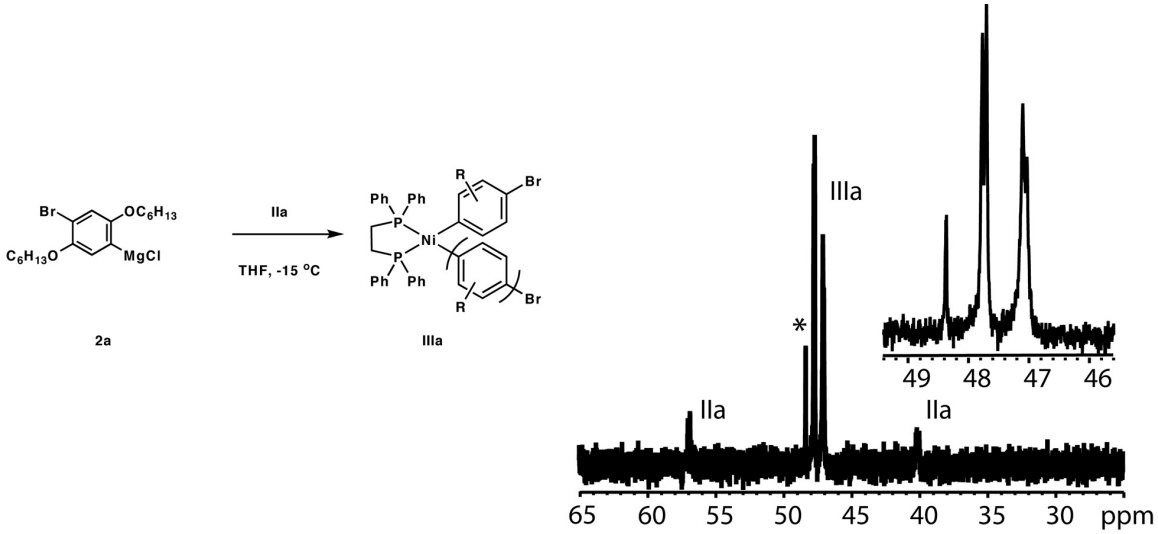

Figure S40. ^{31}P NMR (161 MHz, THF, -15 °C) δ 48.3 ($Ni(dppe)_2X_2$), 47.7 (d, *J* = 11 Hz), 47.0 (d, *J* = 11 Hz).

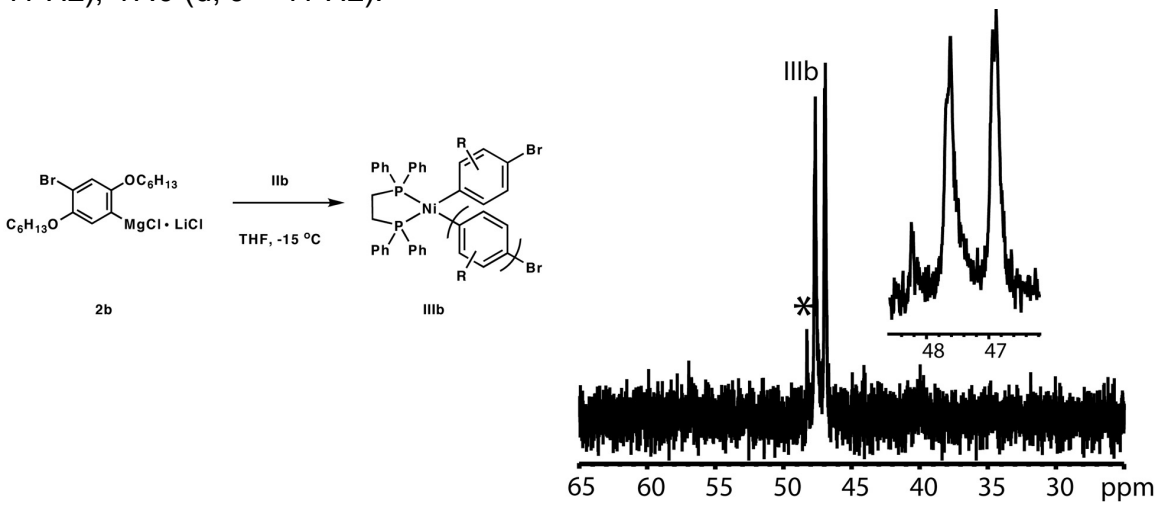

Figure S41. ^{31}P NMR (161 MHz, THF) δ 48.3 ($Ni(dppe)_2X_2$), 47.7 (d, *J* = 9 Hz), 47.0 (d, *J* = 9 Hz).

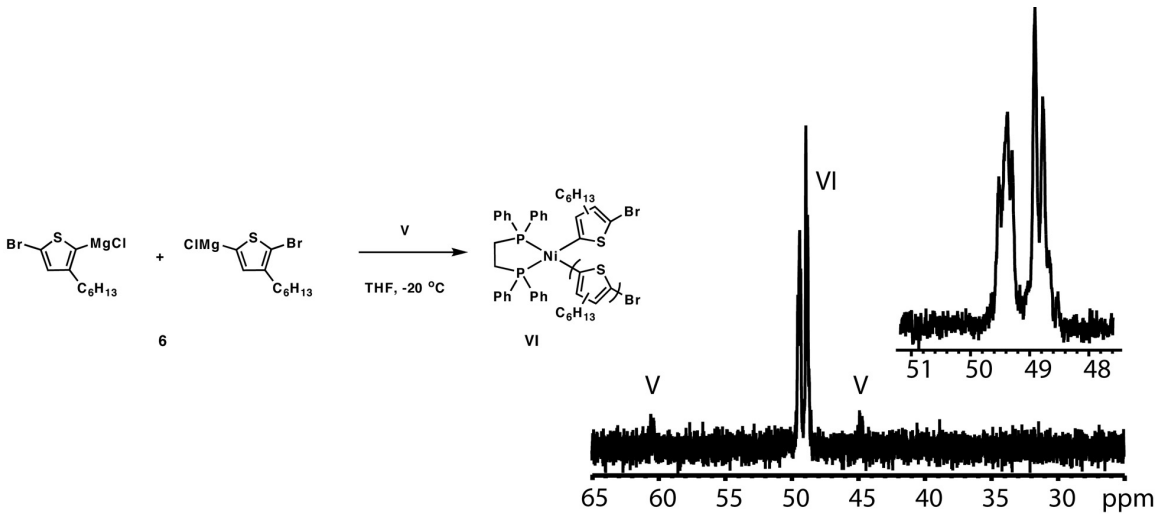

Figure S42 ^{31}P NMR (161 MHz, THF, -20 °C) δ 49.4 (d, *J* = 24 Hz), 49.4 (Ni(dppe)$_2$X$_2$), 48.8 (d, *J* = 24 Hz).

Note that for monomer **6** both regioisomers are consumed under these conditions as demonstrated by the following GC experiment.

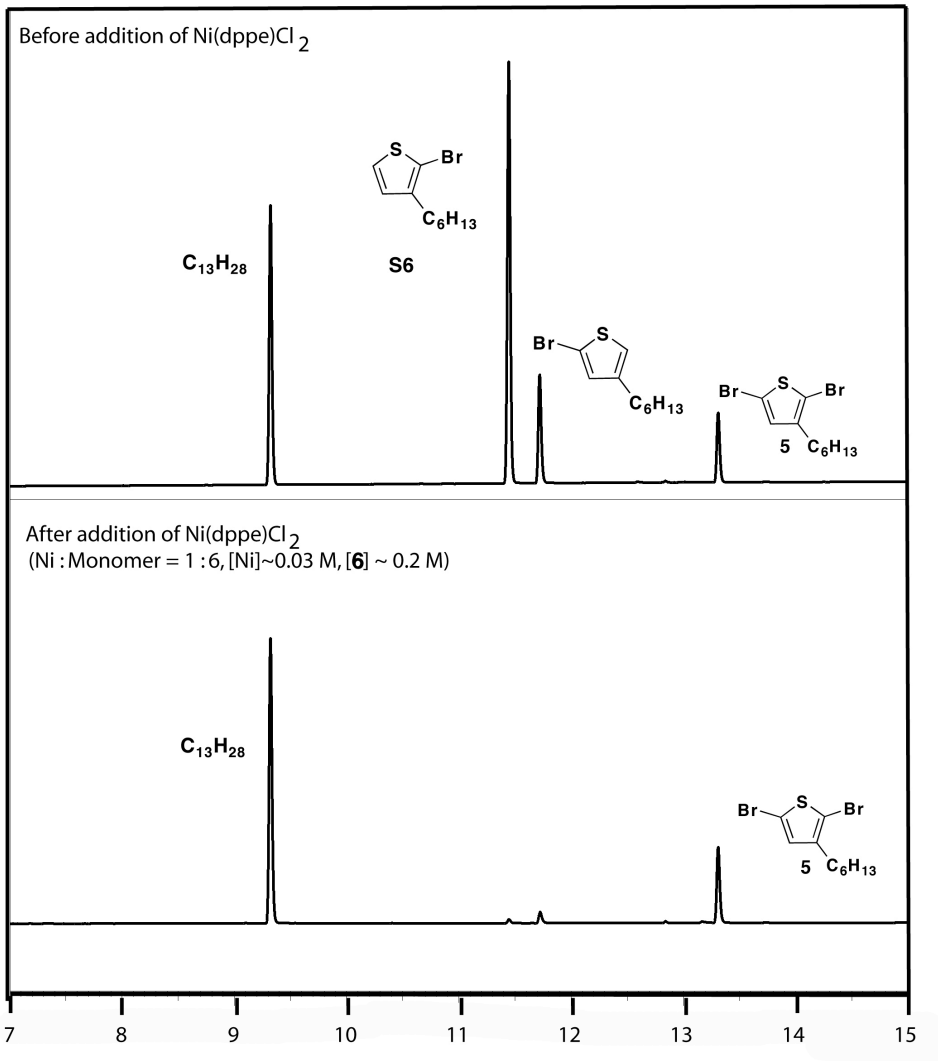

Figure S43. GC chromatograms showing consumption of both thiophene regioisomers.

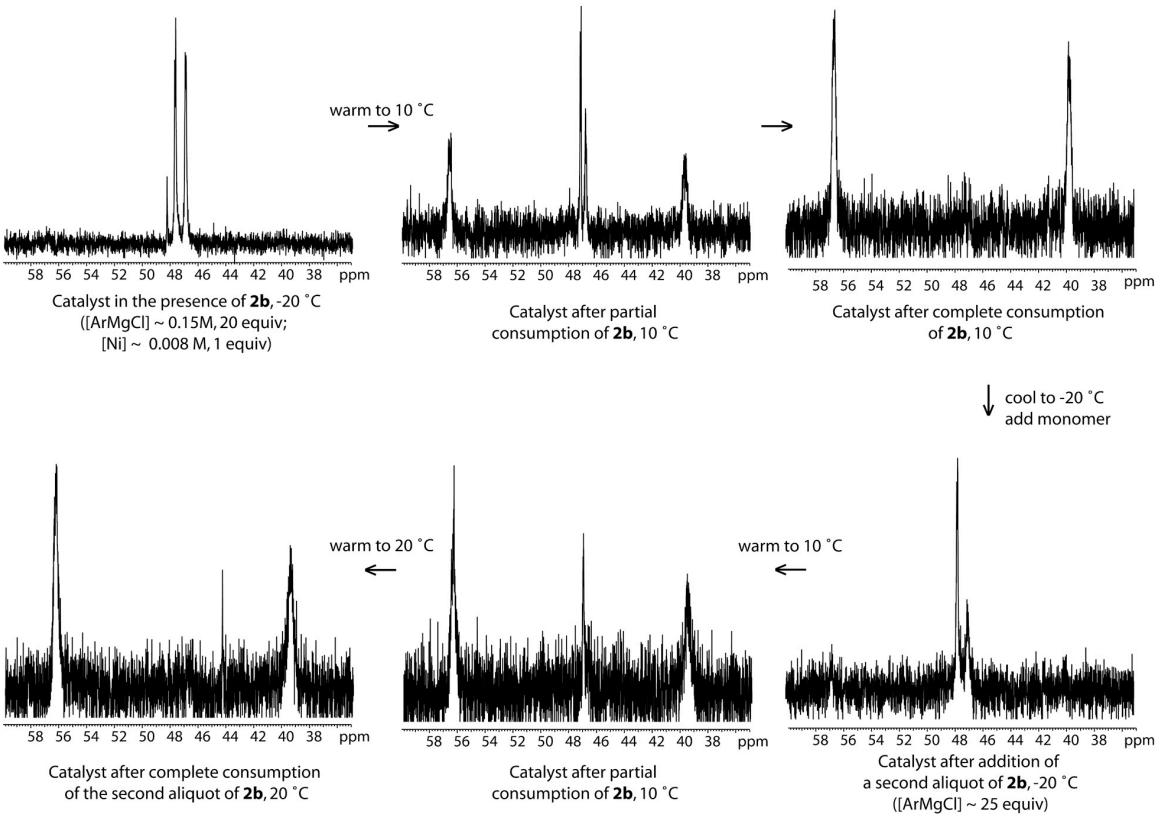

Figure S44.

Interconversion of the catalyst based on presence or absence of **2b**. Loss of signal to noise over time is caused by polymer precipitation at the concentration and temperature required to observe the biaryl nickel species by ^{31}P NMR spectroscopy. Asymmetry and broadening of peaks is believed to be due to the averaging of different sized oligomers on the metal center.

XIII References Cited

[1] Miyakoshi, R.; Shimono, K.; Yokoyama, A.; Yokozawa, T. *J. Am. Chem. Soc.* **2006**, *128*, 16012-16013.

[2] Yokoyama, A.; Miyakoshi, R.; Yokozawa, T. *Macromolecules* **2004**, 37, 1169-1171.

[3] Bogdanović, B; Liao, S-T.; Mynott, R.; Schlichte, K.; Westeppe, U. *Chem. Ber*. **1984**, *117*, 1378-1392.

[4] Touboul, E.; Dana, G.; Convert, O. *Tetrahedron* **1987**, *43*, 543-549.

[5] Iovu, M. C.; Sheina, E. E.; Gil, R. R.; McCullough, R. D. *Macromolecules* **2005**, *38*, 8649-8656.

[6] (a) Stanger, A.; Vollhardt, K. P. C. *Organometallics* **1992**, *11*, 317-320. (b) Jonas, K. *J. Organomet. Chem.* **1974**, *78*, 273-279.

[7] Coronas, J. M.; Muller, G.; Rocamora, M.; Miravitlles, C.; Solans, X. *Dalton Trans.* **1985**, 2333-2341.

[8] Maruyama, S.; Kawanishi Y. *J. Mater. Chem.* **2002**, *12*, 2245-2249.

[9] Tanemura, K.; Suzuki, T.; Nishida, Y.; Satsumabayashi, K.; Horaguchi, T. *Chem. Lett.* **2003**, *32*, 932–933.

[10] Krishna Mohan, K. V. V.; Narender, N.; Kulkarni, S. J. *Tetrahedron Lett.* **2004**, *45*, 8015-8018.

[11] Baker, B. E.; Larock, R. C. *Tetrahedron Lett.* **1988**, *29*, 905-908.

[12] Chatt, J.; Shaw, B. L. *J. Chem. Soc.* **1960**, 1718-1729.

[13] Love, B. E.; Jones, E. G. *J. Org. Chem.* **1999**, *64*, 3755–3756.